Annual Review of LIBRA-LiTE Project: Research Performed During Calendar Year 1990

D. Bruggink, R.L. Engelstad, G.L. Kulcinski, E.G. Lovell, J.J. MacFarlane, E.A. Mogahed, G.A. Moses, R.R. Peterson, M.E. Sawan, G. Sviatoslavsky, I.N. Sviatoslavsky, L.J. Wittenberg

December 1990

FPA-90-3

FUSION POWER ASSOCIATES

2 Professional Drive, Suite 248
Gaithersburg, Maryland 20879
(301) 258-0545

1500 Engineering Drive
Madison, Wisconsin 53706
(608) 263-2308

LIBRA -LiTE Visit
Dec 15 -17, 1990

- Monday, Dec. 16

10:00 Study Background -Kulcinski
10:05 LIBRA LiTE Study Philosophy -
Kulcinski
10:10 Overall LIBRA -LIBRA LiTE
Comparison -Kulcinski
10:30 Beam properties -Peterson
11:00 Cavity Design -Sviatoslavsky

11:30 Break

11:45 Blast Wave - Peterson
12:10 Other Reactor Features -
Sviatoslavsky
12:20 Video -All

12:30 -2 Lunch

2:00 -3:00 Further LIBRA LiTE Discussion
3:00 -4:00 Future Work
4:00 -5:00 Open

6:00 -8:30 Dinner

Background for LIBRA-LiTE Study

- LIBRA study initiated by KfK in 1982
- LIBRA studied for 6 out of 7 years, 1982-89
- Funding for LIBRA mixed with other fundamental research.
- Level of effort is ≈4 PY over 6 years

- SNL joined project in 1988

Background for LIBRA-LiTE Study

- First 6 years based on channel transport; resulted in LIBRA report KfK-4710 (FPA 90-3, and UWFDM-800)
- Most complete self-consistent LIB study published (basis for U.S. FPAC review, 1990)
- Publications
  - 7 reviewed literature papers
  - 2 conference proceedings
  - 15 reports

- Requested by KfK and SNL to examine ballistic focusing for 1990-1

Chronology of LIBRA-Related Reports, 1982–Present

UWFDM 426. The INPORT Concept - An Improved Method to Protect ICF Reactor First Walls; G.L. Kulcinski, G.A. Moses, J. Sapp, M. Sawan, I.N. Sviatoslavsky, D.K. Sze, and W.F. Vogelsang, August 1981 [paper presented at Second Topical Mtg. on Fusion Reactor Materials, August 9-12, 1981, Seattle, WA; J. Nucl. Matls. 103 & 104, 103 (1981)].

FPA-82-4 "Preliminary Considerations of Light Ion Beam Fusion and LIBRA Reactor Design," Presentation at KfK-Karlsruhe, FRG, 3-4 June 1982.

FPA-82-5 "Progress on Modelling of $Pb_{83}Li_{17}$ Recondensation on INPORT Units," L. Pong, D.K. Sze, R.R. Peterson, G.A. Moses, August 1982.

FPA-82-7 "Annual Report of Research Performed on the LIBRA Project Between 1 January and 31 December 1982 by Fusion Power Associates for the Kernforschungszentrum Karlsruhe GmbH, Karlsruhe, FRG," B. Badger, J. Billen, D. Bruggink, R. Engelstad, G.L. Kulcinski, E.G. Lovell, G.A. Moses, K. O'Brien, R.R. Peterson, L. Pong, I.N. Sviatoslavsky, D.K. Sze, W.F. Vogelsang, J. Watrous, 31 December 1982.

FPA-83-2 "An Effective Penetration Shield Design for ICF Reactors," M.E. Sawan, W.F. Vogelsang, and D.K. Sze, May 1983.

FPA-83-3 "Progress Report for the LIBRA Light Ion Beam Fusion Reactor Project for the Period January - June 1983," B. Badger, T. Bartel, J. Billen, M.L. Corradini, R.L. Engelstad, G.L. Kulcinski, E.G. Lovell, G.A. Moses, K.J. O'Brien, R.R. Peterson, L. Pong, M.E. Sawan, I.N. Sviatoslavsky, W.F. Vogelsang, J.J. Watrous, July 1983.

UWFDM 561. Mechanical Analysis of First Wall Tubes for the LIBRA Conceptual Reactor; R. Engelstad and E. Lovell, December 1983 [presented at the IEEE Mtg., Philadelphia, PA, 12-16 December 1983].

FPA-83-8 "Annual Report for the LIBRA Light Ion Beam Fusion Reactor Project for the Period January - December 1983," B. Badger, T. Bartel, J. Billen, M.L. Corradini, R. Engelstad, D. Henderson, G.L. Kulcinski, G.A. Moses, K. O'Brien, R.R. Peterson, L. Pong, M.E. Sawan, I.N. Sviatoslavsky, D.K. Sze, W.F. Vogelsang, J.J. Watrous, December 1983.

FPA-84-1 "Progress Report for the LIBRA Light Ion Beam Fusion Reactor Project for the Period January-June 1984," B. Badger, T.J. Bartel, M.L. Corradini, R.L. Engelstad, D.L. Henderson, G.L. Kulcinski, E.G. Lovell, G.A. Moses, K.J. O'Brien, R.R. Peterson, L. Pong, M.E. Sawan, I.N. Sviatoslavsky, W.F. Vogelsang, and J.J. Watrous, July 1984.

FPA-84-2 "Basic Theory for Three-Dimensional Motion of LIBRA INPORT Tubes," R.L. Engelstad and E.G. Lovell, October 1984.

FPA-84-3 "Planar Vibrations of LIBRA INPORT Tubes Including Gravity Gradient Effects," R.L. Engelstad and E.G. Lovell, October 1984

FPA-84-5 "ION - A Code to Compute Ion Trajectories in Z-Pinch Plasma Channels," G.A. Moses, November 1984.

FPA-84-8 "Annual Progress Report for the LIBRA Light Ion Beam Fusion Reactor Project for the Period

January-December 1984," B. Badger, T.J. Bartel, M.L. Corradini, R.L. Engelstad, D.L. Henderson, G.L. Kulcinski, E.G. Lovell, G.A. Moses, K.J. O'Brien, R.R. Peterson, L. Pong, M.E. Sawan, I.N. Sviatoslavsky, W.F. Vogelsang, and J.J. Watrous, December 1984.

FPA-85-2 "Vibration Analysis of LIBRA INPORTs," R.L. Engelstad and E.G. Lovell, February 1985 [presented at Sixth Topical Meeting on the Technology of Fusion Energy, San Francisco, CA, 3-7 March 1985.]

UWFDM 617. Vibration Analysis of LIBRA INPORTs; R.L. Engelstad and E.G. Lovell, February 1985 [Presented at the Sixth Topical Meeting on the Technology of Fusion Energy, San Francisco, CA, 3-7 March 1985; Fusion Technology, 8, 1884-1889 (July 1985)].

"Vapor Condensation in the Presence of a Noncondensable Gas," Lichung Pong and Gregory A. Moses, Phys. Fluids 29 (6), 1796-1804 (June 1986).

FPA-88-1 "Progress Report on Work Performed on the LIBRA Design During the Period 1 February 1987 to 31 January 1988," B. Badger, G.L. Kulcinski, G. Moses, E. Lovell, R. Engelstad, J. MacFarlane, Z. Musicki, R. Peterson, M. Sawan, I. Sviatoslavsky, and L. Wittenberg, January 1988.

UWFDM 778. Chamber Design for the LIBRA Light Ion Beam Fusion Reactor, M.E. Sawan, I.N. Sviatoslavsky, L.J. Wittenberg, E.G. Lovell, R.L. Engelstad; October 1988 [presented at the 8th Topical Meeting on the Technology of Fusion Energy, 9–13 October 1988, Salt Lake City UT].

UWFDM 781. Overview of the LIBRA Light Ion Beam Fusion Conceptual Design, G.A. Moses, G.L. Kulcinski, D. Bruggink, R.L. Engelstad, E.G. Lovell, J.J. MacFarlane, Z. Musicki, R.R. Peterson, M.E. Sawan, I.N. Sviatoslavsky, L.J. Wittenberg, G. Kessler, U. von Möllendorff, E. Stein, D. Cook, R. Olson, I. Smith, P. Corcoran, H. Nishimoto, J. Fockler; October 1988 [presented at the 8th Topical Meeting on the Technology of Fusion Energy, 9–13 October 1988, Salt Lake City UT].

UWFDM 786. Plasma Channels for the Propagation of Ion Beams in LIBRA, R.R. Peterson, G.A. Moses; July 1988.

UWFDM 787. LIBRA–A Light Ion Beam Fusion Reactor Conceptual Design; G.A. Moses, G.L. Kulcinski, D. Bruggink, R. Engelstad, E. Lovell, J. MacFarlane, Z. Musicki, R. Peterson, M. Sawan, I. Sviatoslavksy, L. Wittenberg, G. Kessler, U. von Möllendorff, E. Stein, I. Smith, P. Corcoran, H. Nishimoto, J. Fockler, D. Cook, R. Olson; July 1988.

UWFDM 800. LIBRA – A Light Ion Beam Fusion Conceptual Reactor Design, B. Badger, G.A. Moses, R.L. Engelstad, G.L. Kulcinski, E. Lovell, J. MacFarlane, R.R. Peterson, M.E. Sawan, I.N. Sviatoslavsky, L.J. Wittenberg, I. Smith, R. Altes, P. Corcoran, R. Kuenning, D. Pellow, D. Wake, J. Ehrhardt, G. Kessler, E. Stein, D.L. Cook, R.E. Olson, R.W. Stinnett; July 1989 (revised February 1990).

UWFDM 804. Activation Analysis for the LIBRA Light Ion Beam Fusion Conceptual Design, Mohamed E. Sawan; October 1989 [Presented at the 13th Symposium on Fusion Engineering, 2–6 October 1989, Knoxville TN].

UWFDM 841. Plasma Channels for the LIBRA Reactor Design; O. Yasar, G.A. Moses and R.R. Peterson, October 1990 [Presented at the 9th Topical Meeting on the Technology of Fusion Energy, 7–11 October 1990, Oak Brook IL].

History of LIBRA Reactor Funding From KfK

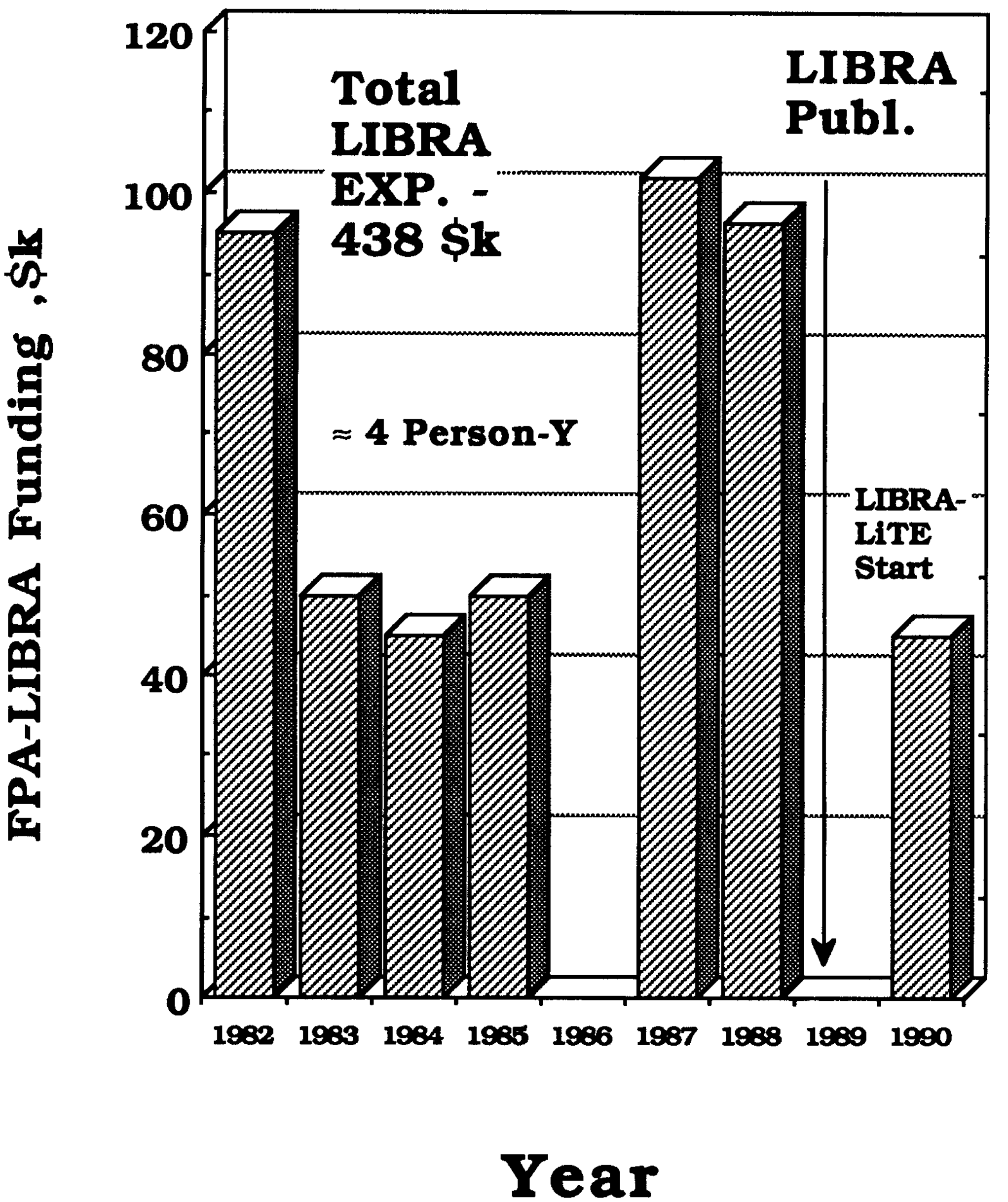

LIBRA LiTE Philosophy

- **Reason to move from channel transport (CT) to ballistic focus (BF) is lack of credibility in CT for focussing to 1 cm diameter beam.**

  Implication :
  - ***Requires significant improvement in microdivergence from diode.***
  - ***Final focussing magnet close to target***

- **Increase power from 330 to 1000 MW_e.**

  Implication:
  - ***Requires larger targets (2 cm dia.)***
  - ***For fixed TW/cm^2, need more TW's***
  - ***For fixed pulse length, requires higher beam energy***
  - ***Higher MJ's ==> larger gain=> higher yield***

- **Main Conflict Between High Yield and Need for Final Focussing Elements Close to Target !**

Logic Behind Present LIBRA - LiTE Design Point

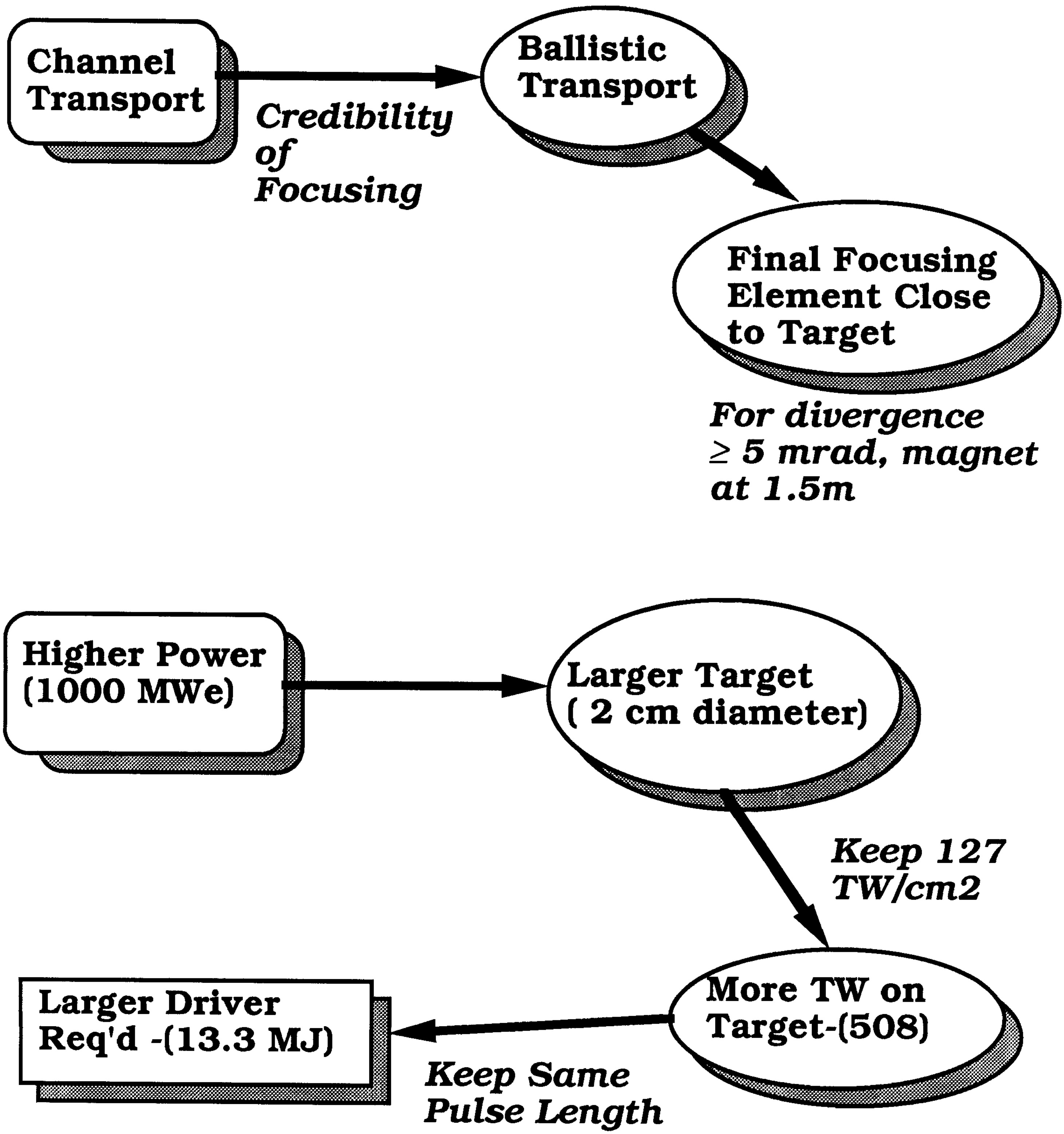

Logic Behind Present LIBRA-LiTE Design (cont.)

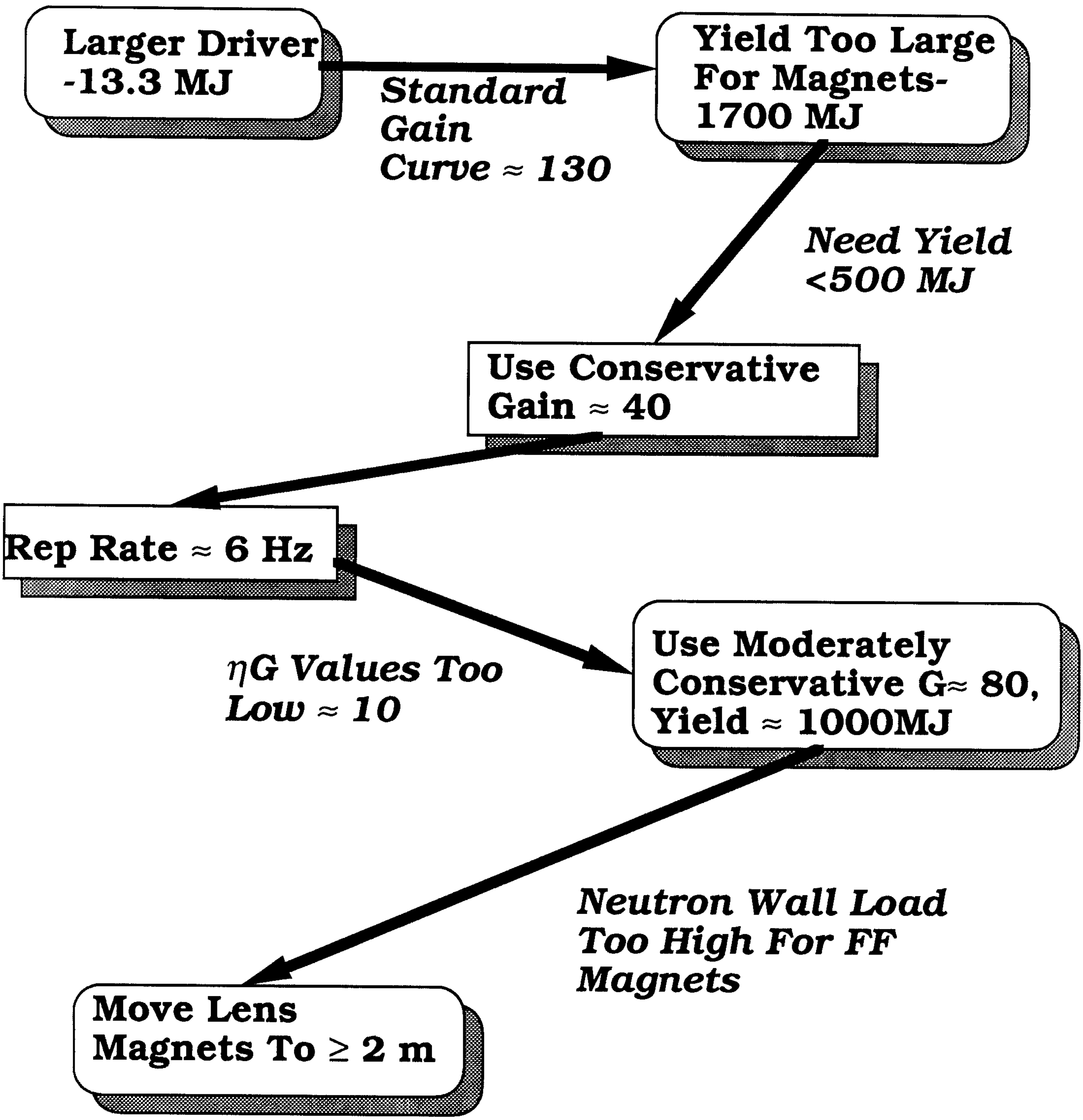

Logic Behind Present LIBRA-LiTE Design (cont.)

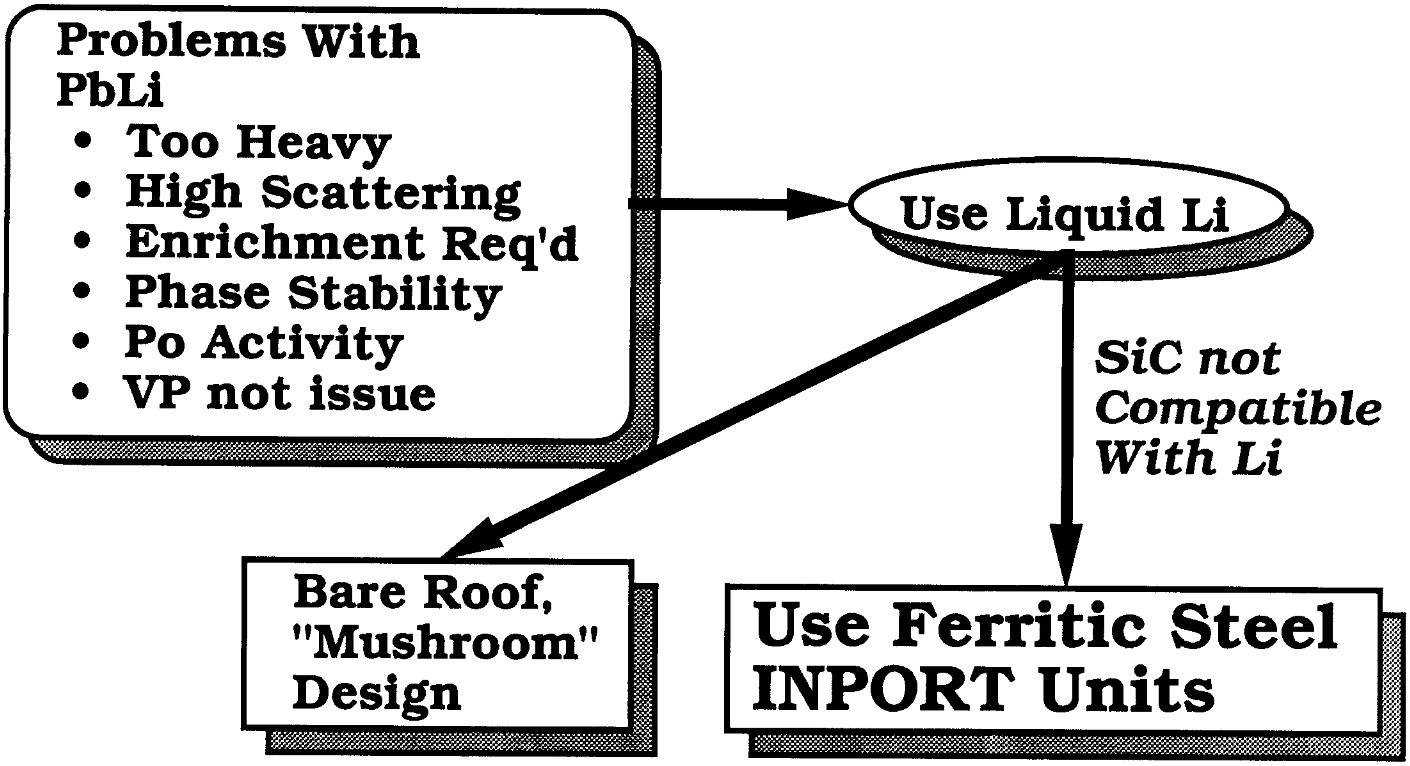

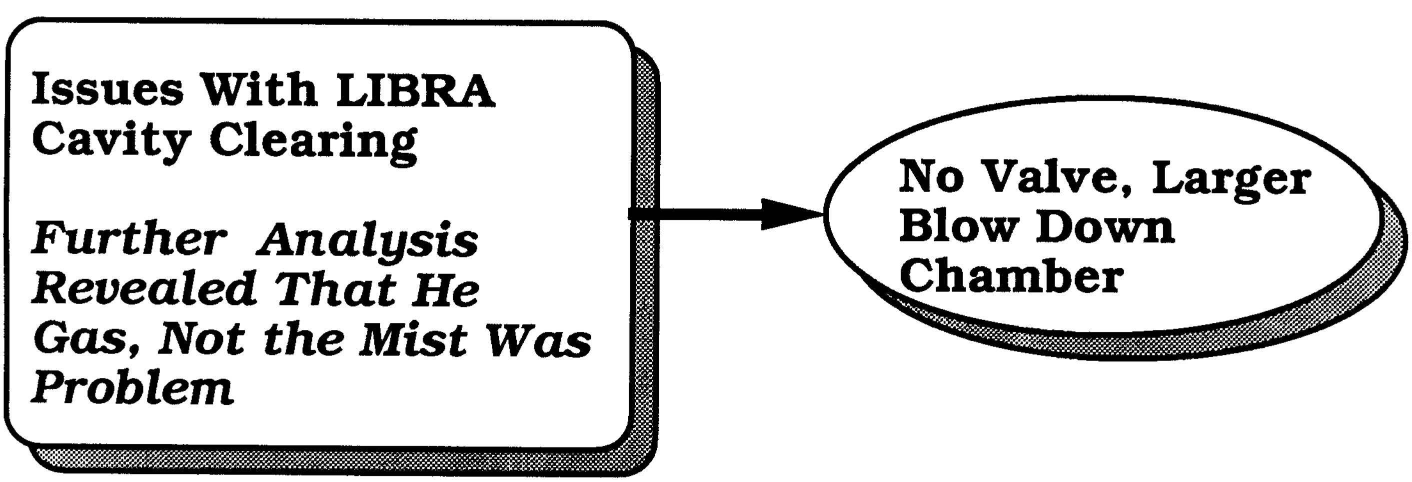

Comparison of Light Ion Beam Fusion Reactors Based on Channel Transport and Ballistic Focusing

General

	LIBRA	LIBRA -LiTE
Net Elec. Power -MWe	331	1284
Gross Elec. Power -MWe	441	1507
Thermal Power -MWt	1161	3377
Recir. Power Frac.	0.25	0.15
Driver Eff. -%	23.5	(23.5)
Driver Rep Rate -Hz	3	3
Target Gain	80	75
ηG	18.8	17.6
Dir. Cap Cost, 89$/kWe	2843	?????

Comparison of Light Ion Beam Fusion Reactors Based on Channel Transport and Ballistic Focussing

Target Performance	LIBRA	LIBRA -LiTE
DT Mass -mg	3.2	10
Input Energy -MJ	4	13.25
Yield -MJ	320	1000
X Ray Yield -MJ	67	197
Neutron Yield -MJ	217	680
Charged Part. Yield -MJ	28.5	102
Endoergic Loss -MJ	7	21
Neutron Multiplication	1.02	1.02

Comparison of Light Ion Beam Fusion Reactors Based on Channel Transport and Ballistic Focusing

Helia Pulsed Power	LIBRA	LIBRA -LiTE
Waterline Energy -MJ	11.1	36.9
# Cells/Module	26	28
Voltage/Cell, MV	1.15	1.07
Cell Diameter -m	2.9	4.06
Module Diameter -m	5.15	6.18
Module Length -m	14.14	20.16
PFL Output Voltage -MV	1.15	1.07
Impedence -Ω	3	????
Dielectric	Water	Water
Switch Type	Metglas Saturable Reactor	Metglas Satur'bl Reactor

Comparison of Light Ion Beam Fusion Reactors Based on Channel Transport and Ballistic Focusing

Target Performance	LIBRA	LIBRA -LiTE
DT Mass -mg	3.2	10
Input Energy -MJ	4	13.25
Yield -MJ	320	1000
X Ray Yield -MJ	67	197
Neutron Yield -MJ	217	680
Charged Part. Yield -MJ	28.5	102
Endoergic Loss -MJ	7	21
Neutron Multiplication	1.02	1.02

Comparison of Light Ion Beam Fusion Reactors Based on Channel Transport and Ballistic Focusing

Li Ion Beams	LIBRA	LIBRA -LiTE
Energy -MeV	25-35	25-35
Number, High Power	16	16
Low Power	2	2
Beam Energy -MJ	4	13.25
Peak Power on Target -TW	400	1325
Pulse Compression Ratio	5	4
Pulse Length on Target -ns	9	10
Current/Channel -MA	~~0.3~~ .83	~~0.51~~ 2.8
Current on Target -MA	~~1.1~~ 13.3	44
Ion Energy Transport	Channel	Ballistic

Comparison of Light Ion Beam Fusion Reactors Based on Channel Transport and Ballistic Focusing

	LIBRA	LIBRA -LiTE
Magnet Properties		
Closest Dist. To Targ. - m	3.3	2.05
Max Impulse To Magnet -Pa-s	< 125	185
Max n Wall Load MW/m^2	4.8	38
Max n damage/CY	18	199
B max - T	3.2	2.0
Max Current /magnet-MAT	0.06	0.41
• Magnet Length -m	2.9	0.3
° Mag. diam, id/od -m	0.2/0.34	0.26/0.46
Magnet Material	TZM	Liq. Li

Comparison of Light Ion Beam Fusion Reactors Based on Channel Transport and Ballistic Focusing

Cavity

	LIBRA	LIBRA -LiTE
Gas Pressure -Torr @STP	100 -He	1 -He
Radius to First surface -m	3	2.05
Pumping Time -ms	300	300
Vap. Liq. Met/Shot -kg	8 (PbLi)	8-(Li)
Chamber Radius -m	4.35	5.7
Max. Chamb. n Damage -dpa/FPY	6.67	6.67

Tritium Inventory and Location

Location	Tritium, g	
	LIBRA	LIBRA-LiTE
Target Fabrication Facility		
In-Process	134	225
In-Storage (1 day)	500	1560
Reactor Hall		
Fuel Targets (1 hr)	21	65
Breeder	0.4	100
Secondary Circuit	1.0	<1
Exhaust	1.3	4
INPORT Tubes	150	<0.1
Fuel Processing		
Purification	1.3	5
Isotope Separation	45	135
Storage Vault (Inactive)	2000	3000
Steam Generator Water	~0	<0.1
Total	2854	5100

Comparison of Light Ion Beam Fusion Reactors Based on Channel Transport and Ballistic Focusing

	LIBRA	LIBRA -LiTE
INPORT TUBES		
Radius to First INPORT -m	3.0	3.45
n Wall Load @ INPORT -MW/m2	5.8	13.6
Tube Material	SiC	Steel
1st Tube od - cm	3	5
Max. INPORT Length. -m	6.4	10
Max. Unsupported Length-m	6.4	5
Impulse to INPORT-Pa-s	125	153
Packing Frac -%	33	33
INPORT Sector Thick. -m	1.35	2.25
Coolant/Breeder	$Li_{17}Pb_{83}$	Li
Tin/Tout °C	340/500	350/500
Li -6 enrichment - %	90	Nat
Energy Multiplication	1.22	1.13
TBR	1.361	1.375

POWER FLOW DIAGRAM FOR LIBRA-LiTE

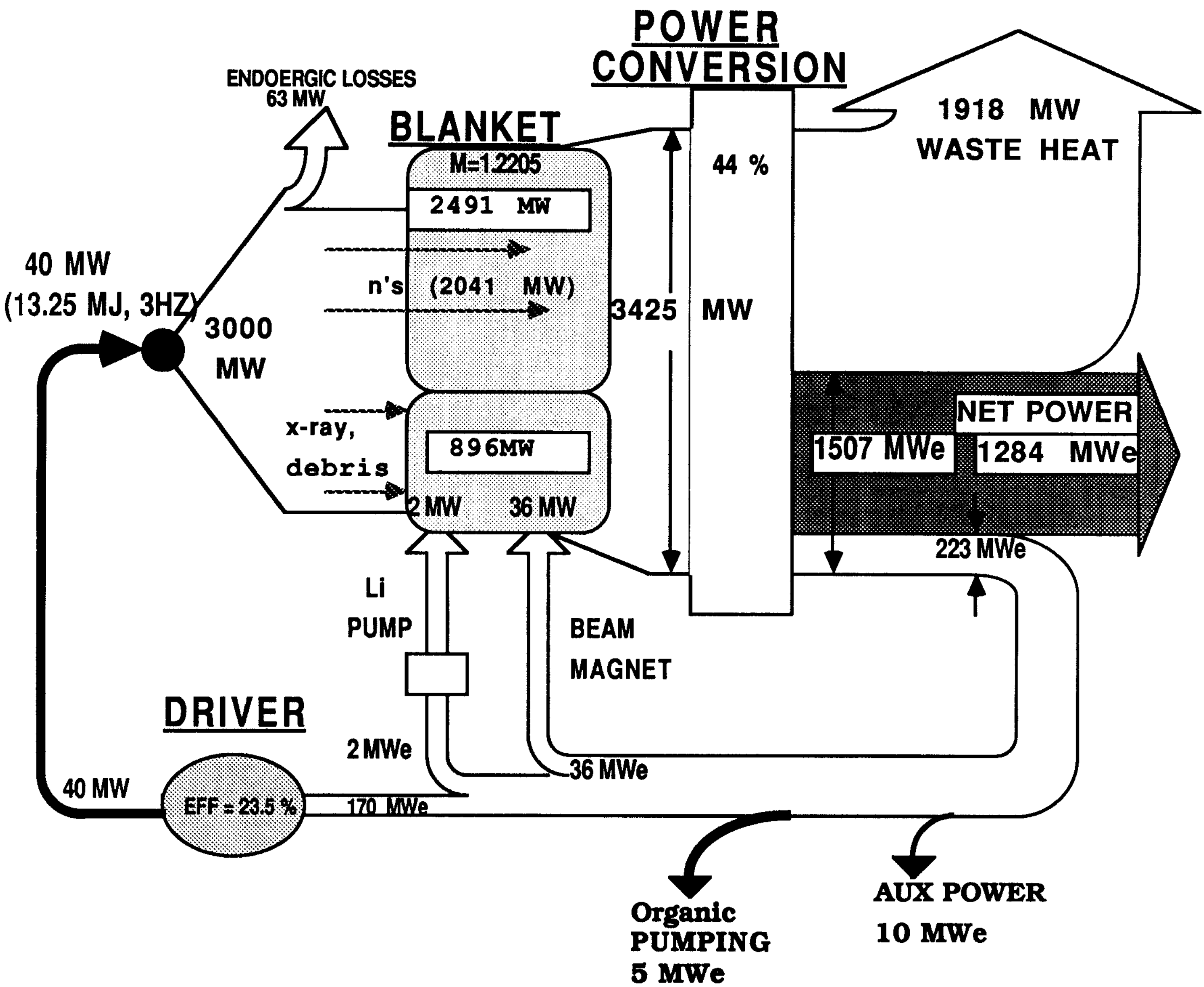

Main Differences Between LIBRA - LiTE and LIBRA

- **Ballistic Focusing**
- **Lens Magnets Close (2m) to Target**

- **1300 MWe vs 330 MWe**
- **13 MJ Driver vs 4 MJ**
- **Conservative Gain Assumptions 75 @ 13 MJ**

Main Differences Between LIBRA - LiTE and LIBRA

- Li Coolant and Breeder vs PbLi
- Steel Inport Units vs SiC
- "Dry", Full Life, Chamber Roof vs "Porous"
- Organic Coolant Secondary vs Helium

LIGHT ION BEAM TRANSPORT IN LIBRA-LiTE

Robert R. Peterson
Layton J. Wittenberg

University of Wisconsin - Madison
and Fusion Power Associates

presented at the LIBRA-LiTE Review
Kernforschungszentrum Karlsruhe
Karlsruhe, Germany

December 17, 1990

LIBRA-LiTE Uses Ballistic Ion Transport

- Ions are transported from diodes through drift tubes to magnetic lenses.
- Achromatic magnetic lenses focus the drifting ion beams.
- The focal spot size is a function of the initial microdivergence, the scattering of the ion beam by the background gas, and the focal length.
- The ions are time-of-flight bunched by ramping of the diode voltage.
- The background gas provides electrons for charge and current neutralization.
- The ion beam heats the gas and increases the plasma conductivity high enough (10^{14} s^{-1}) to avoid the filamentation instability.

Schematic of Ballistic Transport Concept

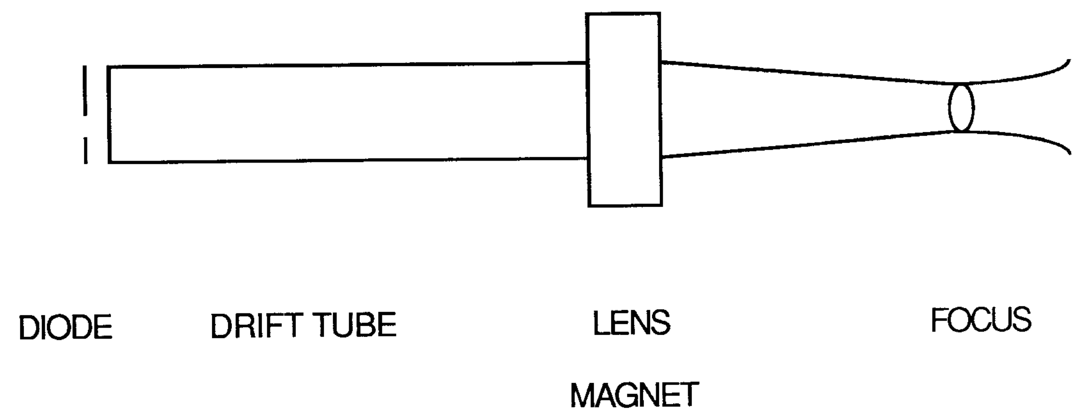

The Driver Energy is a Function of the Ion Beam Spot Size

- Assume that the LIBRA-LiTE target requires conditions similar to the LIBRA target to ignite.

  ▷ Total ion energy fluence on the target surface = 1.27 MJ/cm^2

  ▷ Peak ion power density on the target surface = 127 TW/cm^2

- The LIBRA target is smaller than the ion beam focal spot in LIBRA-LiTE, so more driver energy is required to obtain these conditions.

Choices of Target Size

- The larger focal spot and driver energy allows flexibility of target size and yield.
  - ▷ LIBRA target could be used but it would have a low effective gain because much of the beam would miss the target.
  - ▷ A larger and higher yield target could intercept more of the ion beam and would have a higher effective yield, but this will lead to a larger blast.

The SCATBALL Ballistic Transport Code

- Current density profiles
  - ▷ analytic calculation of ion beam bunching, scattering, and focusing
  - ▷ assume electron return current density equals ion current density.
- Heating of fill gas
  - ▷ modified "Mehlhorn" ion beam energy deposition
  - ▷ ohmic heating by return current
  - ▷ Saha equation-of-State (Coronal and other more complete models available)

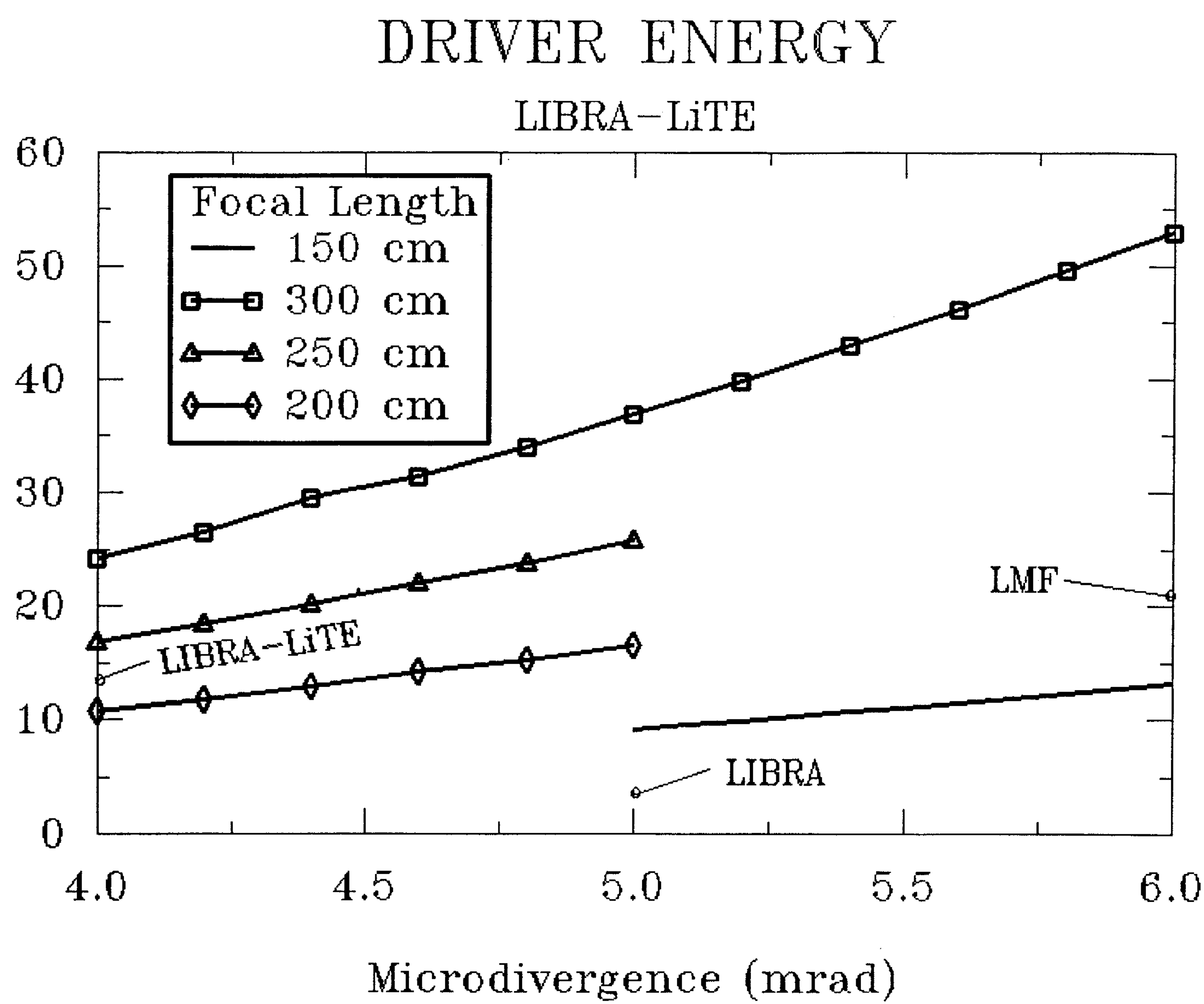
DRIVER ENERGY
LIBRA-LiTE
Focal Length
150 cm
300 cm
250 cm
200 cm
LIBRA-LiTE
LMF
LIBRA
0
10
20
30
40
50
60
4.0
4.5
5.0
5.5
6.0
Microdivergence (mrad)

Drift Tube Length Has Little Effect

- SCATBALL calculations for a magnetic lens centered 220 cm from the target.

- Ion Beam Outer Radius (cm)

θ_μ	4.0 mrad	3.5 mrad
Target-Diode Distance		
6.0 m	11.82	11.62
7.0 m	12.23	12.00

- Driver Energy (MJ)

θ_μ	4.0 mrad	3.5 mrad
Target-Diode Distance		
6.0 m	13.10	10.21
7.0 m	13.25	10.34

Main Pulse Beam Transport Parameters

	LIBRA-LiTE	LMF
Anode Area	278 cm^2	600 cm^2
Focal Length	220 cm	150 cm
Drift Length	480 cm	250 cm
Fill Gas	Helium	Helium
Gas Density	1 Torr	1 Torr
Beam Ion Energy	30 MeV	30 MeV
Diode Pulse Width	40 ns	40 ns
Bunching	4.0	2.67
Micro Divergence	4 mrad	6 mrad
Anode Current Density	2.5 KA/cm^2	2 KA/cm^2
Anode Power Density	74.5 GW/cm^2	60 GW/cm^2
Power per Anode	20.7 TW	36 TW
Energy per Anode	0.828 MJ	1.44 MJ
Ions per Pulse	1.7×10^{17}	3.0×10^{17}
Beam Density	5.40×10^{12} cm^{-3}	4.35×10^{12} cm^{-3}
Z for Neutralization	1.52×10^{-4}	1.23×10^{-4}

Changes in Beam Parameters From LIBRA

	LIBRA-LiTE	LIBRA
Anode Area	278 cm^2	79 cm^2
Focal Length	220 cm	75 cm
Drift Length	480 cm	0 cm
Fill Gas	Helium	Helium
Gas Density	1 Torr	100 Torr
Beam Ion Energy	30 MeV	30 MeV
Diode Pulse Width	40 ns	39 ns
Bunching	4.0	4.0
Micro Divergence	4 mrad	5 mrad
Anode Current Density	2.5 KA/cm^2	3.9 KA/cm^2
Anode Power Density	74.5 GW/cm^2	116 GW/cm^2
Power per Anode	20.7 TW	9.23 TW
Energy per Anode	0.828 MJ	.36 MJ
Ions per Pulse	1.7×10^{17}	5.13×10^{16}
Beam Density	5.40×10^{12} cm^{-3}	1.67×10^{12} cm^{-3}
Z for Neutralization	1.52×10^{-4}	4.71×10^{-7}

LIBRA-LiTE Diode Concept

- Diode Requirements:

microdivergence:	3.5 - 6.0 mrad
current density:	2 - 5 kA/cm^2
purity:	90%
ion production η:	80%
repetition rate:	3 - 6 Hz

- Ion Source Options:

solid LiF:	best to date, low rep rate
Liquid Li EHD:	high rep rate, still untested on PBFA-II
magnetically shaped anode plasma:	high rep rate, expts. at Cornell

- Discussions with Cook and Stinnett (SNL): go with EHD.

LIBRA-LiTE Diode Parameters

	Main	Pre-Pulse
Energy on Target(MJ)	11.92	1.33
# of Beams	16	2
Transport η (%)	90	90
Energy per Beam on Target (kJ)	745	665
Energy per Beam at Diode (kJ)	828	739
Pulse Width at Diode (ns)	40	40
Ave. Power per Diode (TW)	20.7	18.5
Ion Energy (MeV)	26 - 32	30
Ion Current per Beam (MA)	0.69	0.62
Peak Current Density at Diode (kA/cm^2)	2.5	2.6
Anode Area per Diode (cm^2)	278	235
Physical Diode Gap (cm)	3.39	3.33
Dynamic Diode Gap (cm)	2.75	2.69
Diode Anode Outer Radius (cm)	10.26	9.16
Diode Anode Inner Radius (cm)	4.12	3.02
Critical Magnetic Field (T)	2.46	2.50
Applied Magnetic Field (T)	4.92	5.00

GAS BREAKDOWN PROCESSES

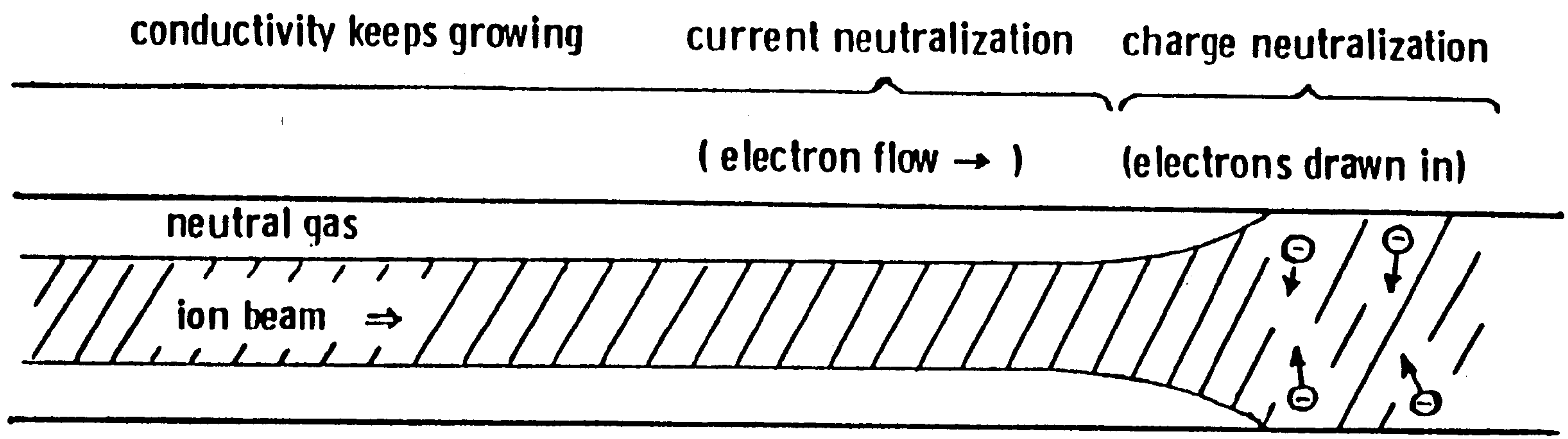

$$\frac{\partial n_e(t)}{\partial t} = \frac{n_b(t)}{\tau_i}$$

ion impact ionization

single particle effect
continues through whole pulse

$$\frac{\partial n_e(t)}{\partial t} = \frac{n_e(t)}{\tau_e}$$

electron avalanche

fed by collective fields
of whole beam

ohmic heating

continues to heat plasma

$$\frac{\mathcal{P}}{\pi R^2 L} = \frac{E^2}{\sigma}$$

Beam Current Density Profiles in LIBRA-LiTE

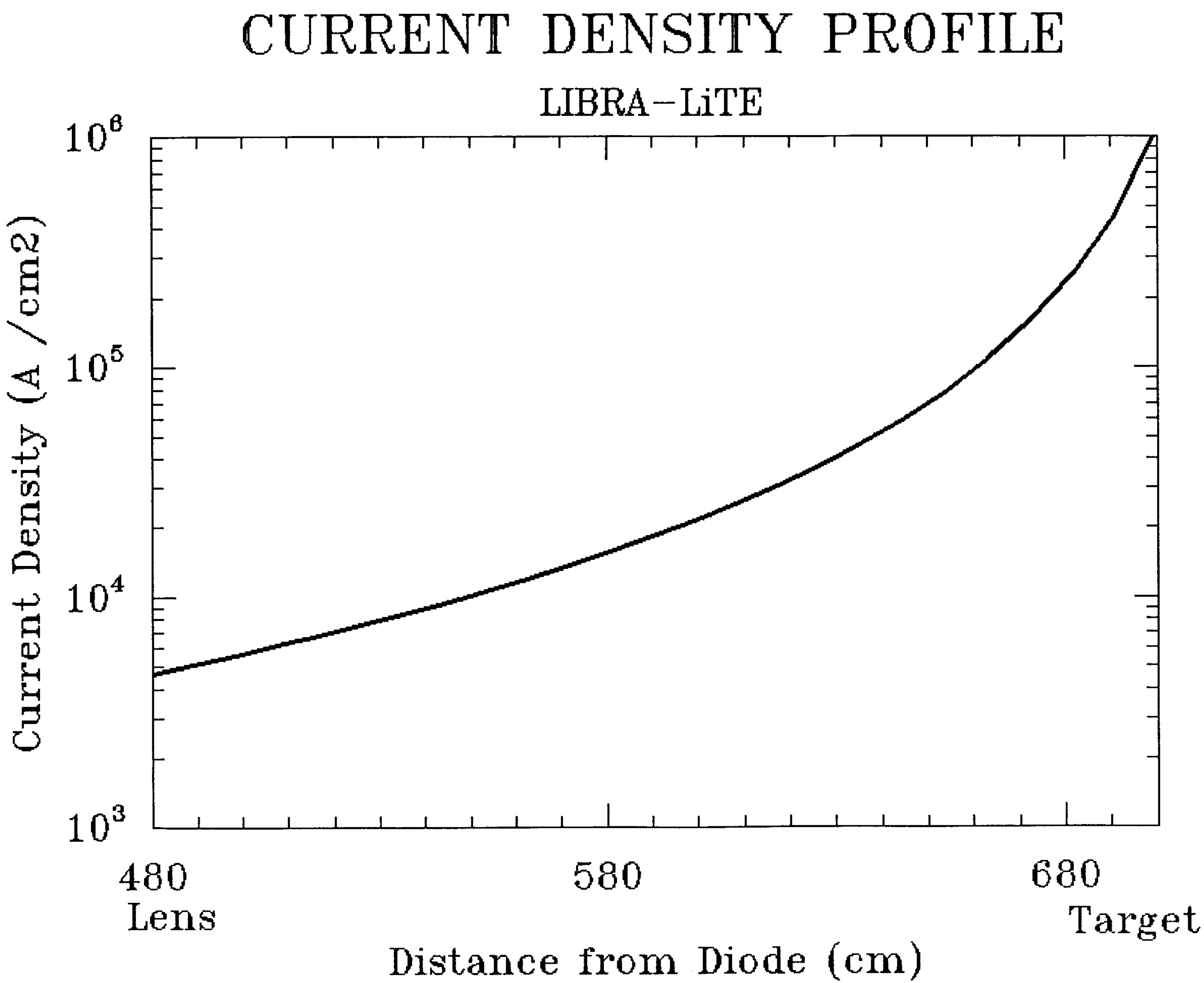

Temperature and Energy Density Profiles

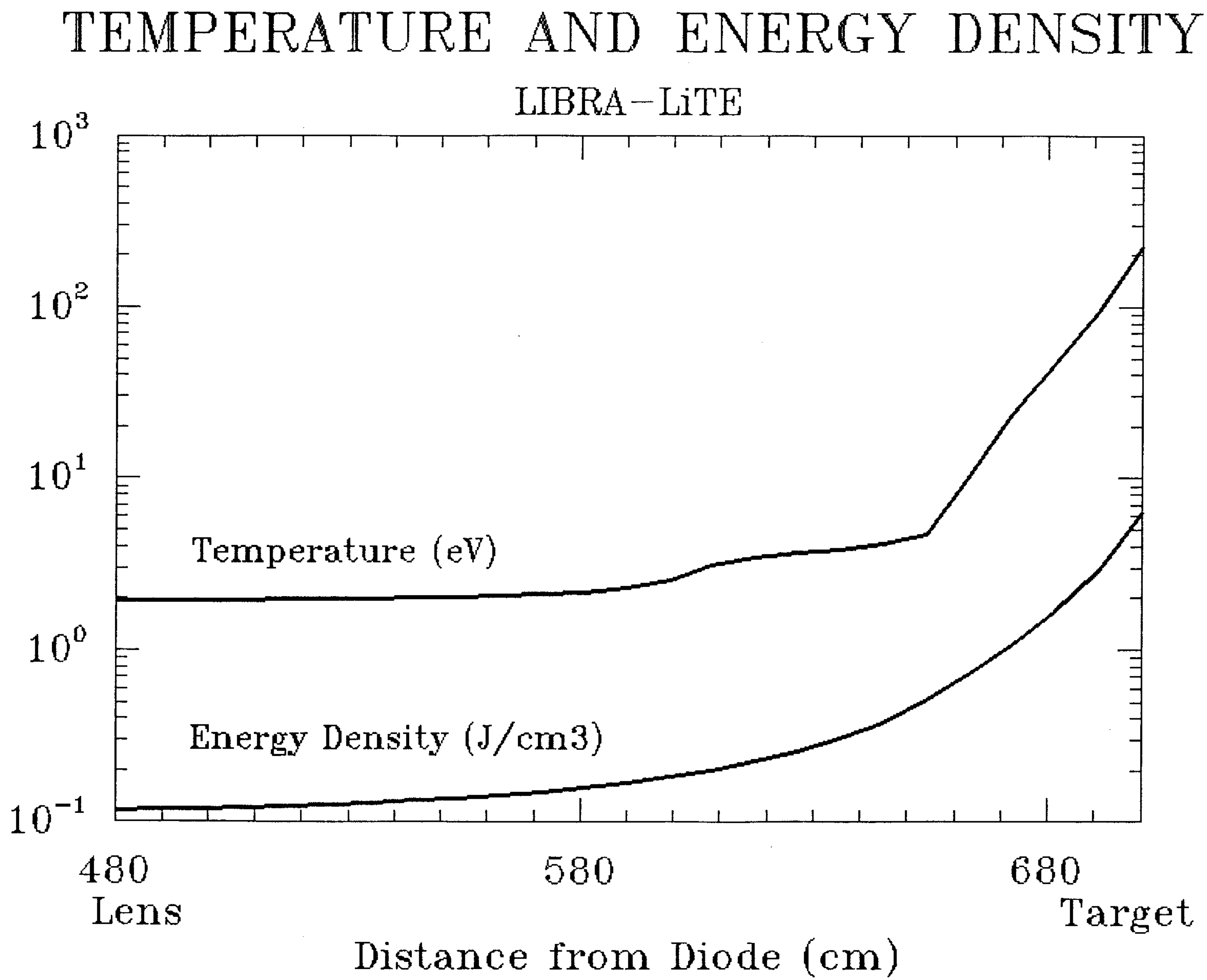

Charge State and Conductivity Profiles

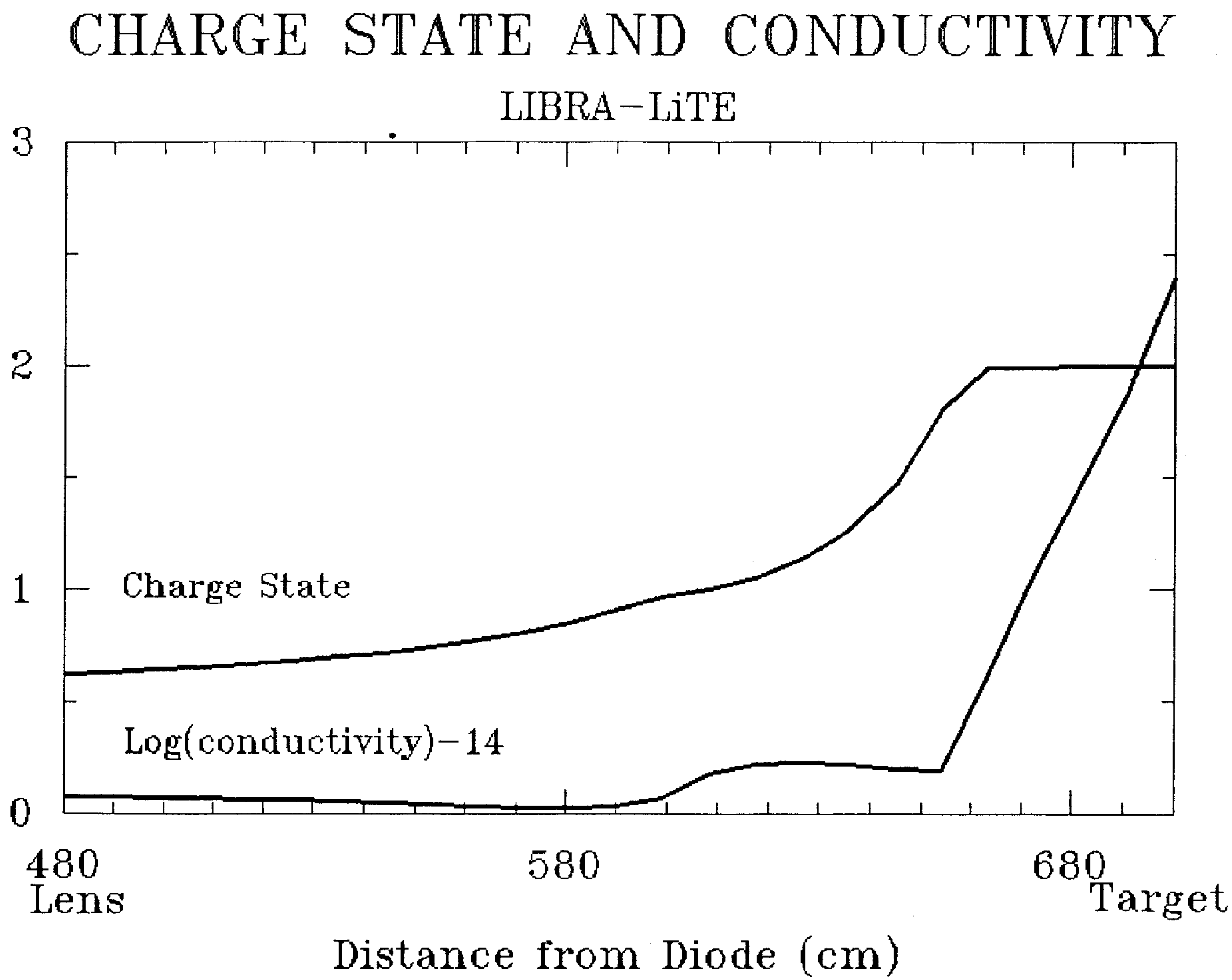

Final Focus Lens

- Intense neutron flux close to the target causes large nuclear heating and high radiation damage.

- Utilize a single-turn solenoid magnet fabricated from a ferritic steel shell containing flowing liquid lithium.

- The liquid lithium serves as the electrical conductor and the heat transfer fluid.

- The circulating lithium removes the nuclear heating and avoids the radiation damage to a metallic conductor and a ceramic insulator.

- The heat generated by the electrical conductance and the neutronic interactions is retained in the heat transfer fluid and recirculated to the electrical power system.

- The lifetime of the magnet is determined by the radiation damage to the steel shell.

FINAL FOCUS LENS

SINGLE-TURN SOLENOID MAGNET, FERRITIC STEEL CASE FILLED WITH LIQUID LITHIUM

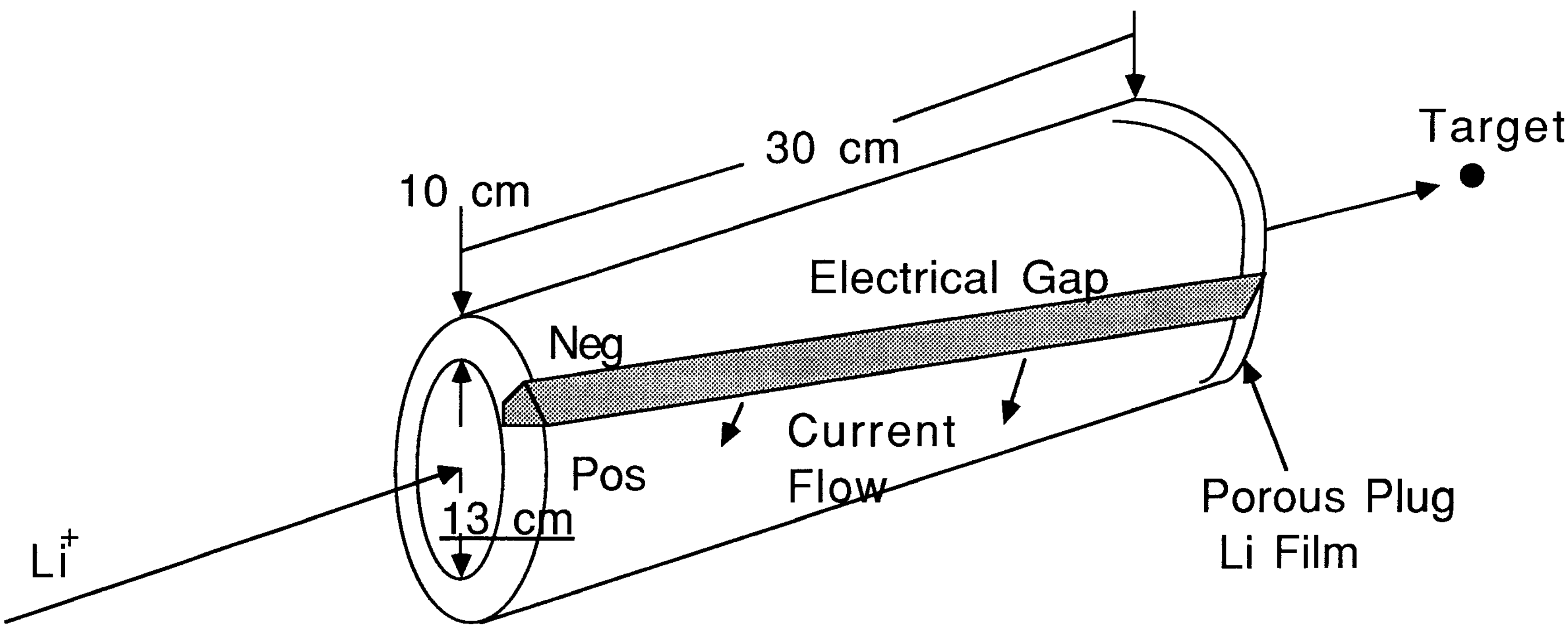

LIQUID LITHIUM CAN NOT FLOW ACROSS THE GAP BUT REVERSES FLOW AND EXITS AT THE INLET SIDE

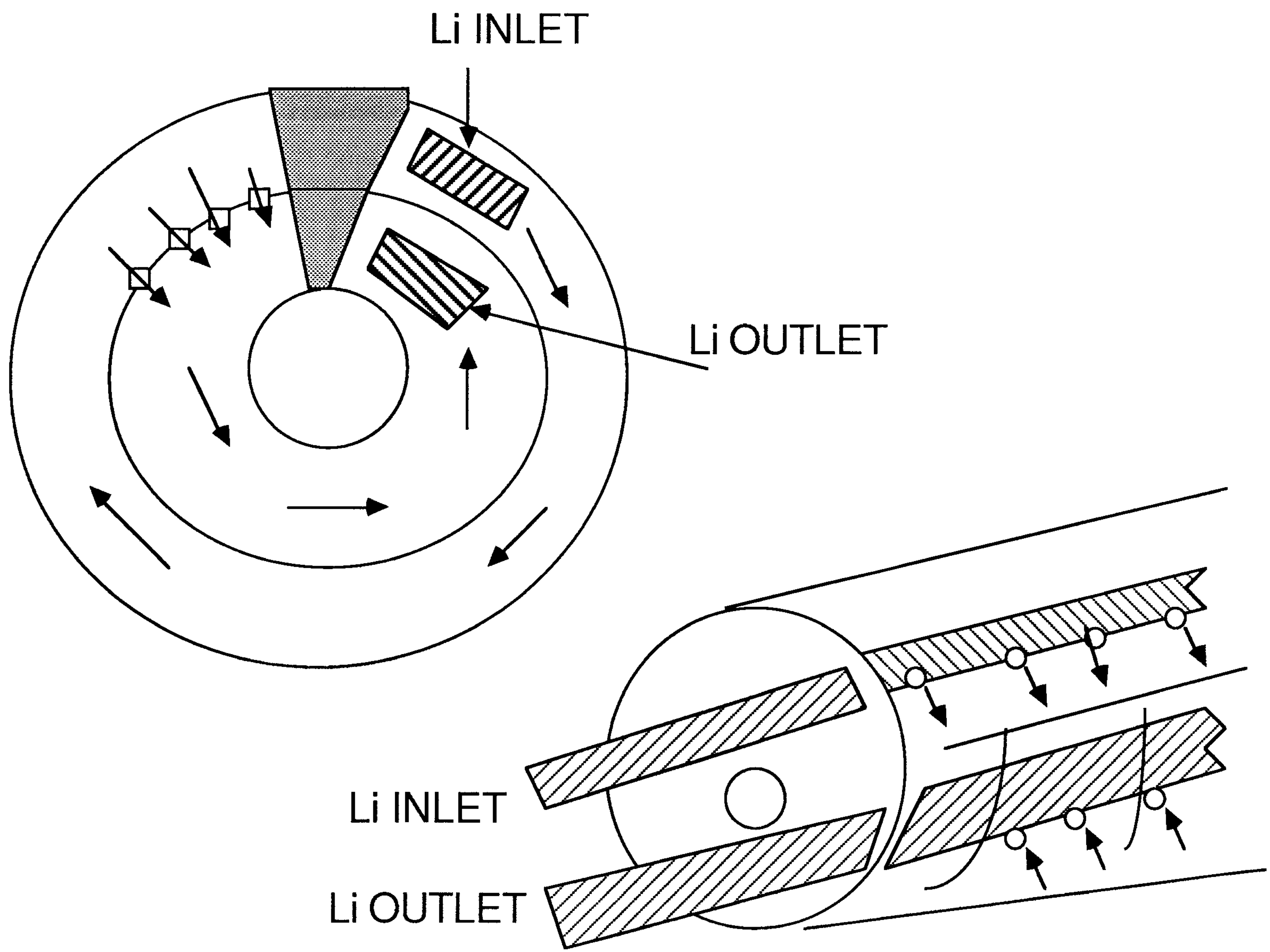

Final Focus Lens – Parameter List

Magnetic Field, T	2
Radius, OD, m	0.23
Radius, ID, m	0.13
Length, m	0.30
Current, MA	0.41
Current Flux, MA/m^2	15.0
EMF, V	4.83
Power, MW/coil	2.0
MW/18 coils	36.0
Lithium Flow Rate, kg/s	7.7
Lithium Velocity, m/s	1.1
Lithium Mass, kg/coil	17.0
Nuclear Heating (Li+Fe), MW	6.85
Resistive Heating, MW	2.0
Li Temperature Rise, K	250
LOFA Response Time, s	7

Final Focus Lens – Parameter List (contd.)

MHD Pressure	
Poloidal, MPa	1.1
Entrance+Exit, MPa	3.7
Total, MPa	4.8
MHD Pumping Power, MW/18 coils	1.3
Steel Container Wall Thickness, mm	2.5
Membrane Stress, MPa	130
Useful Radiation Lifetime, CY	1

Conclusions

- **Ballistic transport of ion beams, though more efficient than channel transport, leads to low required microdivergence (θ_μ) and large focal spot sizes.**

- **Large focal spots require large driver energies and, therefore, large yields to obtain high ηG.**

- **Diodes can be designed that are similar to the LIBRA diodes, but which have higher energy per diode.**

- **Conductivities of the order of 1×10^{14} s^{-1} are achievable throughout the ion beam transport by ion beam and return current heating of the background gas.**

- **Neutron damage to lens magnets has led to a novel magnet design using liquid lithium as a conductor.**

LIBRA-LiTE Chamber Description

I.N. Sviatoslavsky, M.E. Sawan, G.L. Kulcinski,
E.A. Mogahed, G.I. Sviatoslavsky

Fusion Power Associates
and
Fusion Technology Institute
University of Wisconsin
Madison, Wisconsin, USA

LIBRA-LiTE Review Meeting
17 December 1990
Karlsruhe, Germany

Topics Covered

- Overall Reactor Description
- Chamber Description
- Neutronics Analysis
- Thermal Hydraulics
- Chamber Evacuation

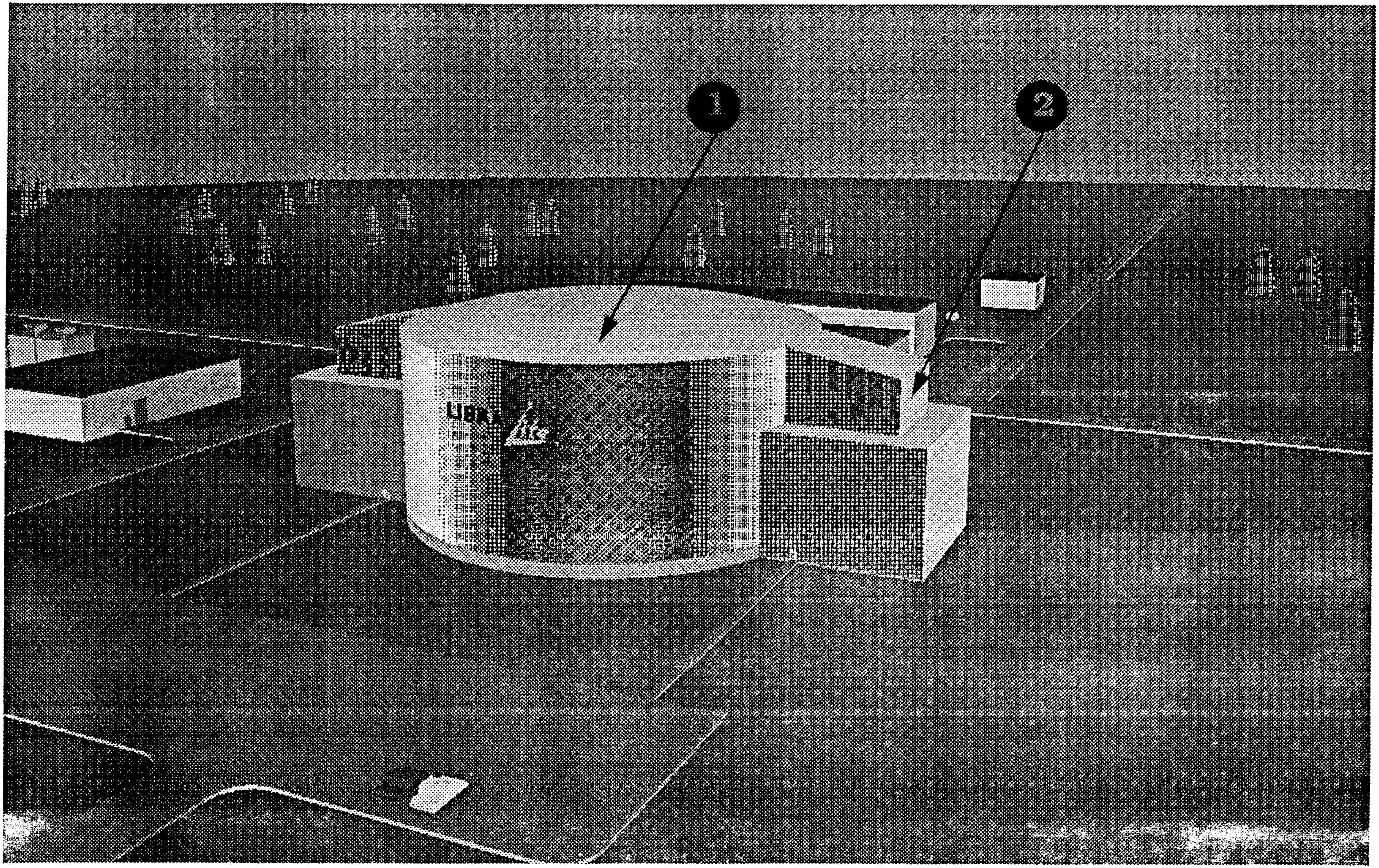

Overall View of LIBRA-LITE Power Plant

(1) Reactor containment building

(2) Hot cells, one on each side of containment building

Overall View of LIBRA-LiTE Power Plant

(1) Reactor containment building

(2) Hot cells, one on each side of containment building

Overall View of Containment Building with Translucent Walls

(1) Hot cell

(2) Viewing windows

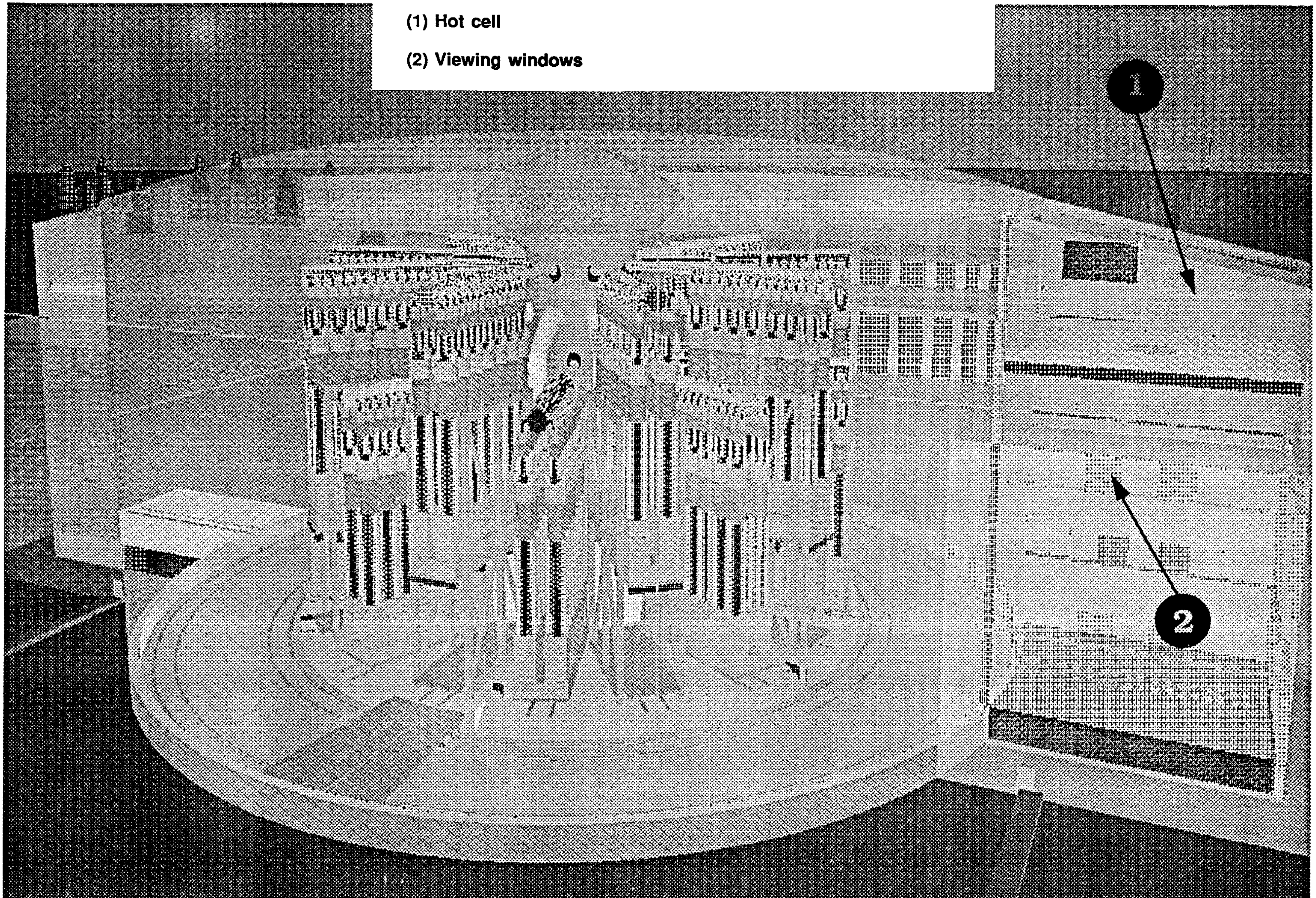

Overall View of Containment Building with Translucent Walls

(1) Hot cell

(2) Viewing windows

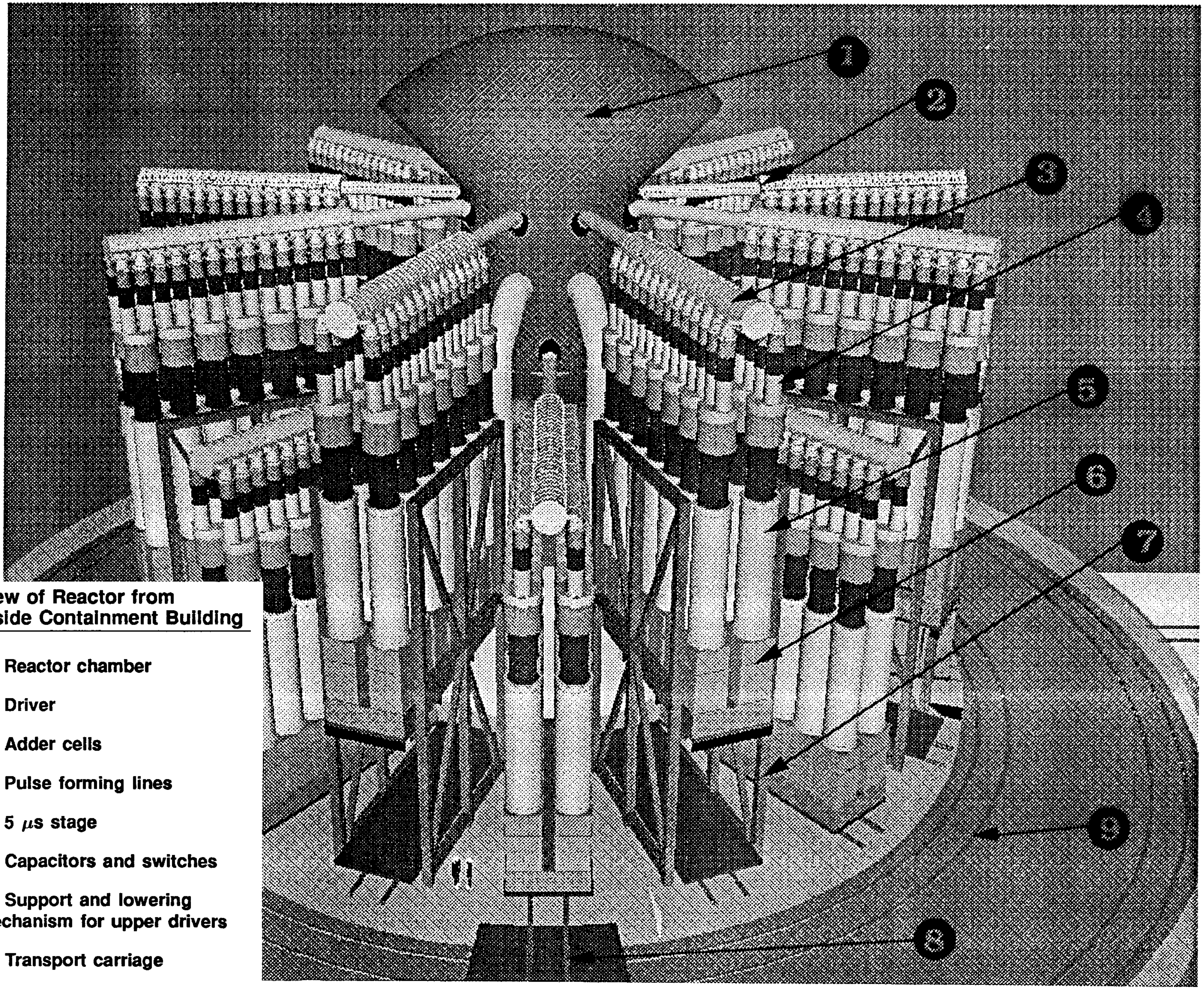

View of Reactor from Inside Containment Building

(1) Reactor chamber

(2) Driver

(3) Adder cells

(4) Pulse forming lines

(5) 5 μs stage

(6) Capacitors and switches

(7) Support and lowering mechanism for upper drivers

(8) Transport carriage

(9) Circumferential rails

View of Reactor from Inside Containment Building

(1) Reactor chamber

(2) Driver

(3) Adder cells

(4) Pulse forming lines

(5) 5 μs stage

(6) Capacitors and switches

(7) Support and lowering mechanism for upper drivers

(8) Transport carriage

(9) Circumferential rails

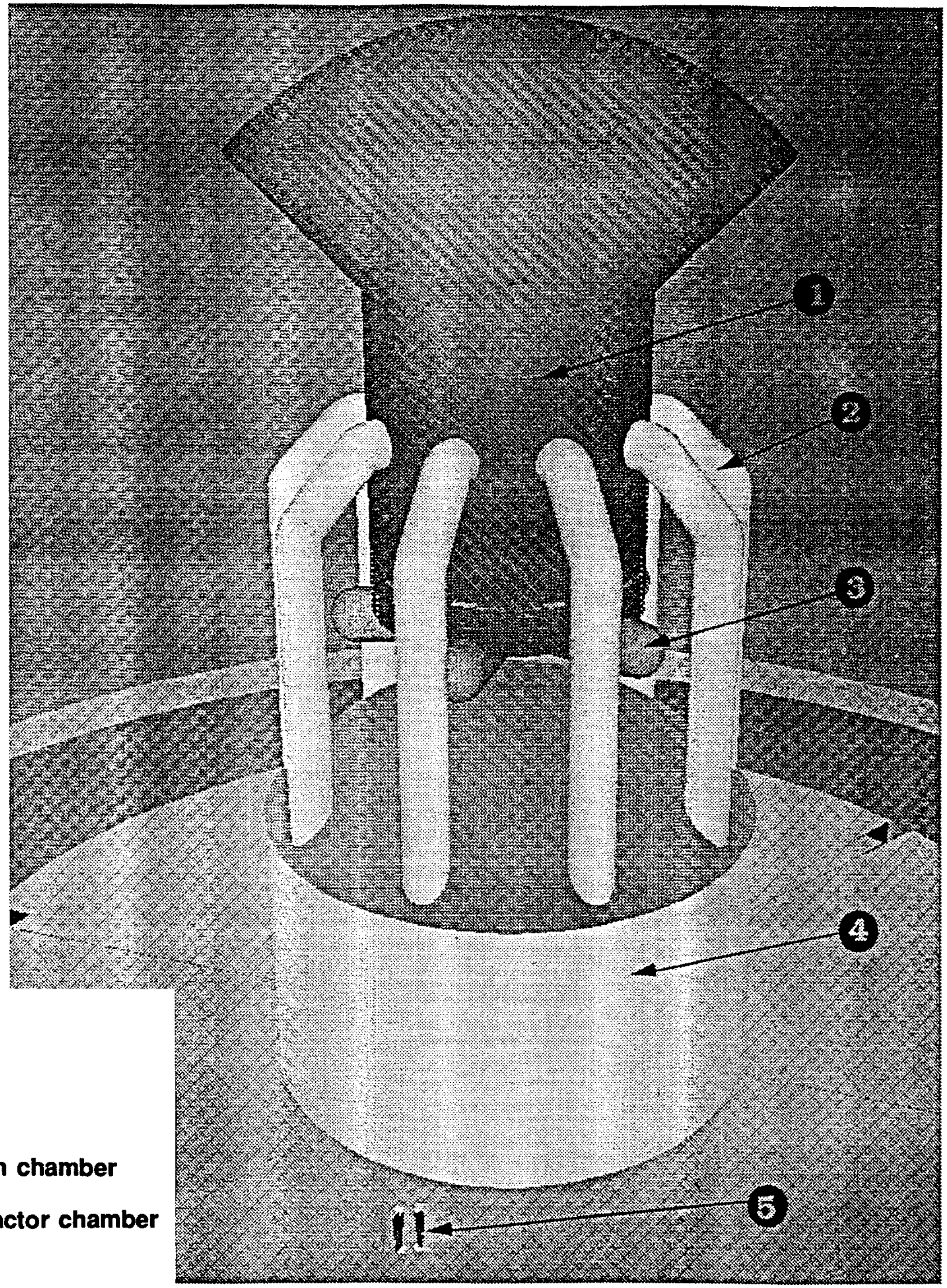

External View of Reactor Chamber and Expansion Chamber

(1) Reactor chamber

(2) Vacuum lines leading to expansion chamber

(3) Heat exchangers (5) in base of reactor chamber

(4) Expansion chamber

(5) 2 m men

External View of Reactor Chamber and Expansion Chamber

(1) Reactor chamber

(2) Vacuum lines leading to expansion chamber

(3) Heat exchangers (5) in base of reactor chamber

(4) Expansion chamber

(5) 2 m men

Top View of Reactor Within Containment Building

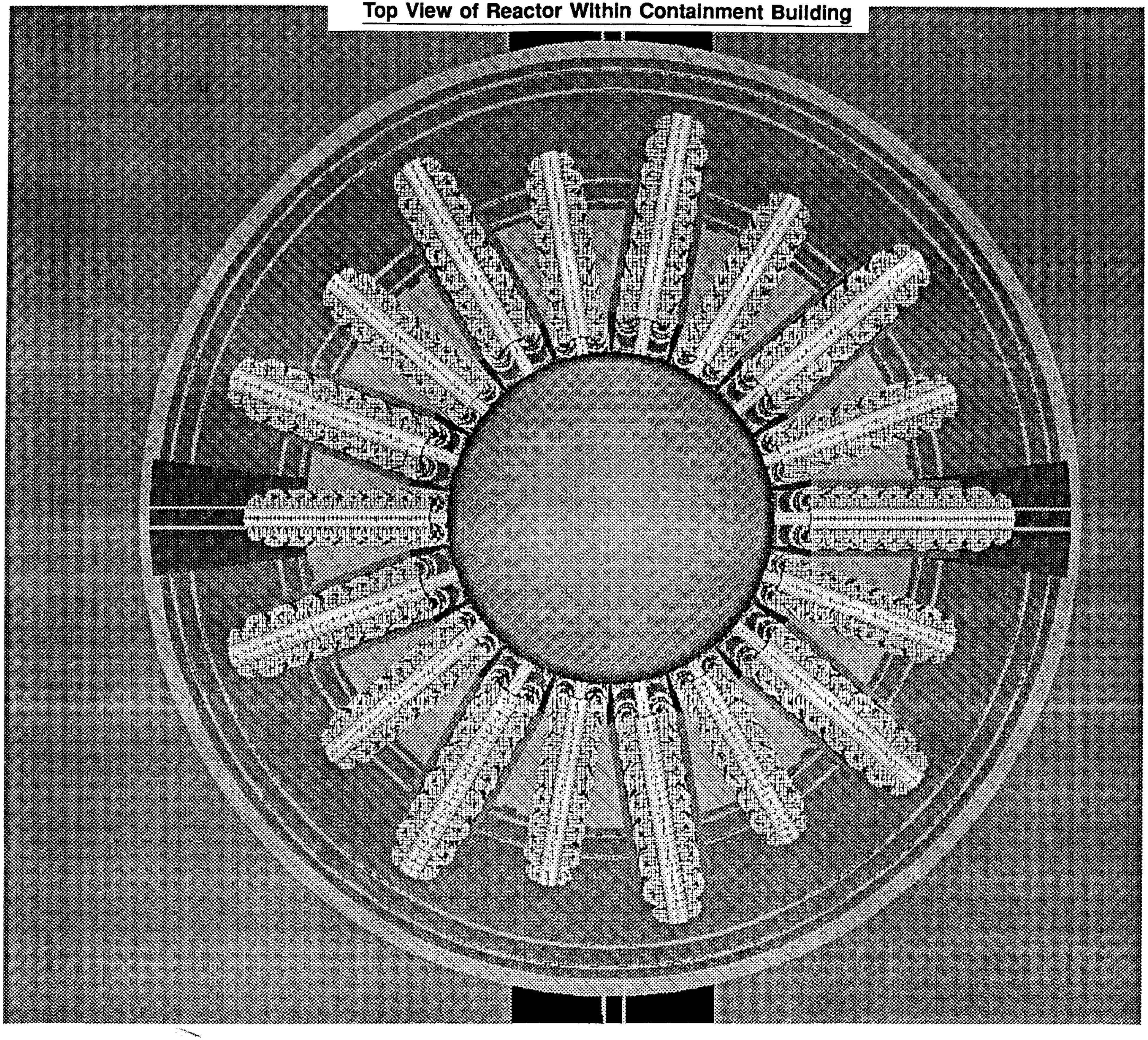

Top View of Reactor Within Containment Building

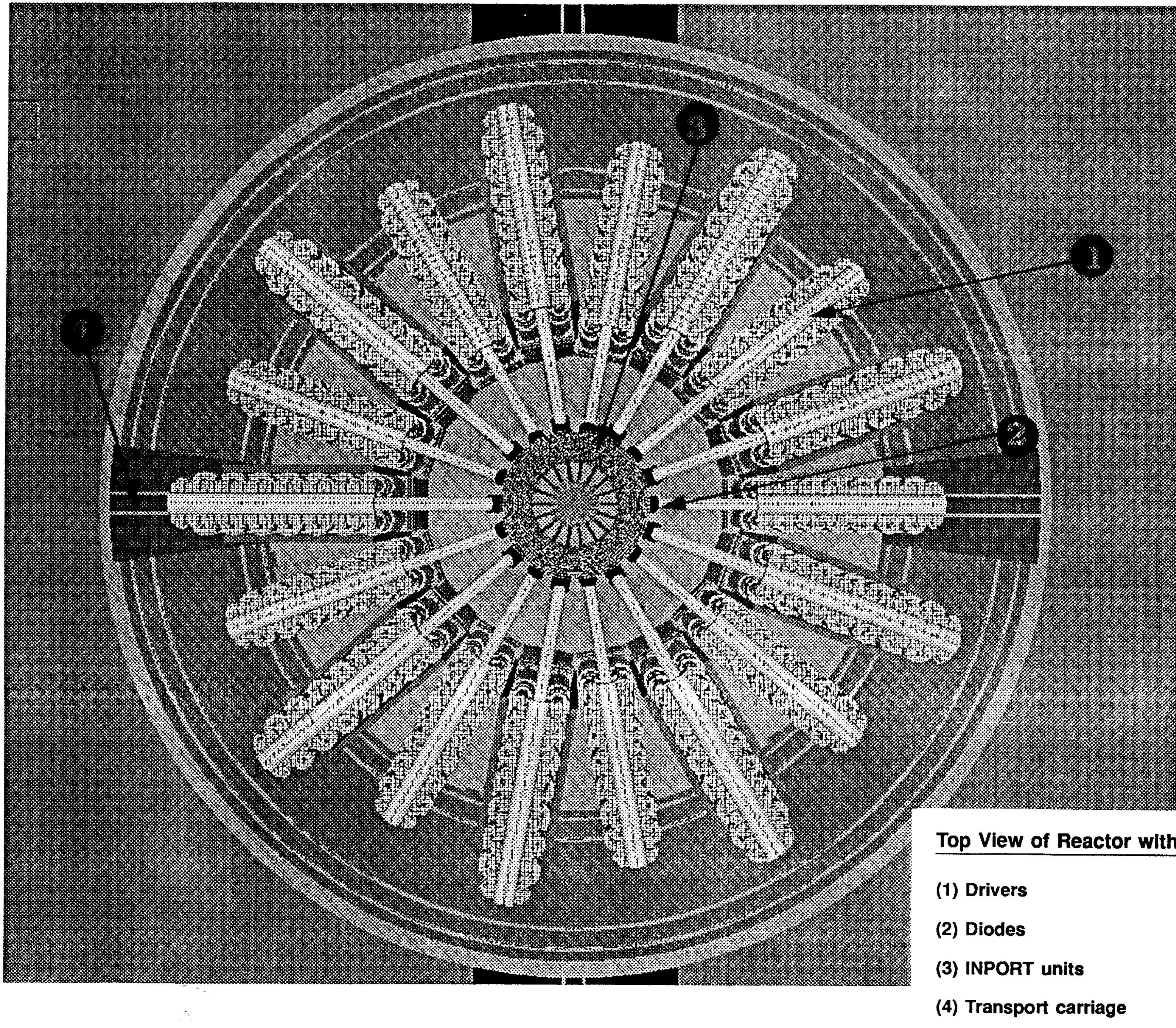

Top View of Reactor with Roof Removed

(1) Drivers

(2) Diodes

(3) INPORT units

(4) Transport carriage

Top View of Reactor with Roof Removed

(1) Drivers

(2) Diodes

(3) INPORT units

(4) Transport carriage

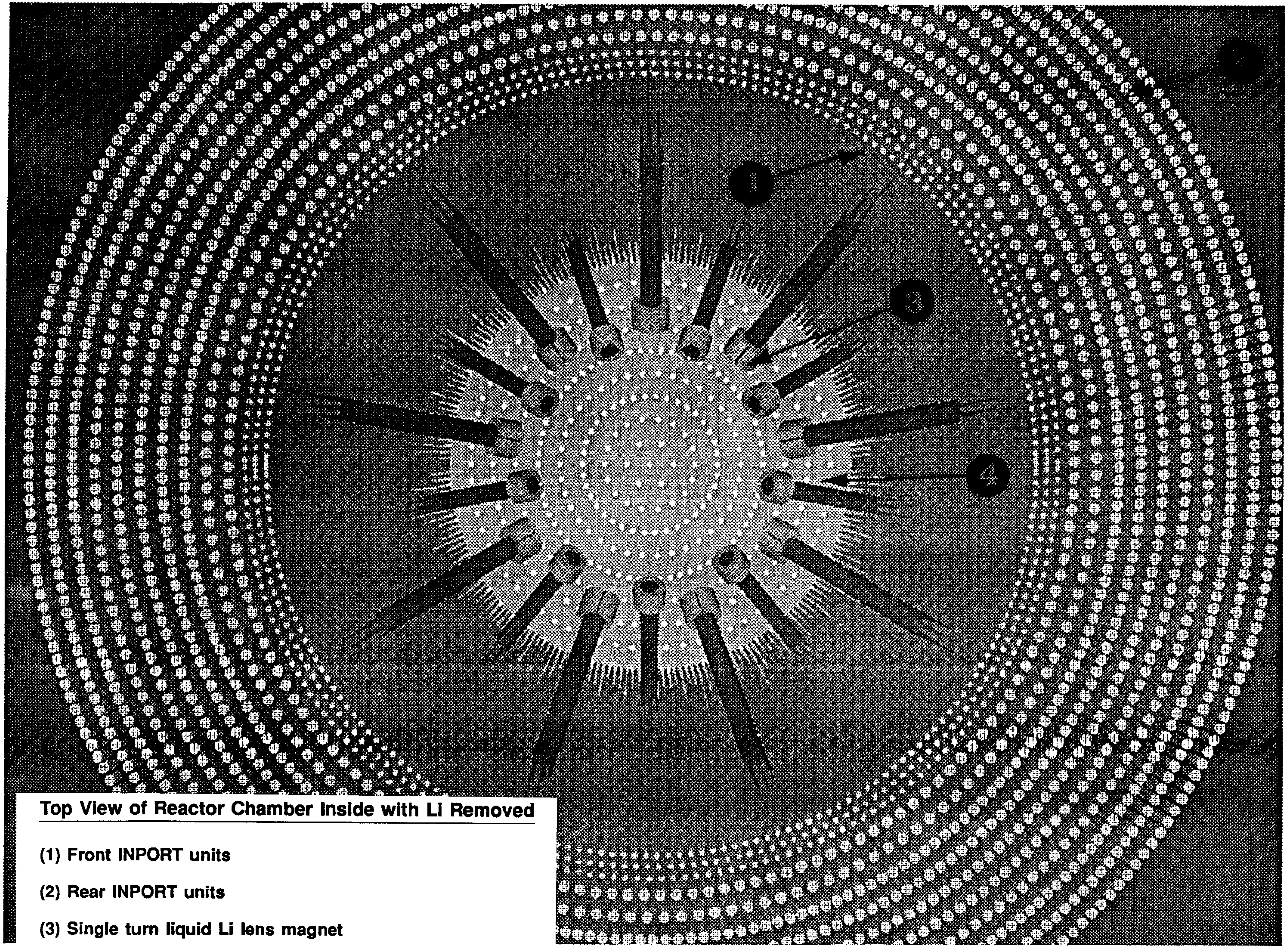

<u>Top View of Reactor Chamber Inside with Li Removed</u>

(1) Front INPORT units

(2) Rear INPORT units

(3) Single turn liquid Li lens magnet

(4) Perforated bottom plate

Top View of Reactor Chamber Inside with Li Removed

(1) Front INPORT units

(2) Rear INPORT units

(3) Single turn liquid Li lens magnet

(4) Perforated bottom plate

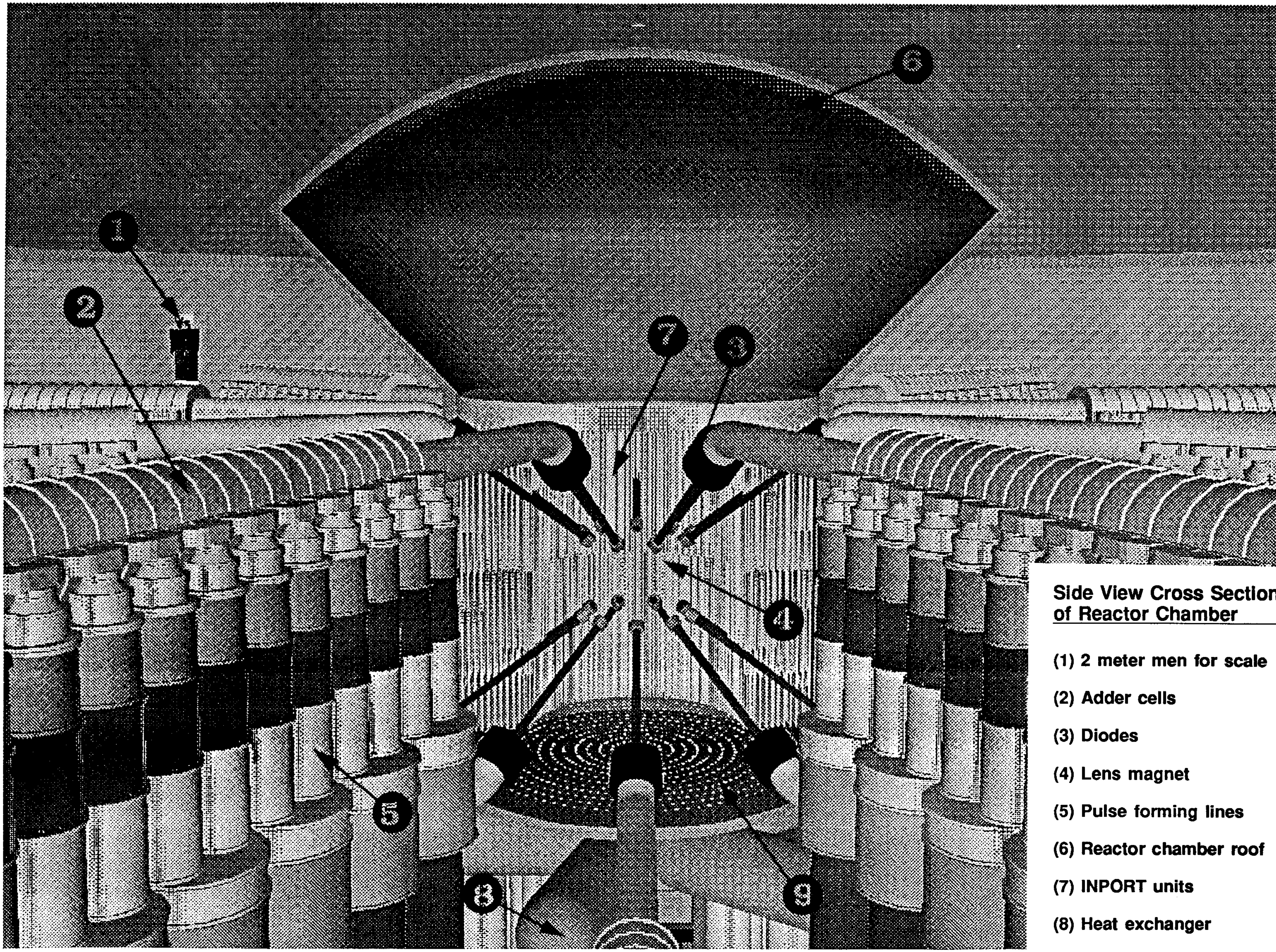

Side View Cross Section of Reactor Chamber

(1) 2 meter men for scale

(2) Adder cells

(3) Diodes

(4) Lens magnet

(5) Pulse forming lines

(6) Reactor chamber roof

(7) INPORT units

(8) Heat exchanger

(9) Perforated bottom plate

Side View Cross Section of Reactor Chamber

(1) 2 meter men for scale

(2) Adder cells

(3) Diodes

(4) Lens magnet

(5) Pulse forming lines

(6) Reactor chamber roof

(7) INPORT units

(8) Heat exchanger

(9) Perforated bottom plate

Special Features of Chamber

- Ferritic steel (HT-9) INPORT units
- Single turn liquid Li lens magnets
- Roof designed as a lifetime component
- Expansion chamber is used to help evacuate reactor chamber
- Lens magnets replaced every calendar year
- INPORT units replaced every two FPY

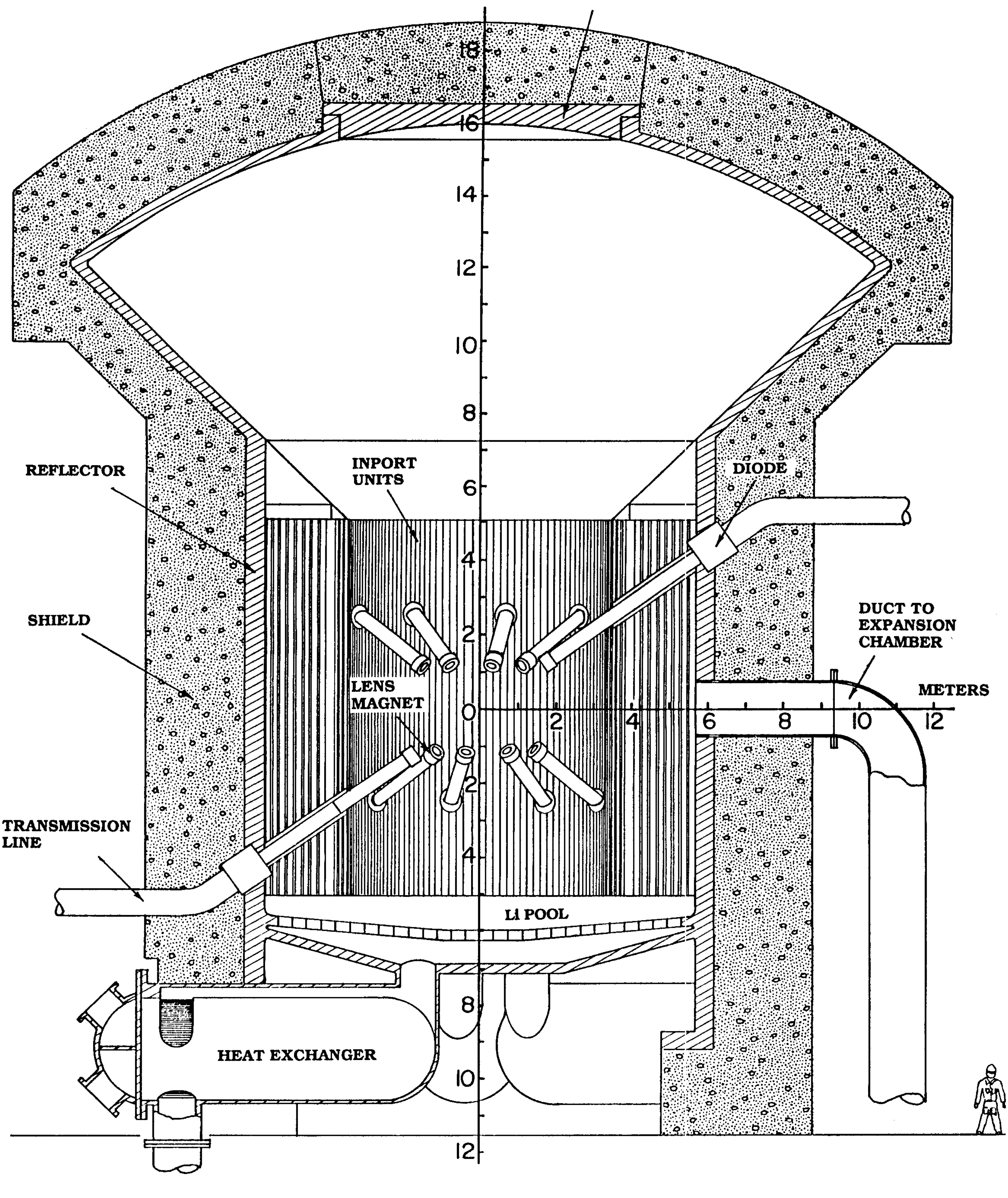

CROSS SECTION OF LIBRA LiTE CHAMBER

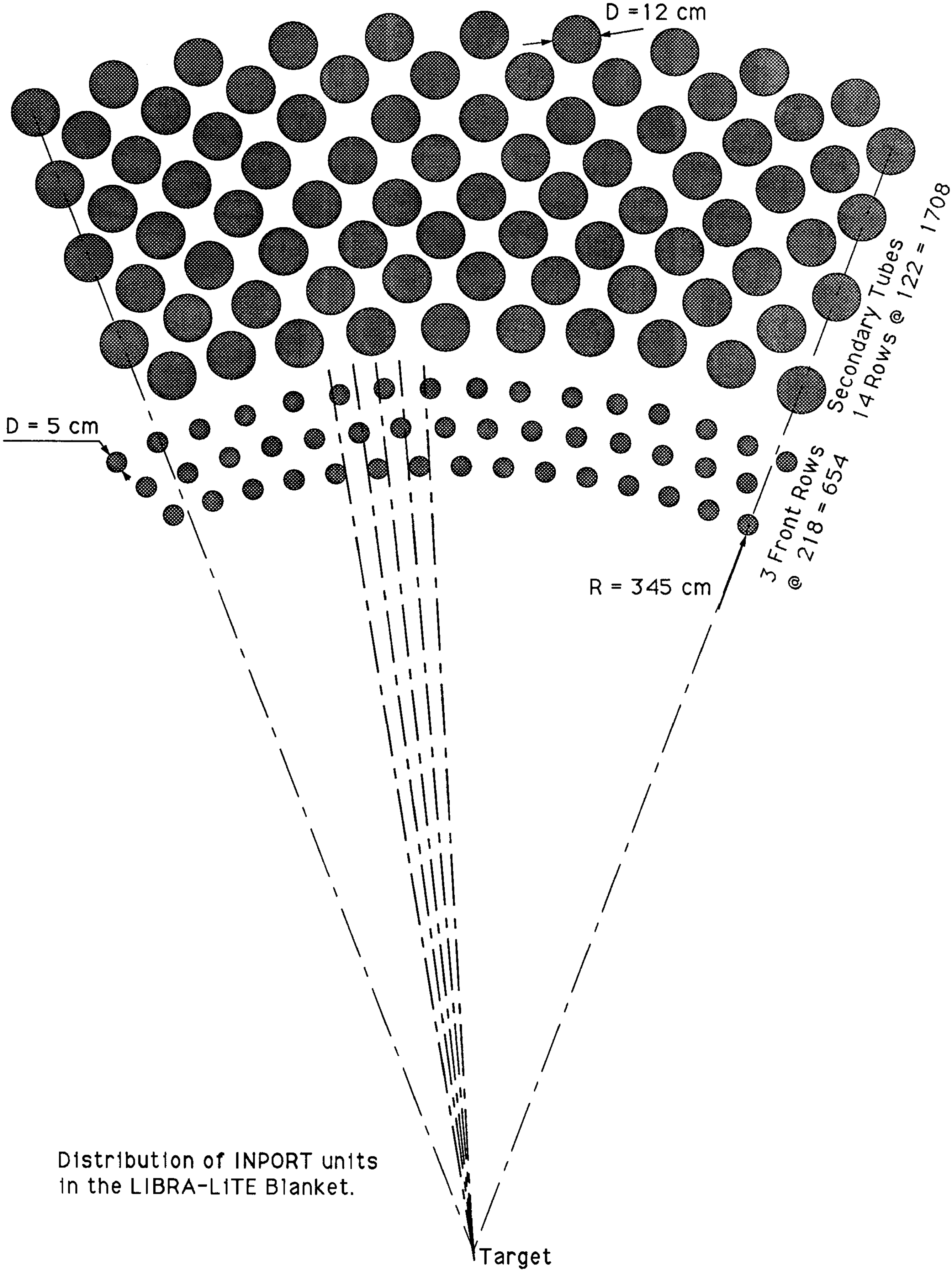

Distribution of INPORT units
in the LIBRA-LITE Blanket.

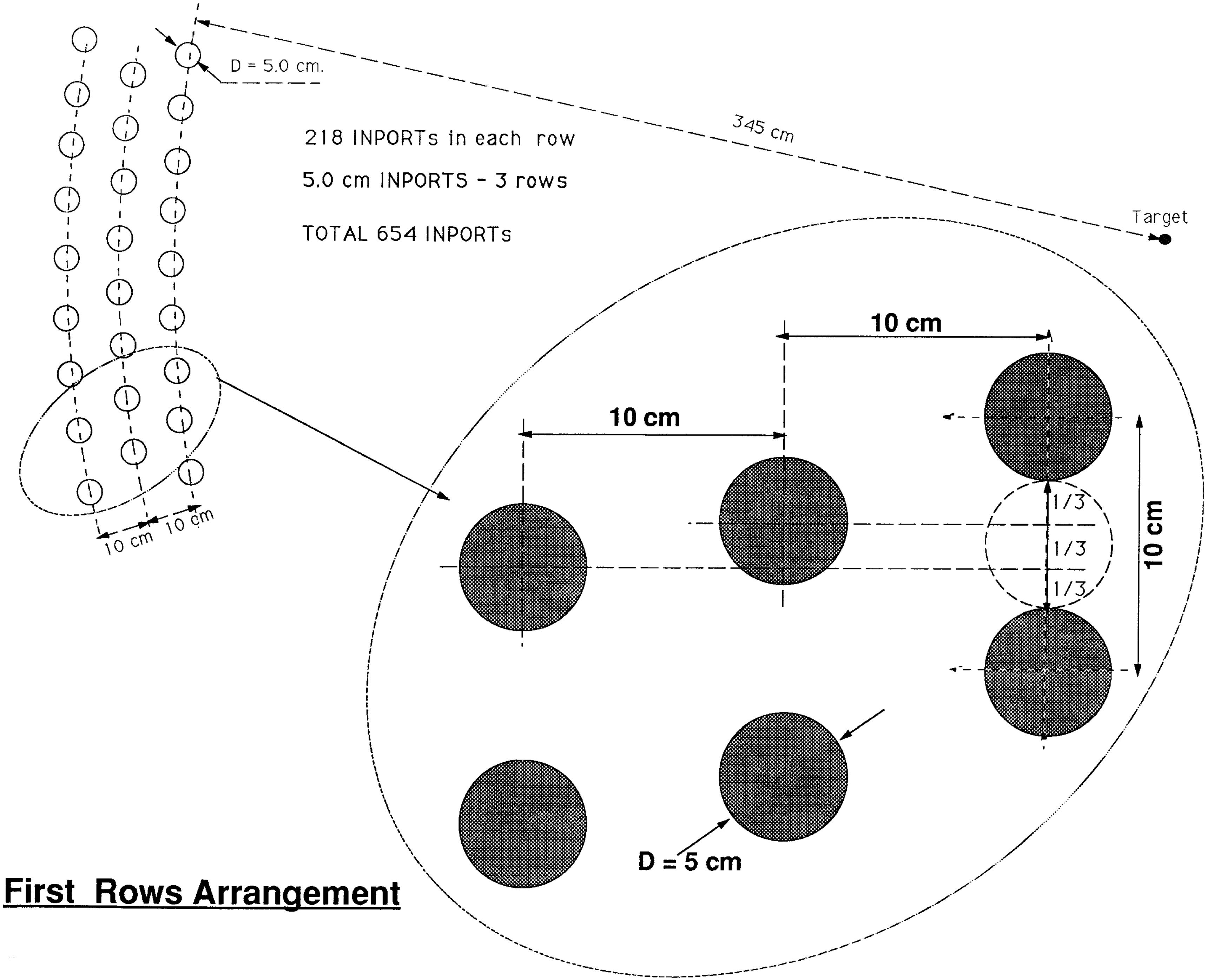

First Rows Arrangement

General Description

- Structural material is HT-9 ferritic steel

- Breeding/cooling material is natural Li

- The chamber is an upright cylinder with an accentuated domed roof

- There are 18 drivers, 9 on the top and 9 on the bottom

- The beam lines have lens magnets at a distance of 2.2 m from the target to the magnet center, and 2.05 m to the front surface

General Description (contd.)

- The lens magnets are single turn with flowing liquid Li as the conductor

- The side walls of the cylinder are protected with wetted INPORT units made of HT-9 at a radius of 3.45 m

- The INPORT units are integrated with the beam lines to insure uniform coverage

- The blanket is 2.25 m thick consisting of INPORT units with flowing Li. The packing fraction is 33%.

- The bottom is protected by a pool of Li

General Description (contd.)

- The accentuated domed roof is designed as a lifetime component. The roof is not self wetting but will condense Li on its surface. It is cooled with Li. The roof has an access port for maintenance.

- The cylindrical shield is 2.6 m thick made of reinforced concrete.

- After the shot the expanding He buffer gas flows through the INPORT units and blows out through ducts into an expansion chamber.

- The hot Li in the pool flows to 5 heat exchangers in the base of the reactor.

- The Li exchanges heat with an organic coolant which then goes to a conventional steam cycle.

Selected Chamber Parameters

Radius to Front INPORT Units (m)	3.45
Radius to Inner Reflector Surface (m)	5.70
Distance from Target to Bottom Pool (m)	5.0
Distance from Target to Roof (m)	16.0
Reflector Thickness (m)	0.5
Average Bottom Pool Thickness (m)	0.75
Radius to Center of Lens Magnet (m)	2.20
Radius to Face of Lens Magnet (m)	2.05
Diameter of Front INPORT Units (m)	0.05
Diameter of Rear INPORT Units (m)	0.12

Selected Parameters (contd.)

Total Number of Drivers	18
Distance of Diode from Target (m)	7.0
Inclination of Beams to Horizontal (degrees)	35
Radius of Beam at Lens Magnet (m)	0.12
Li Inlet Temperature (^{o}C)	350
Li Outlet Temperature (^{o}C)	500
Li Mass Flow Rate (kg/s)	4.84×10^{3}
Total Thermal Power (MWt)	3425
Temperature of Organic Coolant (^{o}C)	425
Estimated Power Cycle Efficiency (%)	44
Gross Electric Power (MWe)	1507
Estimated Net Electric Power (MWe)	1284

Neutronics Analysis for LIBRA-LiTE

Mohamed Sawan
Fusion Technology Institute
The University of Wisconsin

LIBRA-LiTE Review Meeting
17 December 1990
Karlsruhe, Germany

Chamber Neutronics Analysis

- ONEDANT spherical geometry calculations.
- 30n-12g group cross section data based on ENDF/B-V.
- Point source at center of chamber emitting neutrons and gamma photons having the LIBRA target spectrum.
- Per DT fusion, 1.025 neutrons are emitted from the target with 11.64 MeV average energy. In addition, 0.013 gamma photons are emitted with 3.85 MeV average energy.
- Overall energy multiplication determined in terms of the blanket nuclear energy multiplication via

$$M_o=0.979[0.695M_n+0.305]$$

- Results normalized to 1000 MJ DT yield and 3 Hz repetition rate.

- Chamber radius= 5.7 m.
- INPORT tubes with 0.33 packing fraction. 2% HT-9 and 98% Li in tubes.
- 0.5 m thick side reflector consisting of 90% Ht-9 and 10% Li.
- 0.5 m thick roof consisting of 80% HT-9 and 20% Li.
- 0.25 m thick bottom splash plate consisting of 80% HT-9 and 20% Li.
- Max length of INPORT units= 10 m.

Design Requirements

- 1D TBR in INPORT units > 1.3.
- Peak end-of-life dpa in the ferritic steel chamber wall < 200 dpa. For 30 FPY reactor life, the peak dpa rate should not exceed 6.66 dpa/FPY.
- Peak damage rate in magnets < 200 dpa/CY.

TBR vs. dpa Rate for the Different Design Options

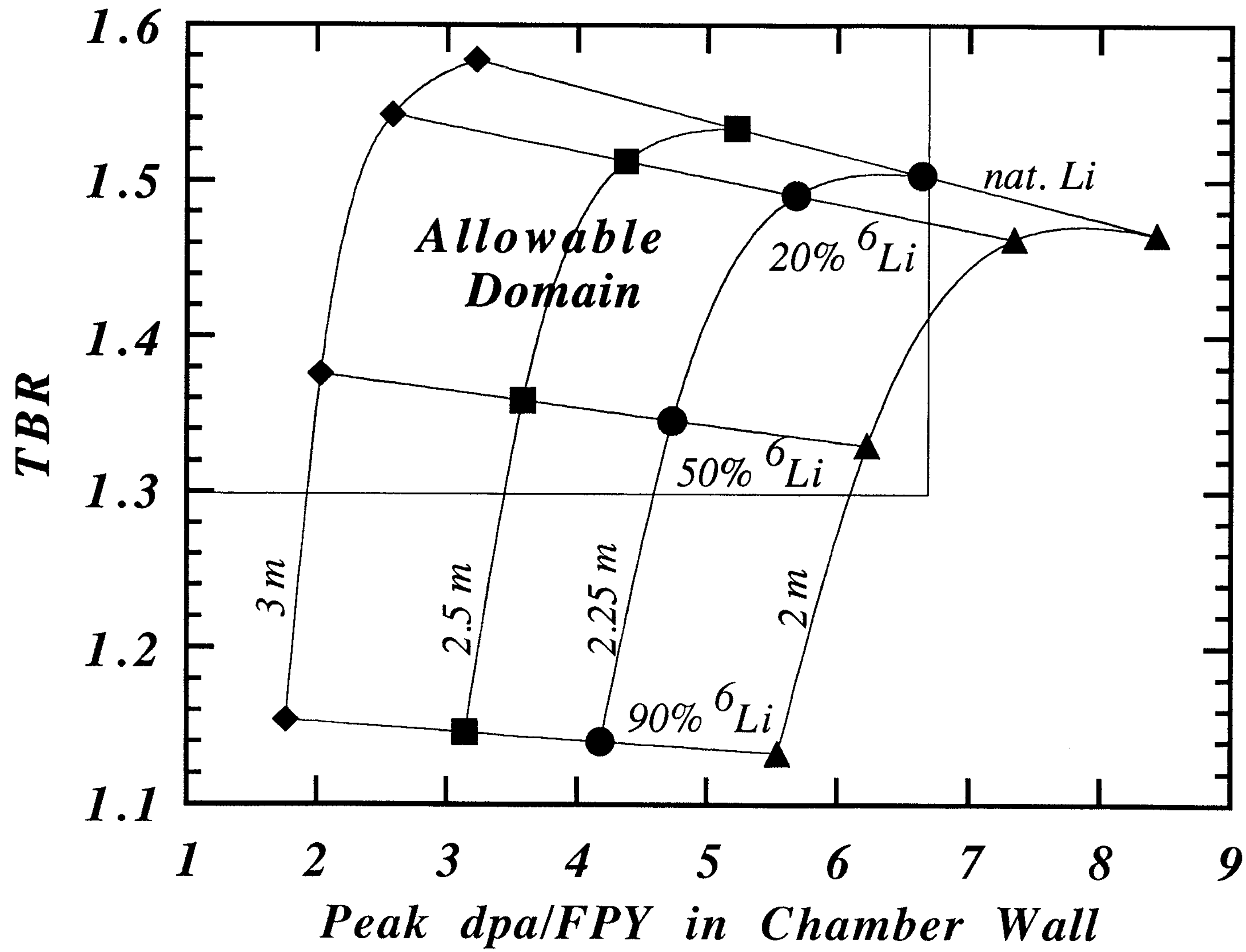

Effect of Blanket Thickness on Peak Damage in the Permanent Chamber Wall

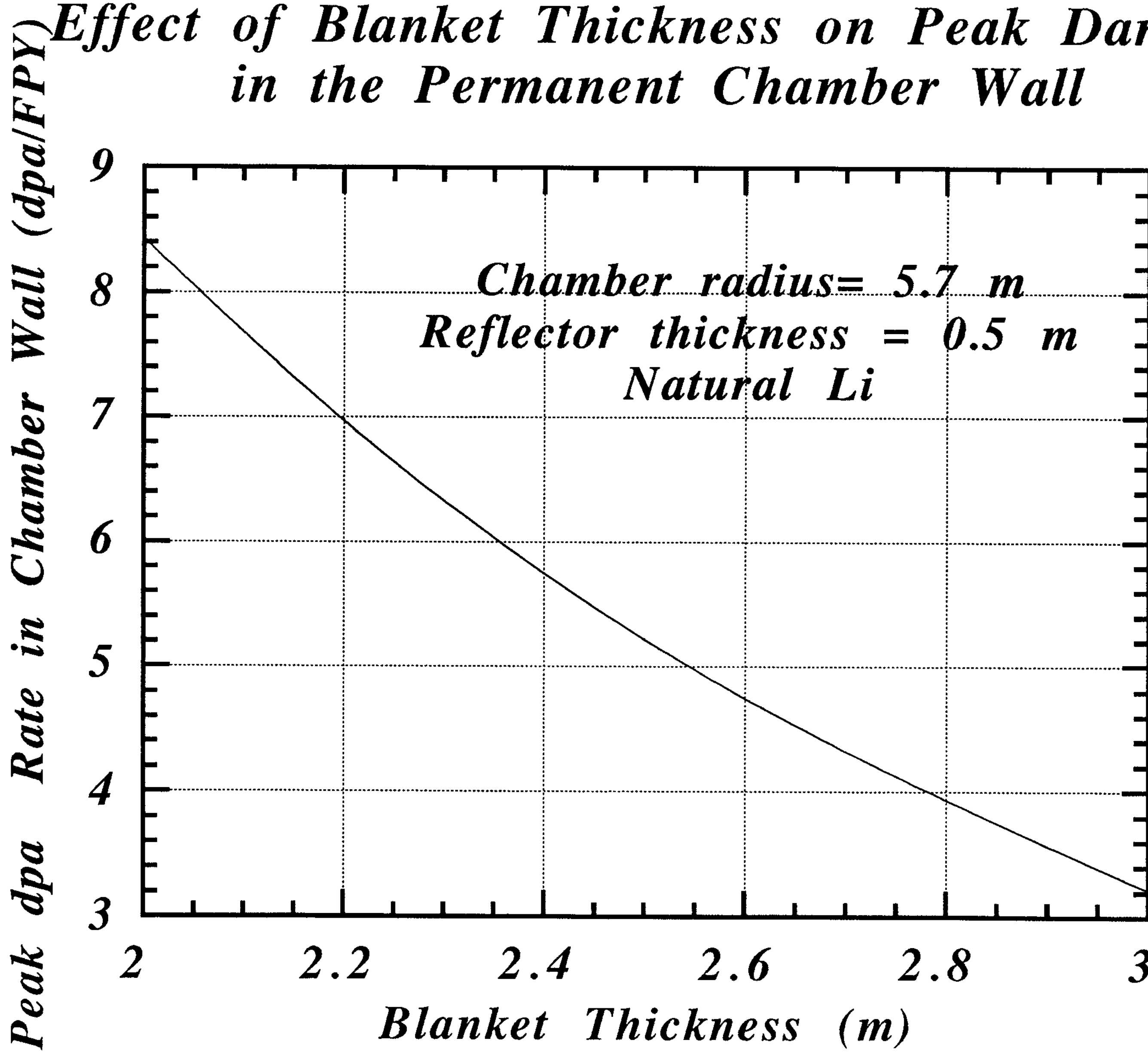

Neutronics Parameters for the Reference Blanket Design

- Blanket thickness= 2.25 m.
- Front surface of INPORT units at 3.45 m from target.
- Neutron wall loading= 13.6 MW/m^2.
- Natural Li is used.
- Local TBR= 1.504.
- Local M_n= 1.242.
- Local M_0= 1.144.
- Peak dpa rate in INPORT units= 90 dpa/FPY.
- Peak dpa rate in side chamber wall= 6.64 dpa/FPY.

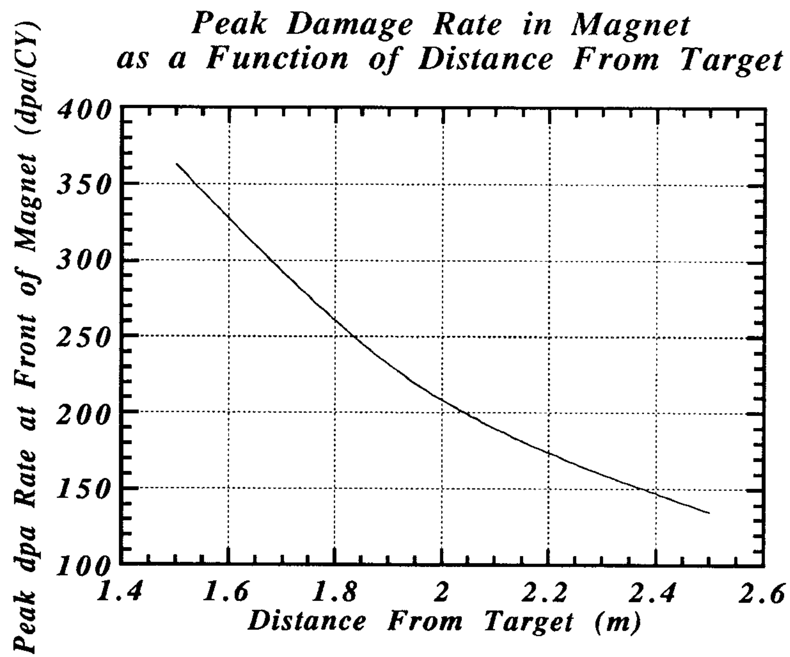

- Front of magnet at 2.05 m from target. Center of magnet at 2.2 m.
- Neutron wall loading at front of magnet= 38.5 MW/m^2.
- Peak dpa rate= 199 dpa/CY.
- Local TBR= 0.883.
- Local M_n= 1.13.
- Local M_o= 1.068.

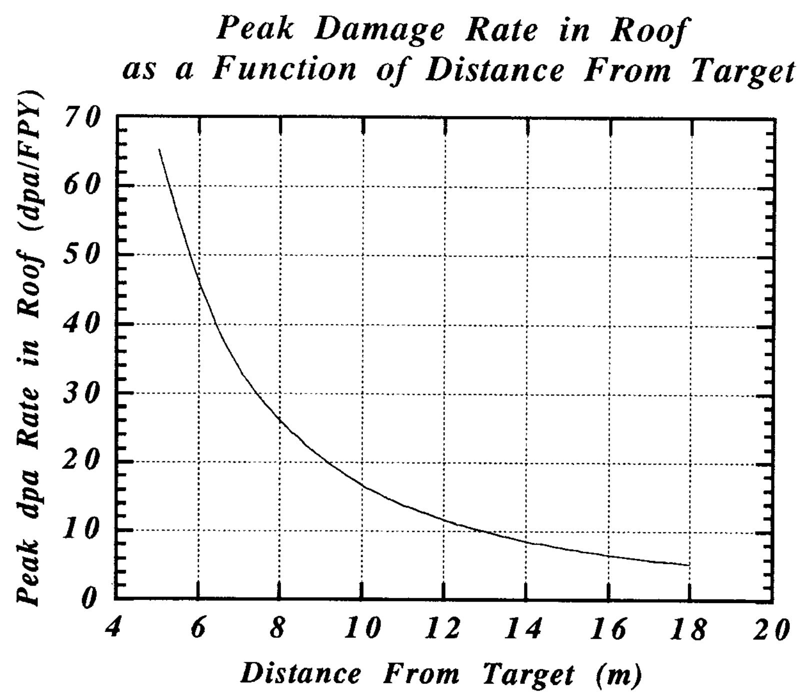

- Front surface of roof at 16 m from target.
- Neutron wall loading= 0.63 MW/m^2.
- Peak dpa rate in roof= 6.57 dpa/FPY.
- Local TBR= 0.558.
- Local M_n= 1.299.
- Local M_o= 1.182.

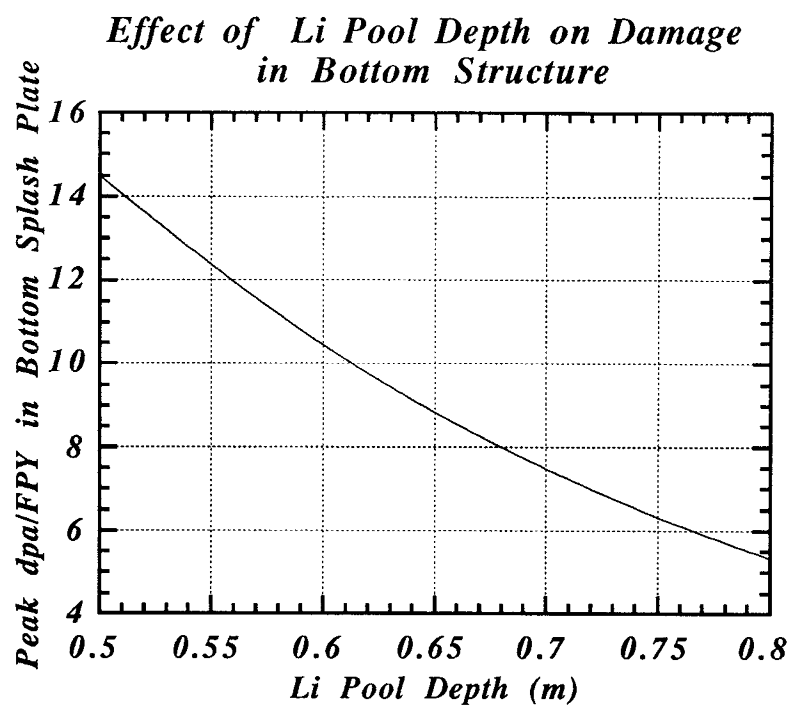

- Depth of pool= 0.75 m.
- Peak dpa rate in bottom structure= 6.32 dpa/FPY.
- Local TBR= 1.575.
- Local M_n= 1.221.
- Local M_o= 1.129.

Effect of Side Biological Shield Thickness on Dose Rate During Reactor Operation

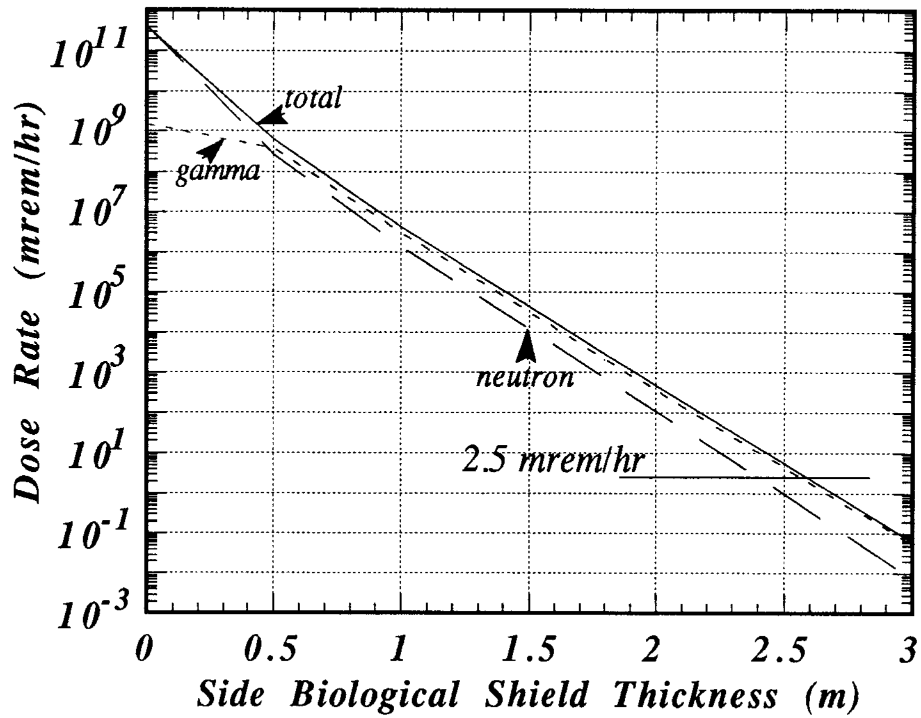

- Required concrete shield thickness= 2.6 m.
- Biological shield consists of 70% concrete, 20% carbon steel C1020, and 10% He.

Overall Reactor Neutronics Parameters

Region	Coverage Fraction	TBR	M_n
INPORT	76.64%	1.5036	1.242
Beam Ports	1.81%	0	0
Magnets	3.85%	0.883	1.13
Roof	8.85%	0.558	1.299
Bottom	8.85%	1.575	1.221
Total Reactor	100%	1.3751	1.2184

Reactor thermal power= 3000x0.979[0.695x1.2184+0.305]= 3383 MW

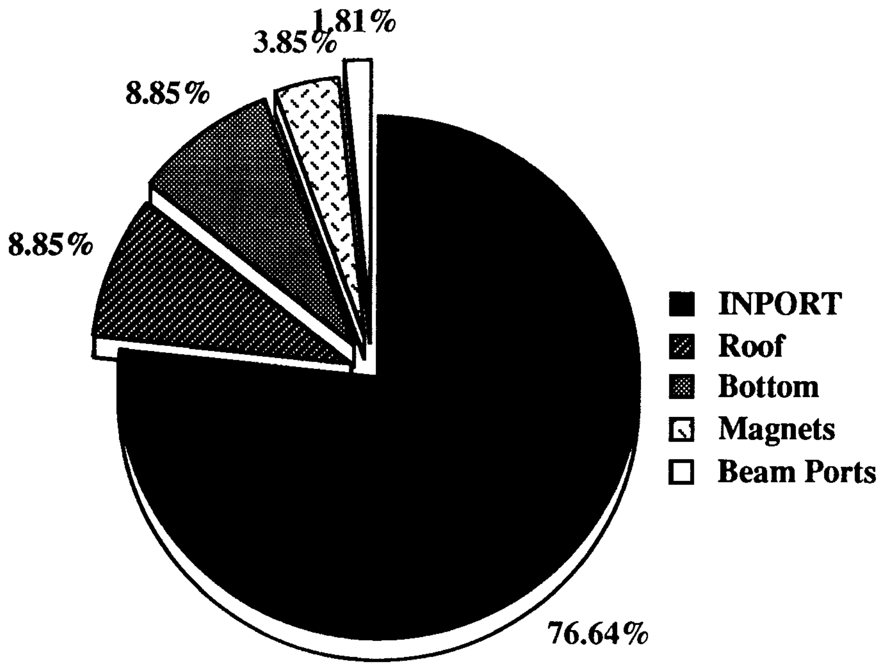

Fractions of Source Neutrons Going to Different Reactor Regions

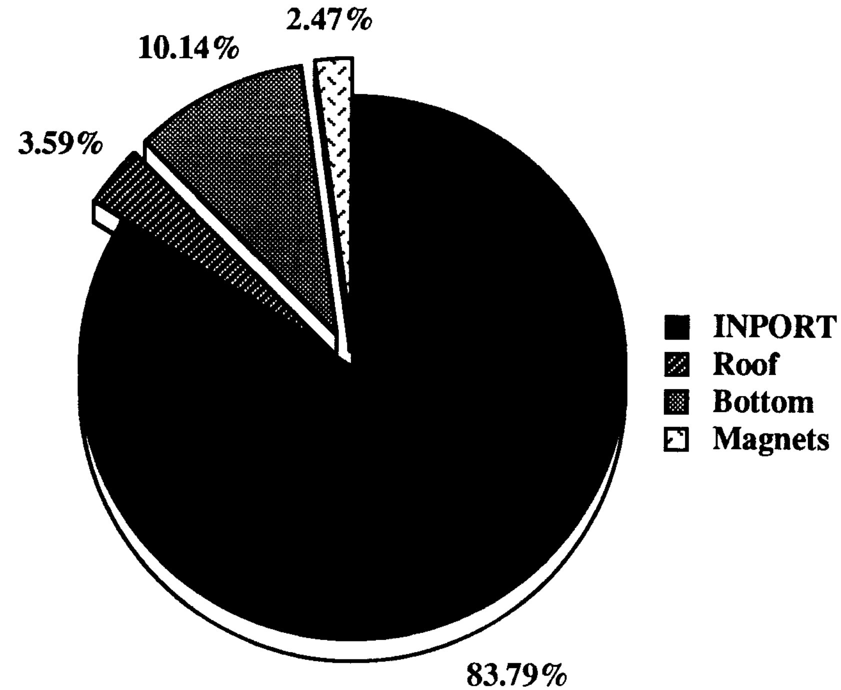

Contributions from the Different Regions to the Overall TBR (1.375)

Nuclear Heating in INPORTS & Reflector of LIBRA-LiTE

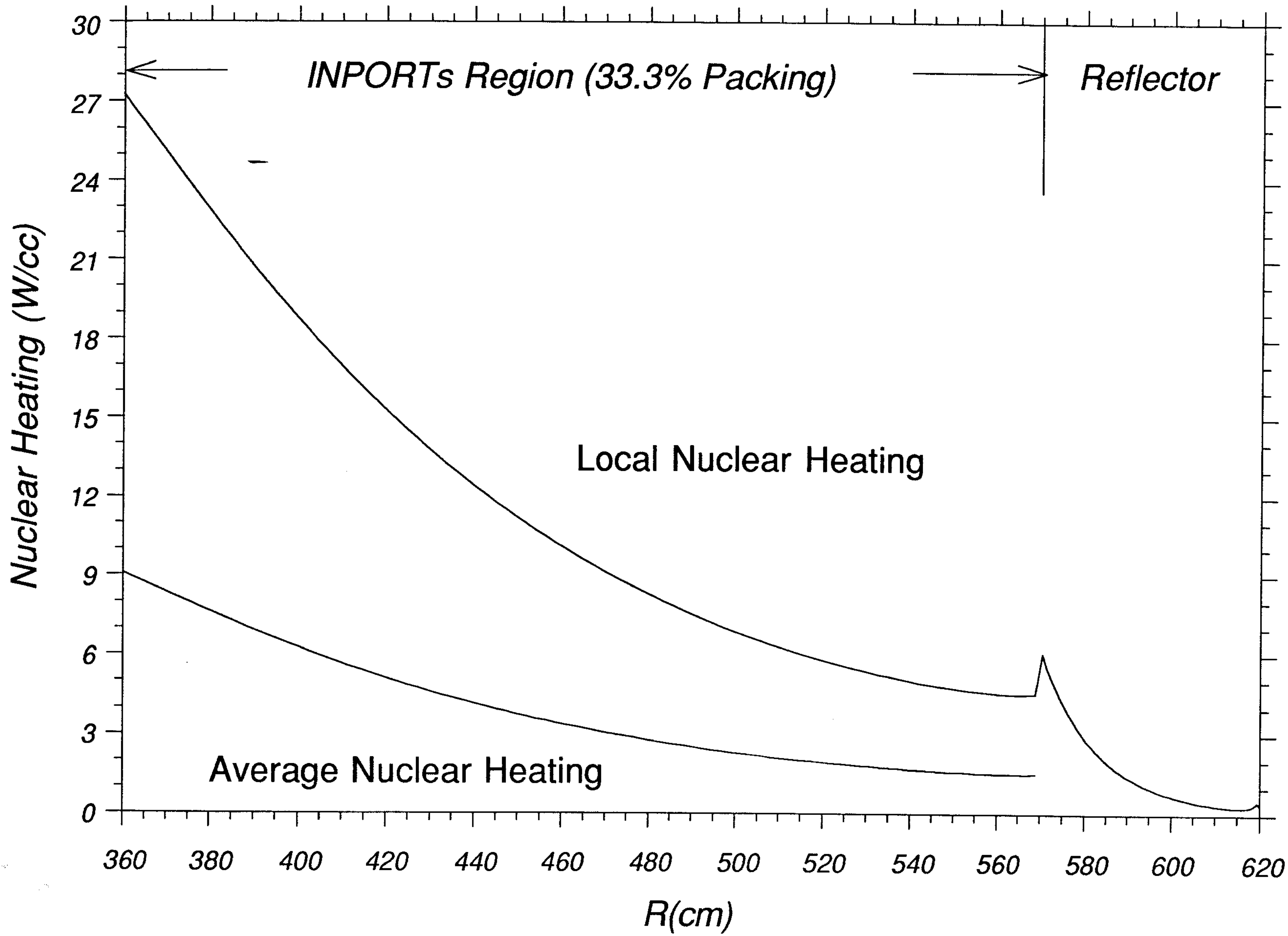

A Comparison Between {LIBRA-I} and {LIBRA-LiTE}

a) *Geometry*

	LIBRA-I	LIBRA-LiTE
INPORT Structural Material	SiC	HT-9
First Surface Radius (m)	3.00	3.45
Tube Bank Thickness (m)	1.35	2.25
Packing Fraction	1/3	1/3
Chamber Radius (m)	4.35	5.70
INPORT Zone Cross Sect. Area (m^2)	31.2	65.0
INPORT Max. Height (m)	6.4	10.0
Front tubes		
# of Rows	2	3
Diameter (cm)	3	5
Total Number	628	654
Secondary tubes		
# of Rows	9	14
Diameter (cm)	10	12
Total Number	1260	1708

b) *Thermal Parameters*

	LIBRA-I	LIBRA-LiTE
Average Surface Heat Flux(MW/m²)	**1.46**	**4.628**
Max. Surface Heat Flux(MW/m²)	**1.8**	**6.464**
Surface Heating in first INPORT Rows (MW)	**124**	**1003**
Nuclear Heating in first INPORT Rows (MW)		**641**
Total Heating (MW)		**1644**
Power Consumed in Li evaporation from first INPORT Rows (MW)		**852**
Surface Heating Due to Uniform recondensation (kW/m²)		**95.2**
Total Heating in first INPORT Rows (MW)		**988.3**
Total Heating in Secondary tubes (MW)		**2055**

c) *Coolant System Parameters [340°C-500°C]*

	LIBRA-I	LIBRA-LiTE
Coolant	**LiPb**	**Li**
Density (g/cc)	**9.82-9.56**	**0.5-0.485**
Heat Capacity (kJ/kg.deg.)	**0.19-0.187**	**4.2**
Melting Pt. (°C)	**235**	**180**
ρ . **Cp (kJ/m3.deg.)**	**1828**	**2100**
Thermal Conductivity (W/m.K)	**13.77-17.71**	**46.2-50.4**
Coolant Inlet Temp. (°C)	**340**	**350**
Coolant Outlet Temp. (°C)	**500**	**500**
Diam. of First Surface Tubes(cm)	**3.0**	**5.0**
# of Tubes in First INPORT zone	**628**	**654**
Velocity in First Surface Tubes (cm/s)	**260**	**244**
Velocity in Secondary Tubes (cm/s)	**50**	**34**
Average Velocity (cm/s)	**52**	**47**
Mass flow Rate (kg/s)	5.07×10^4	4.84×10^3

Chamber Evacuation

<u>Parameters:</u>	
• Chamber Volume (m^3)	$2.553\text{x}10^3$
• Fill Gas	He
• Atom Density (#/cm^3)	$3.55\text{x}10^{16}$
• He Pressure at 273 K (torr)	1
<u>Before Shot:</u>	
• He Gas Temperature (K)	800
• He Gas Pressure (torr)	3
<u>After Shot:</u>	
• He Gas Temperature (K)	$30\text{x}10^3$
• He Gas Pressure (torr)	200
<u>Before Expansion:</u>	
• He Gas Cools Down to	$\sim 20\text{x}10^3$ K
• Corresponding He Gas Pressure (torr)	132

Assumptions Used to Determine Pumping Speed

1) An expansion chamber is connected to the reaction chamber

2) The following processes occur:

- Li vapor condenses on INPORT units
- He gas cools down to $\sim$20,000 K
- He gas expands isentropically into expansion chamber
- Li spray mist cools down He gas in expansion chamber to 800 K
- He gas remaining in reaction chamber continues to cool down approaching 800 K
- Pressure in both chambers equilibrates to some value $>$ 2 torr

Subsequent Processes

1) Vacuum system capacity is based on evacuating both chambers down to 2 torr in 1/3 second.

2) Fresh He gas is injected into reaction chamber to achieve the needed atom density for the next shot.

EQUILIBRATED PRESSURE AFTER EXPANSION AND REQUIRED PUMPING SPEED AS A FUNCTION OF RATIO OF EXPANSION TO CHAMBER VOLUME

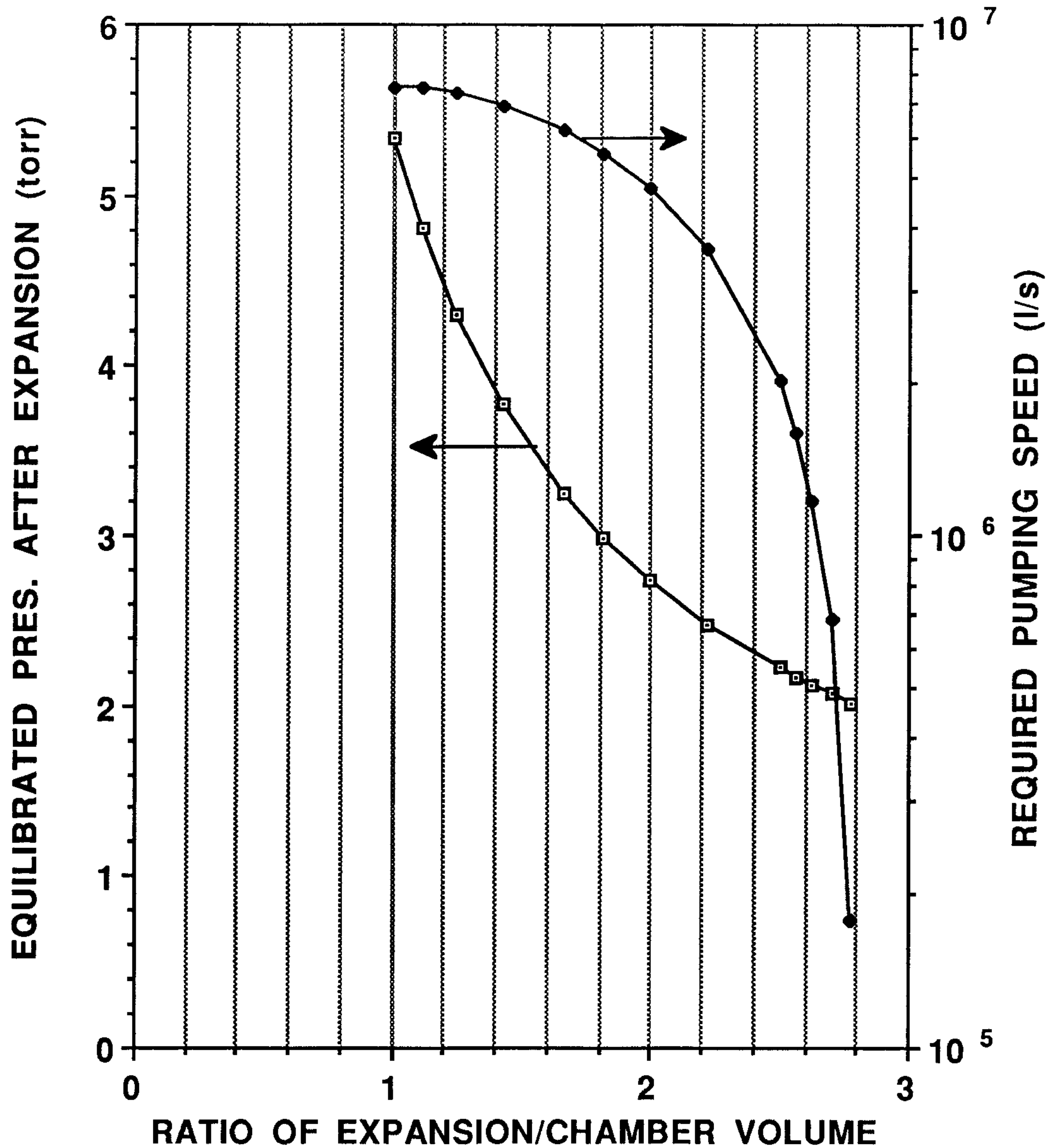

* T in expansion chamber=800K
Initial He pressure = 132 torr
Initial He temp.=20000K

Results

- Expansion chamber volume $\sim$1.75 x reactor chamber volume, or $\sim$4500 m^3

- Required pumping speed is $\sim 1.8\times10^5$ ℓ/s

Observations

- System is insensitive to the temperature to which the He gas cools down to before expansion

- Energy in the reactor and in expansion chambers recovered as high grade for use in power cycle

REQUIRED PUMPING SPEED FOR TWO He GAS COOLDOWN TEMP. AS A FUNCTION OF RATIO OF EXPANSION TO CHAMBER VOLUME

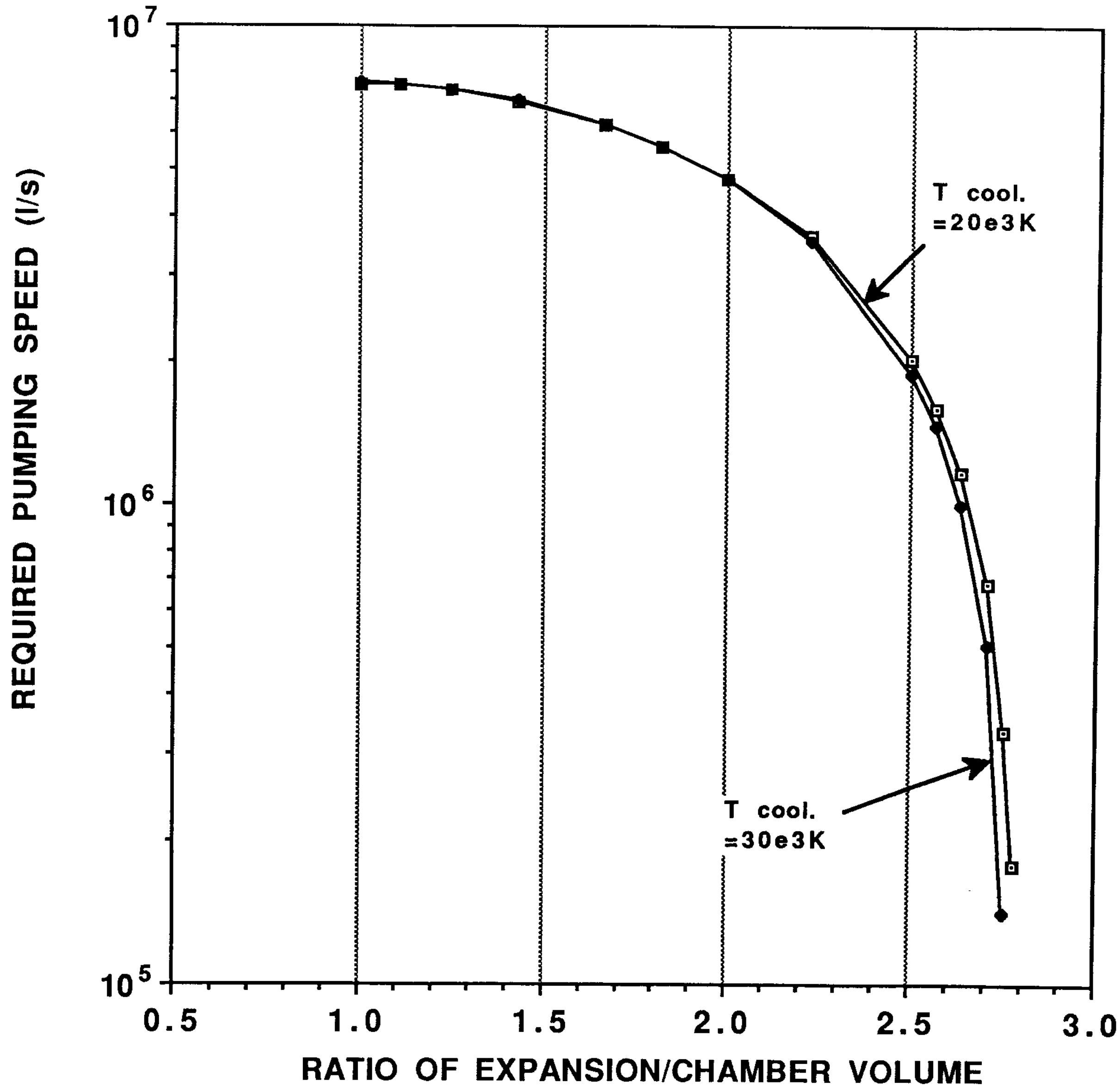

TARGET EXPLOSION BLASTS IN LIBRA-LiTE

Robert R. Peterson
Roxann L. Engelstad
Edward G. Lovell

University of Wisconsin - Madison
and Fusion Power Associates

presented at the LIBRA-LiTE Review
Kernforschungszentrum Karlsruhe
Karlsruhe, Germany

December 17, 1990

Vaporization and Gas Dynamics Determine Target Chamber Wall Loadings

- High fluence x-rays from target explosion vaporizes large masses of lithium from target chamber surfaces. High fluence debris ions from the target are deposited in the background gas, generating a blast wave moving toward the target chamber structures.

- A shock wave passes through the vapor while it is still at liquid density and strikes the remaining unvaporized part of the wall, leading to a very high magnitude but short duration pressure pulse on the wall.

- The pressure peak drives a shock into the cold unvaporized material.

- The vapor moves toward the center of the target chamber until it collides with the blast in the background gas.

Vaporization and Gas Dynamics Determine Target Chamber Wall Loadings (cont.)

- The vapor and gas begin a complicated motion in the target chamber volume. Much of the material passes through the field of INPORTs, which acts as a cross-flow heat exchanger and removes energy from the gas and condenses the vapor.

- The gas motion eventually subsides, leaving energy in the gas that causes a residual pressure in the gas that affects the mechanical response and the pumping of gas from the chamber.

Schematic Picture of Gas Flow in Target Chamber

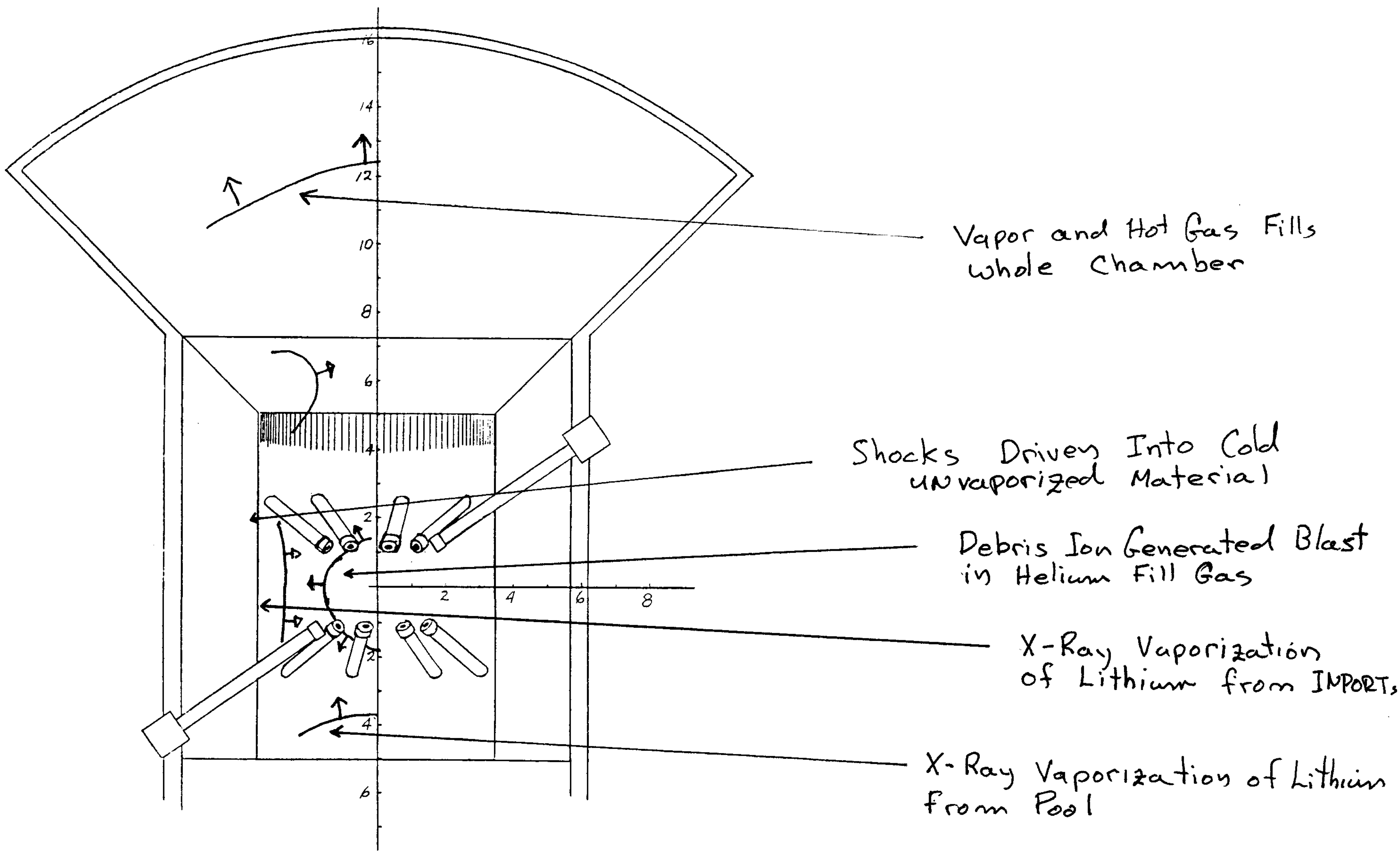

Important Issues

- Can target chamber structures be designed to survive the impulsive pressure loadings from x-ray vaporization?

- Do the shocks in the cold material cause damage?

- Where does the vaporized mass re-condense?

- How much energy remains in the target chamber gases for long periods and how can that energy be recovered?

CONRAD Computer Code

- 1-D Lagrangian radiation-hydrodynamics.
- 20 group radiation diffusion.
- Table look-up of equations-of-state and opacities from SESAME or IONMIX.
- Time-dependant target x-ray and ion depostion in fill gas and structures.
- Vaporization, condensation and heat transfer modeled in structures.

Base Case Parameters

	at INPORTs	at Lens Magnets
Target Yield (MJ)	1000	1000
X-Ray Yield (MJ)	197	197
Debris Ion Yield (MJ)	102	102
Distance from Target (cm)	345	205
X-Ray Fluence (J/cm^2)	132	373
X-Ray Spectrum	Bangerter	Bangerter
X-Ray Pulse Width (ns)	1	1
Ion Species	Lead	Lead
Ion Energy (keV)	257	257
Fill Gas	Helium	Helium
Gas Density (cm^{-3})	3.55×10^{16}	3.55×10^{16}
Wall Material	Liquid Lithium	Liquid Lithium

X-Ray Spectrum from "Bangerter" Target

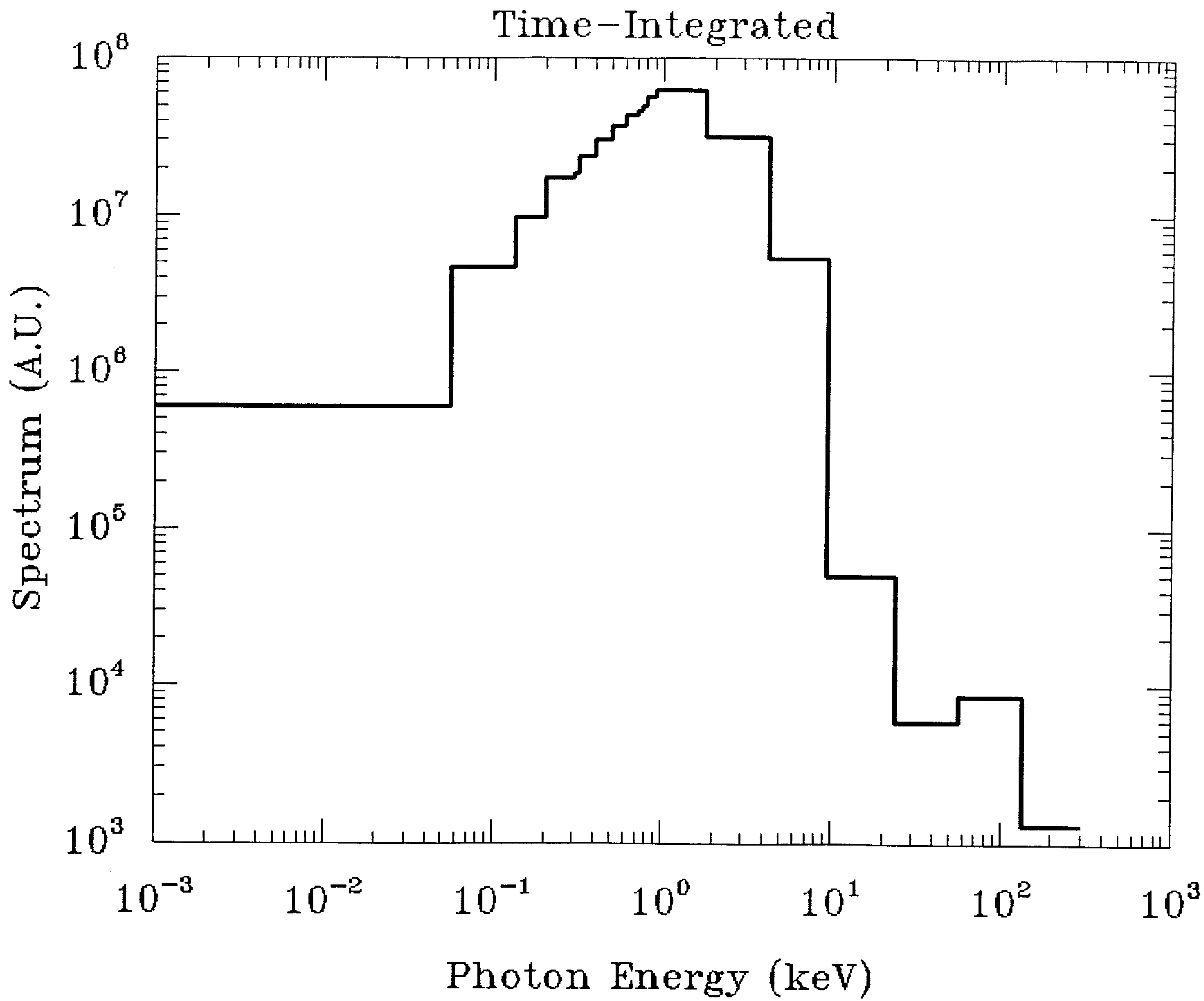

Table of Results

	at INPORTs	at Lens Magnets
Whole Sphere Vaporized Mass (kg)	8.062	5.790
Vaporized Areal Density (mg/cm^2)	5.39	10.96
Vaporized Thickness (μ)	102	207
Peak Pressure at Vapor/Liquid (GPa)	5.39	9.18
Time of Peak Pressure (ns)	24.6	46.3
Duration of Vaporization Pulse (ns)	20	50
Impulse at 100 ns (Pa-s)	126	287
Impulse at 10 μs (Pa-s)	153	360
Energy in Gas and Vapor at 10 μs (MJ)	138	—

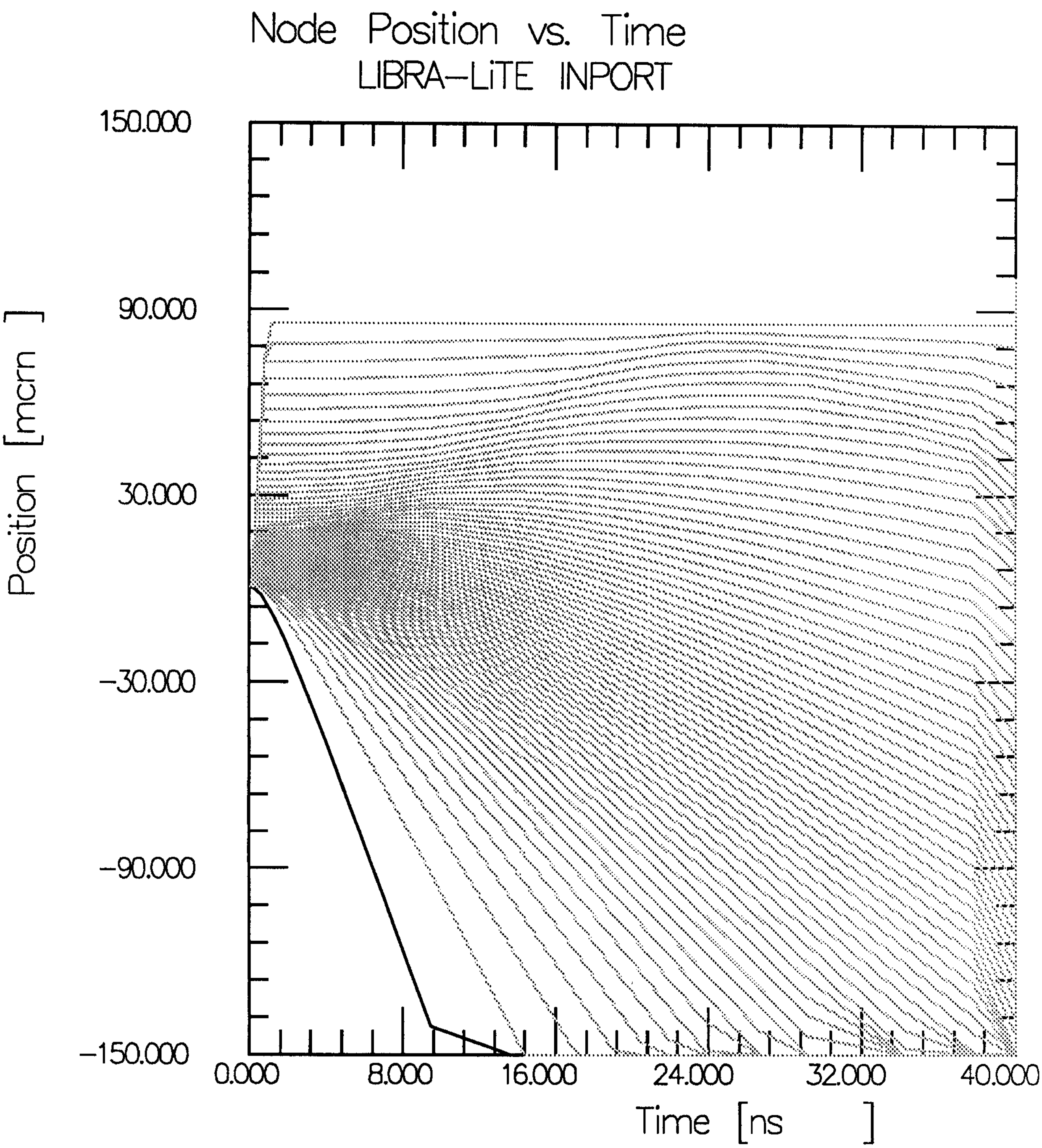
Node Position vs. Time
LIBRA-LiTE INPORT
150.000
90.000
30.000
-30.000
-90.000
-150.000
Position [mcrn]
0.000
8.000
16.000
24.000
32.000
40.000
Time [ns]

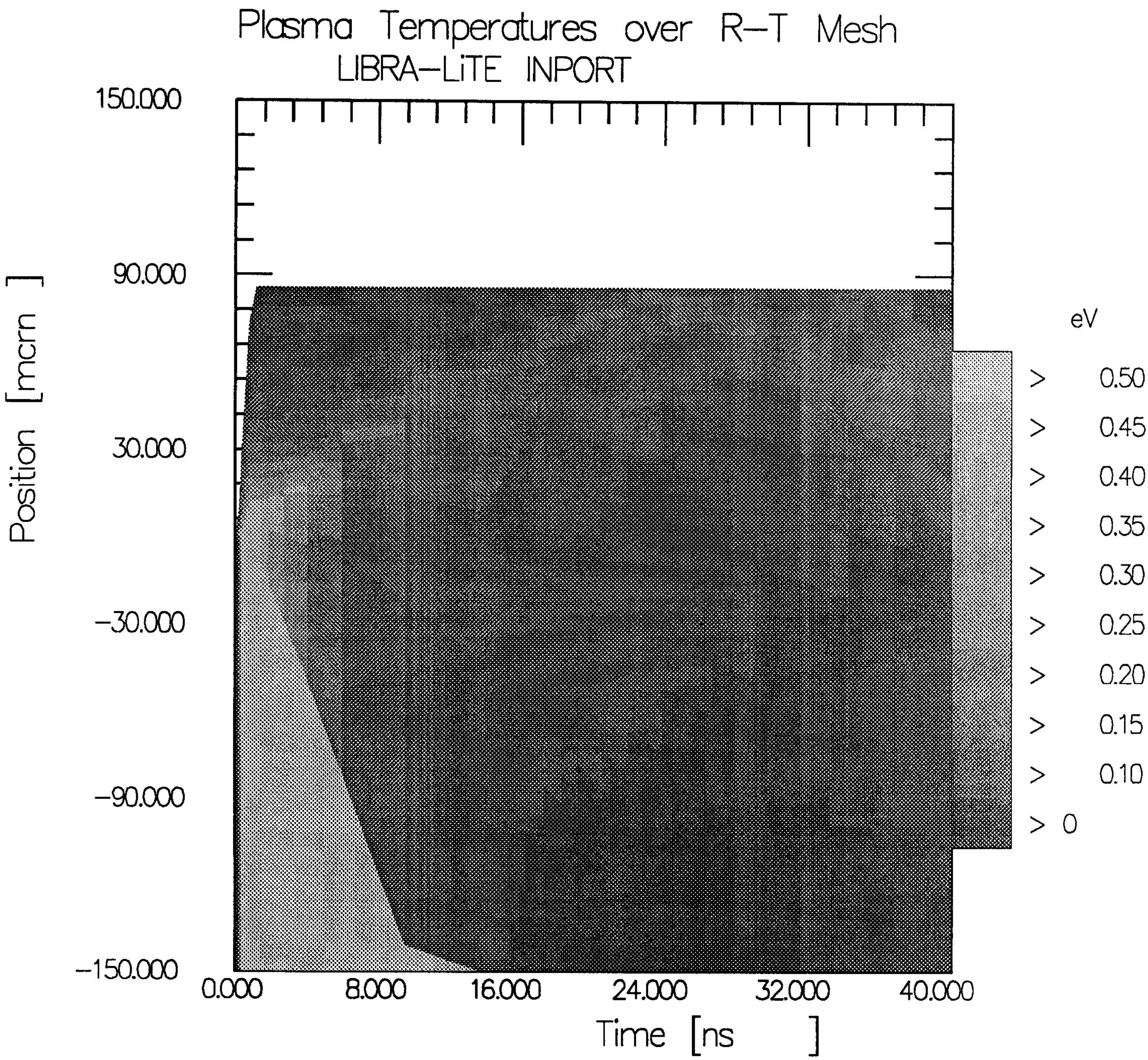

Plasma Temperatures over R–T Mesh
LIBRA–LiTE INPORT
150.000
90.000
30.000
–30.000
–90.000
–150.000
Position [mcrn]
0.000
8.000
16.000
24.000
32.000
40.000
Time [ns]
eV
> 0.50
> 0.45
> 0.40
> 0.35
> 0.30
> 0.25
> 0.20
> 0.15
> 0.10
> 0

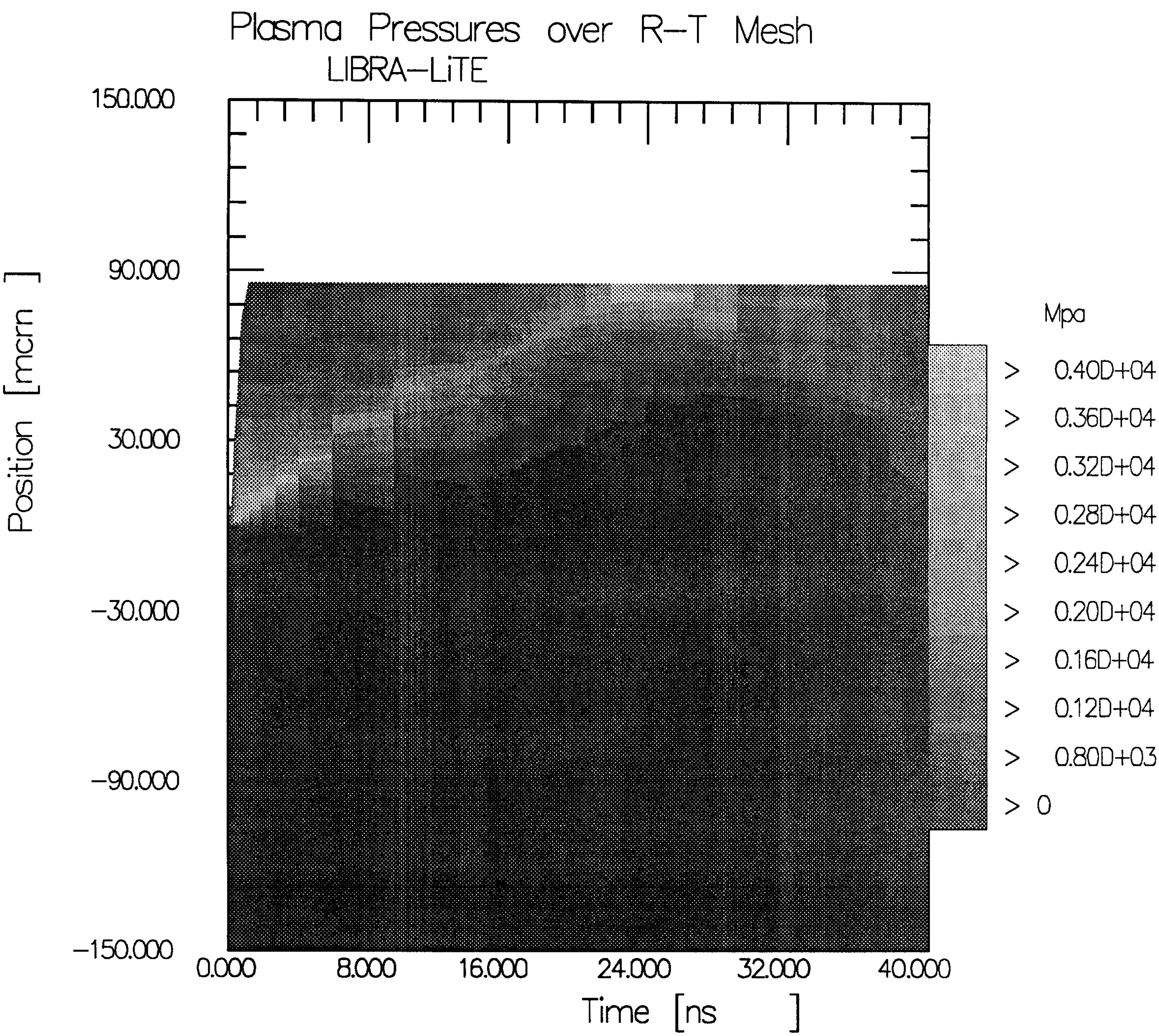

Plasma Pressures over R-T Mesh
LIBRA-LiTE
150.000
90.000
30.000
-30.000
-90.000
-150.000
Position [mcrn]
0.000
8.000
16.000
24.000
32.000
40.000
Time [ns]
Mpa
> 0.40D+04
> 0.36D+04
> 0.32D+04
> 0.28D+04
> 0.24D+04
> 0.20D+04
> 0.16D+04
> 0.12D+04
> 0.80D+03
> 0

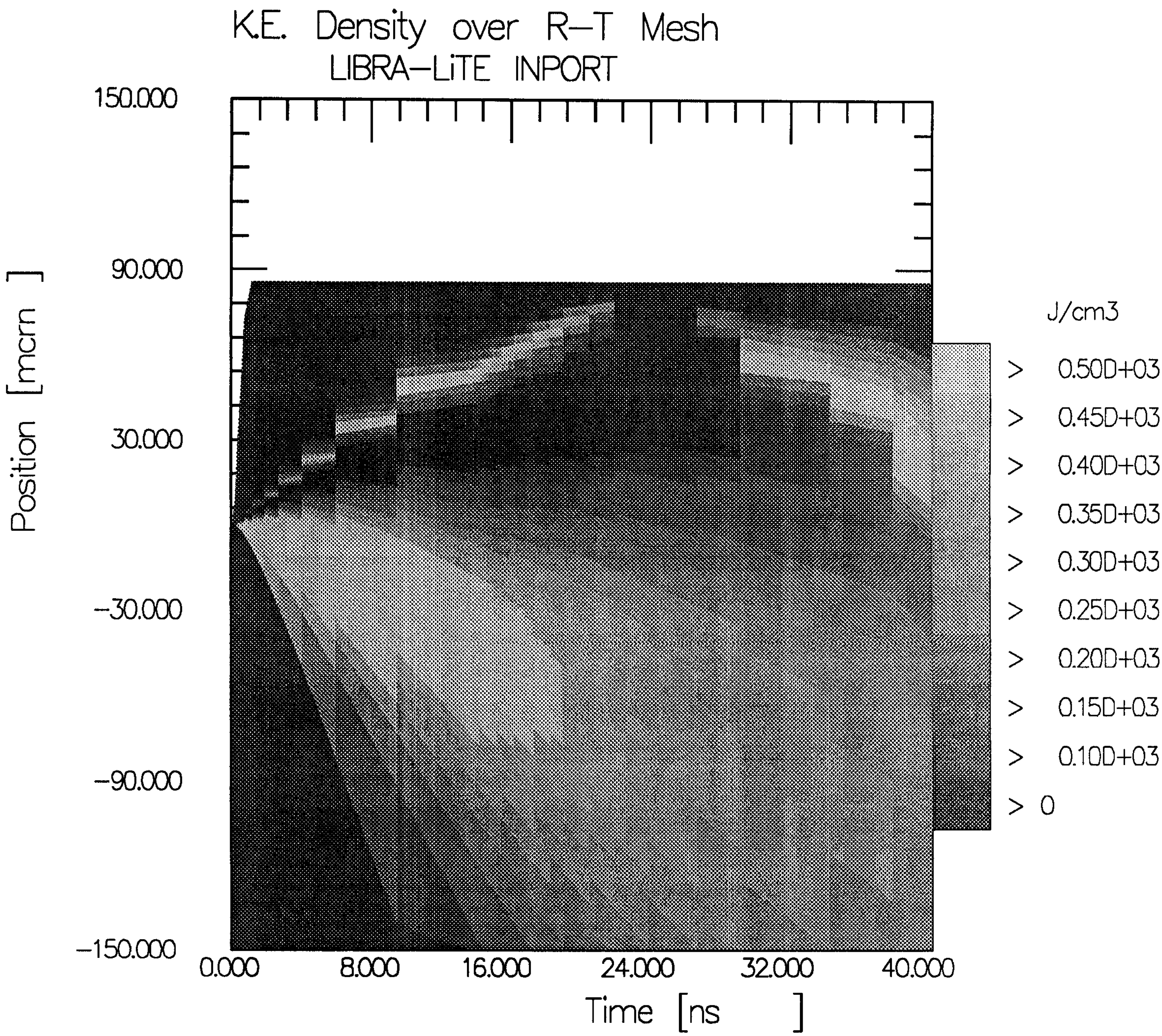

K.E. Density over R–T Mesh
LIBRA–LiTE INPORT
150.000
90.000
30.000
–30.000
–90.000
–150.000
Position [mcrn]
0.000
8.000
16.000
24.000
32.000
40.000
Time [ns]
J/cm3
> 0.50D+03
> 0.45D+03
> 0.40D+03
> 0.35D+03
> 0.30D+03
> 0.25D+03
> 0.20D+03
> 0.15D+03
> 0.10D+03
> 0

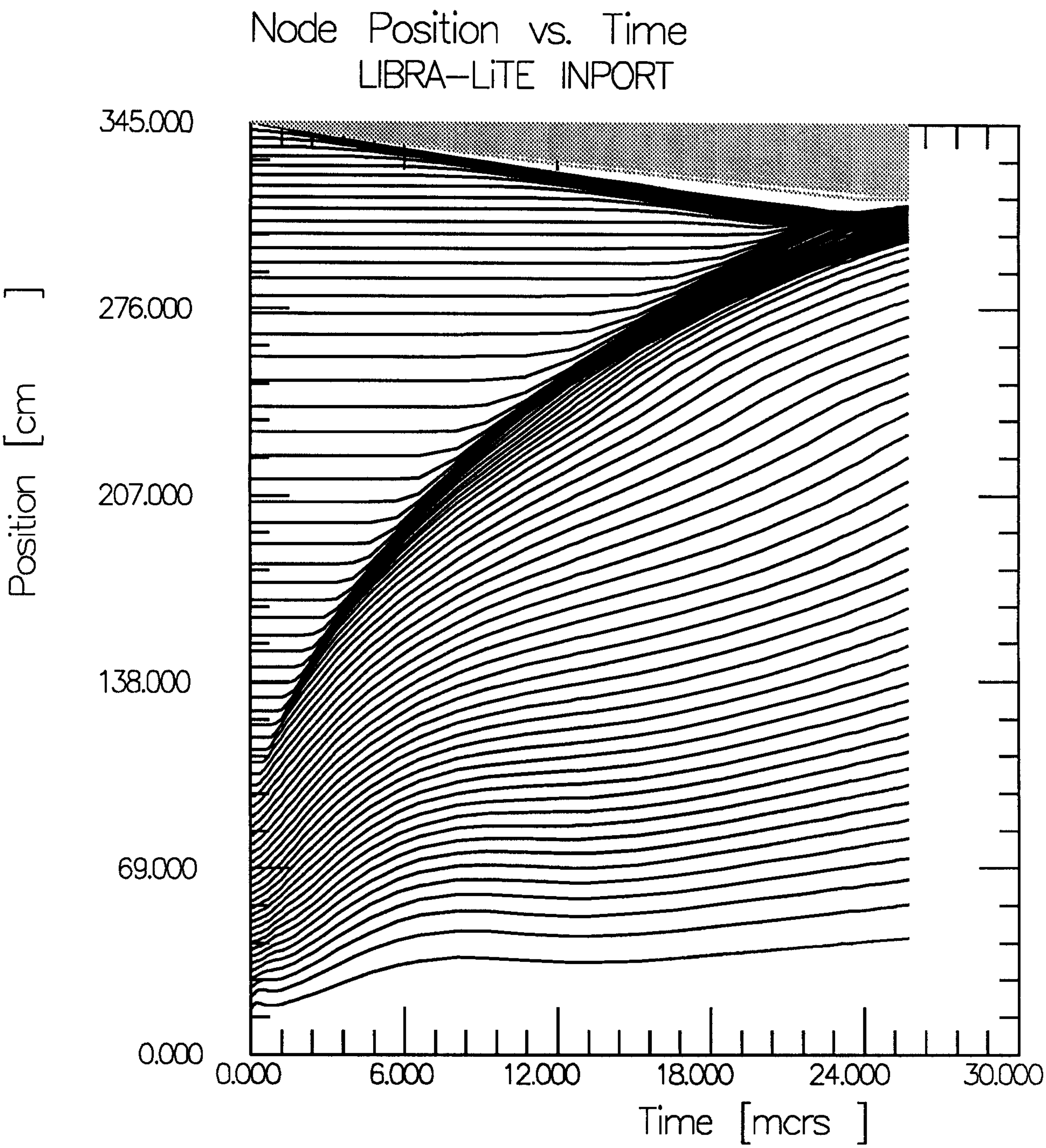

Node Position vs. Time
LIBRA-LiTE INPORT
345.000
276.000
207.000
138.000
69.000
0.000
Position [cm]
0.000
6.000
12.000
18.000
24.000
30.000
Time [mcrs]

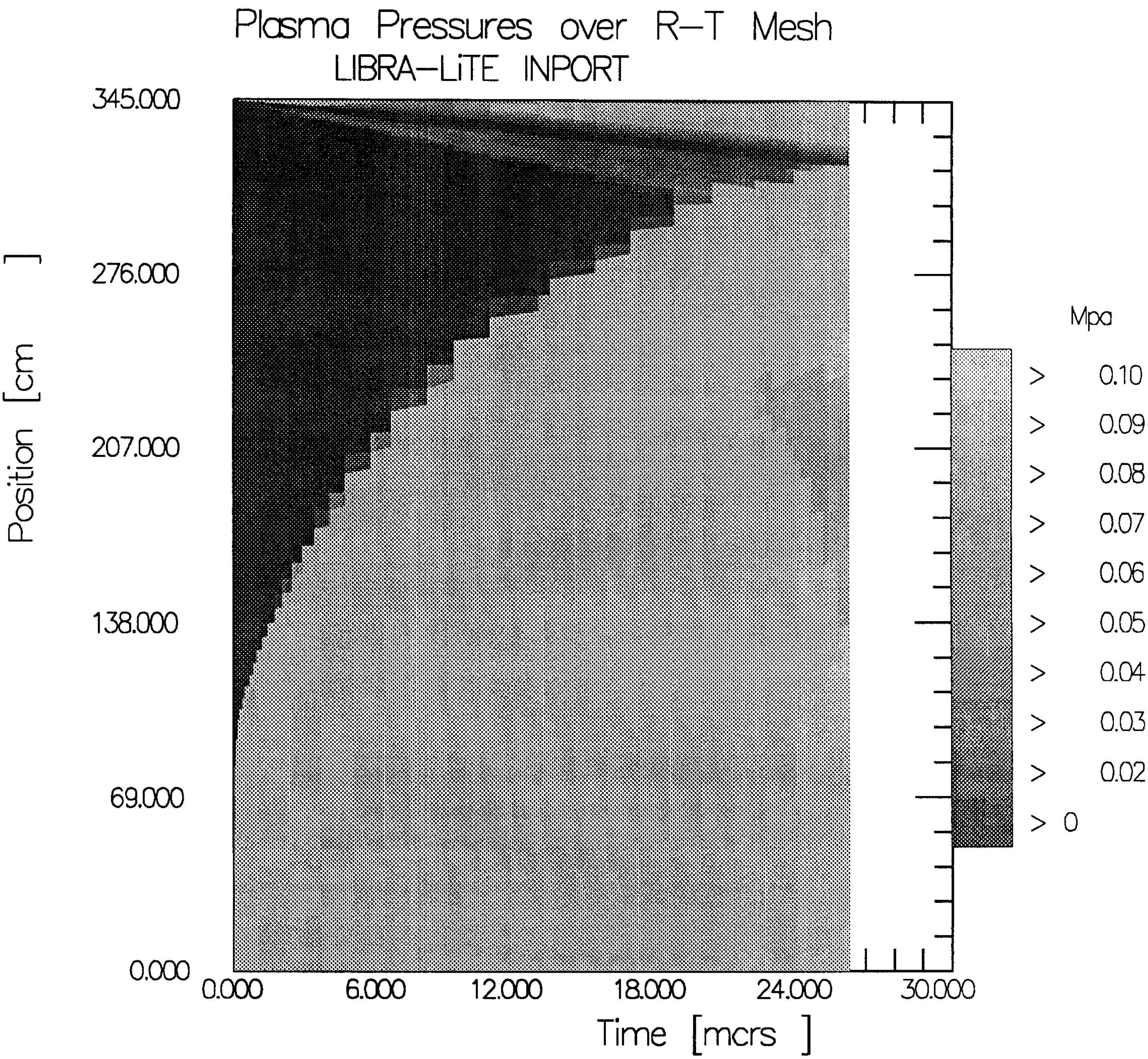

Plasma Pressures over R-T Mesh
LIBRA-LiTE INPORT
345.000
276.000
207.000
138.000
69.000
0.000
Position [cm]
0.000
6.000
12.000
18.000
24.000
30.000
Time [mcrs]
Mpa
> 0.10
> 0.09
> 0.08
> 0.07
> 0.06
> 0.05
> 0.04
> 0.03
> 0.02
> 0

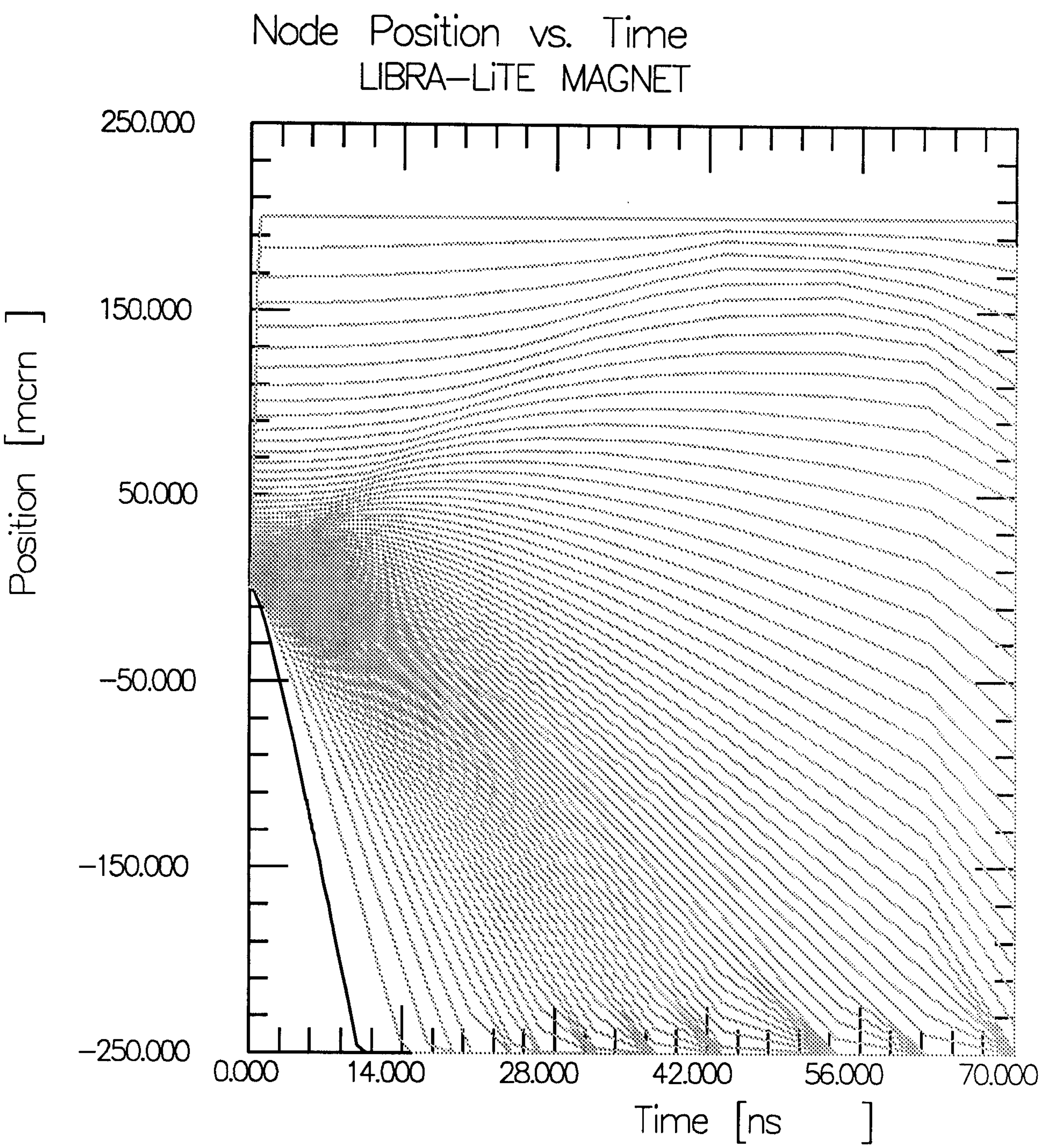

Node Position vs. Time
LIBRA-LiTE MAGNET
250.000
150.000
50.000
-50.000
-150.000
-250.000
Position [mcrn]
0.000
14.000
28.000
42.000
56.000
70.000
Time [ns]

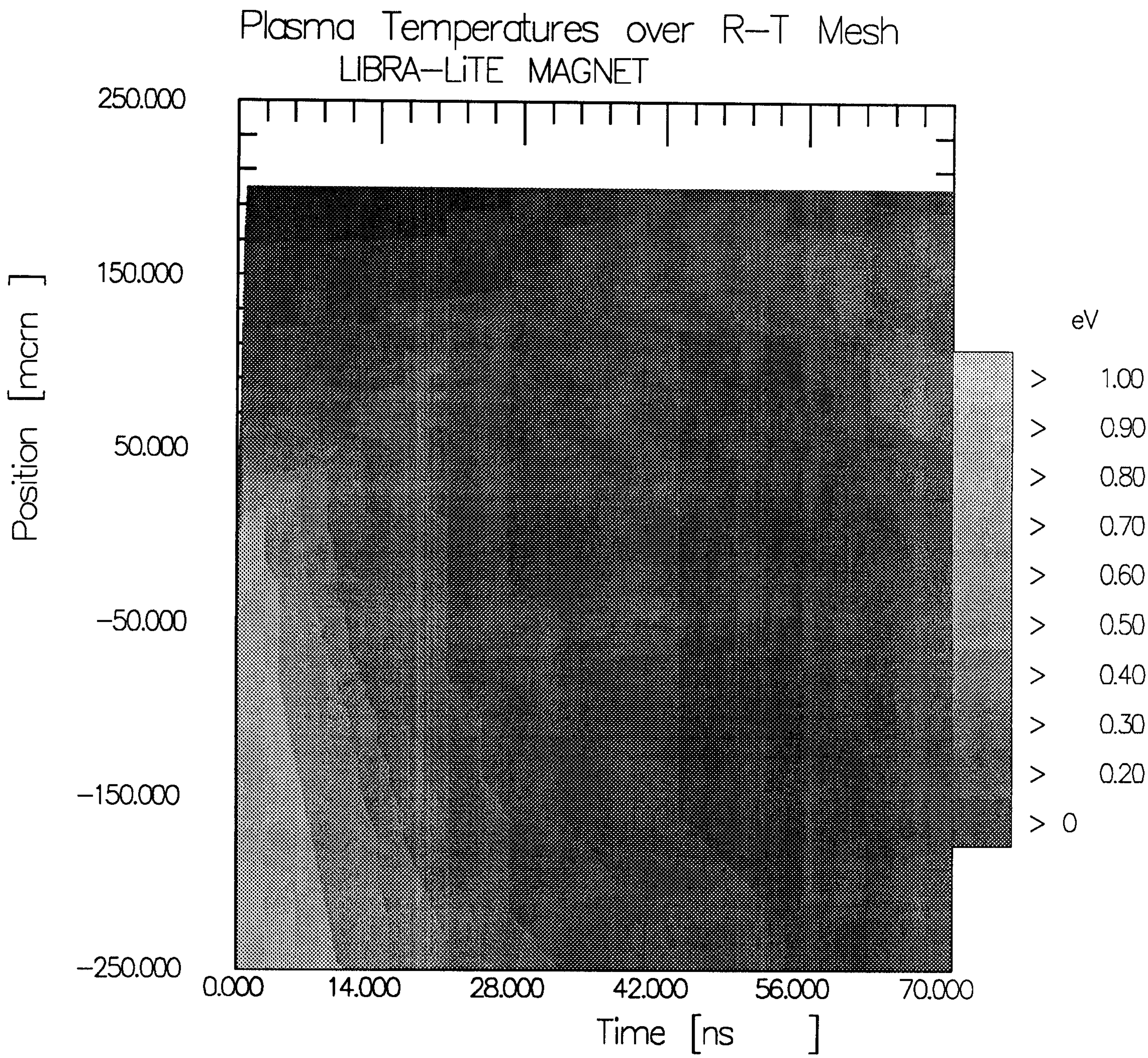

Plasma Temperatures over R-T Mesh
LIBRA-LiTE MAGNET
250.000
150.000
50.000
-50.000
-150.000
-250.000
Position [mcrn]
0.000
14.000
28.000
42.000
56.000
70.000
Time [ns]
eV
> 1.00
> 0.90
> 0.80
> 0.70
> 0.60
> 0.50
> 0.40
> 0.30
> 0.20
> 0

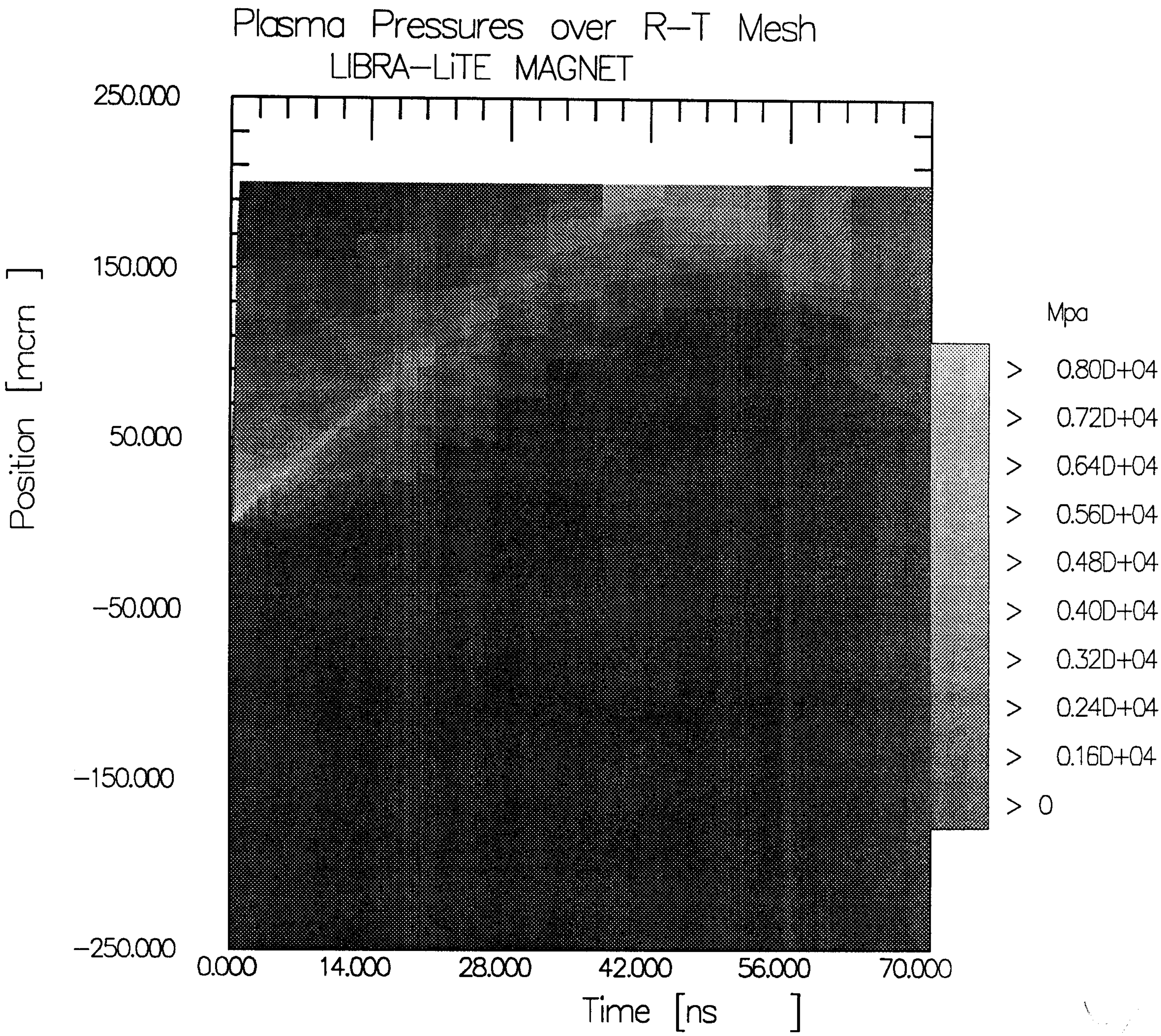

Plasma Pressures over R-T Mesh
LIBRA-LiTE MAGNET
250.000
150.000
50.000
-50.000
-150.000
-250.000
Position [mcrn]
0.000
14.000
28.000
42.000
56.000
70.000
Time [ns]
Mpa
> 0.80D+04
> 0.72D+04
> 0.64D+04
> 0.56D+04
> 0.48D+04
> 0.40D+04
> 0.32D+04
> 0.24D+04
> 0.16D+04
> 0

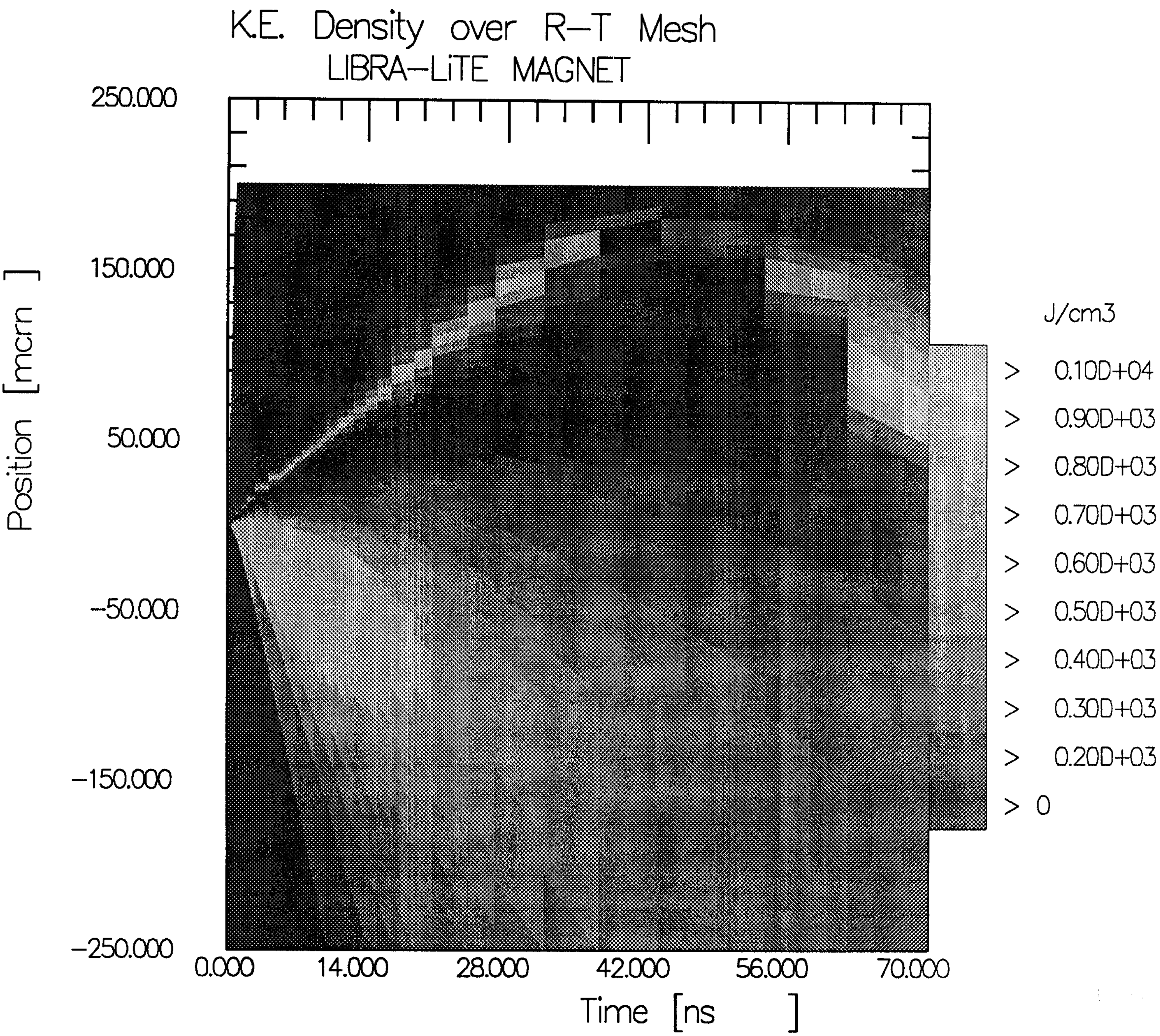

K.E. Density over R–T Mesh
LIBRA–LiTE MAGNET
250.000
150.000
50.000
–50.000
–150.000
–250.000
Position [mcrn]
0.000
14.000
28.000
42.000
56.000
70.000
Time [ns]
J/cm3
> 0.10D+04
> 0.90D+03
> 0.80D+03
> 0.70D+03
> 0.60D+03
> 0.50D+03
> 0.40D+03
> 0.30D+03
> 0.20D+03
> 0

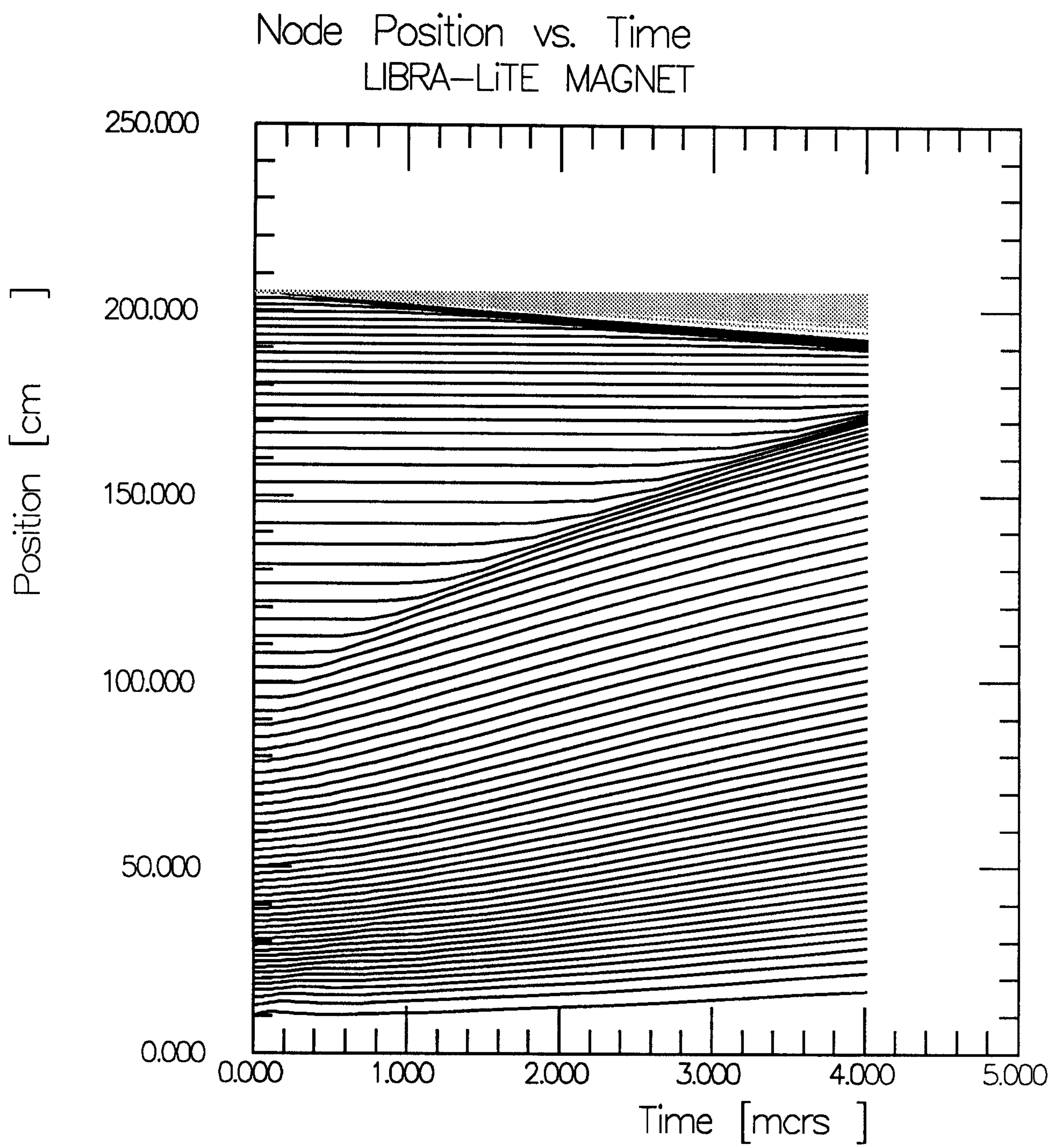

Node Position vs. Time
LIBRA-LiTE MAGNET
250.000
200.000
150.000
100.000
50.000
0.000
Position [cm]
0.000
1.000
2.000
3.000
4.000
5.000
Time [mcrs]

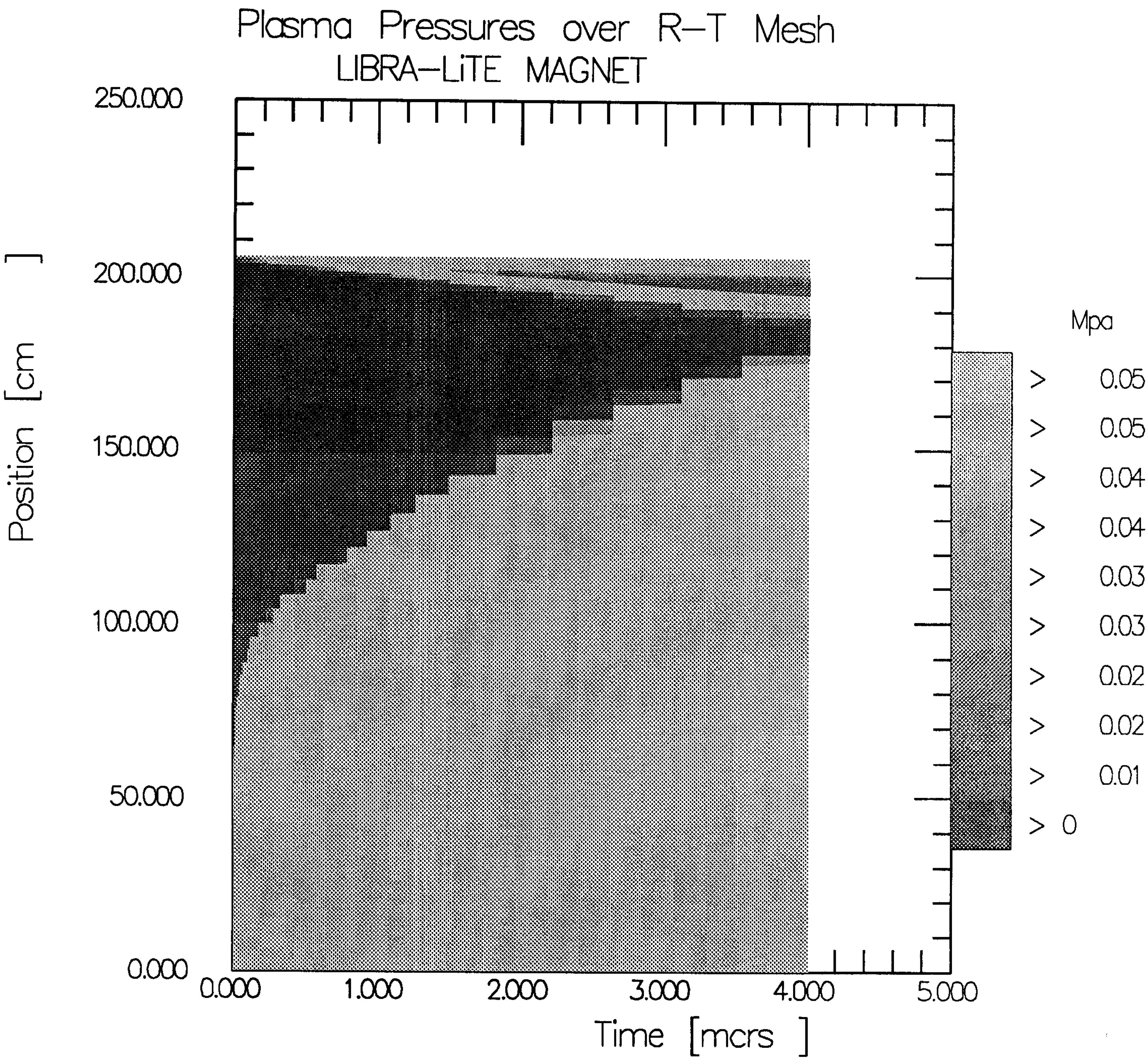

Plasma Pressures over R-T Mesh
LIBRA-LiTE MAGNET
Position [cm]
250.000
200.000
150.000
100.000
50.000
0.000
0.000
1.000
2.000
3.000
4.000
5.000
Time [mcrs]
Mpa
> 0.05
> 0.05
> 0.04
> 0.04
> 0.03
> 0.03
> 0.02
> 0.02
> 0.01
> 0

Pressure Pulse on INPORT's

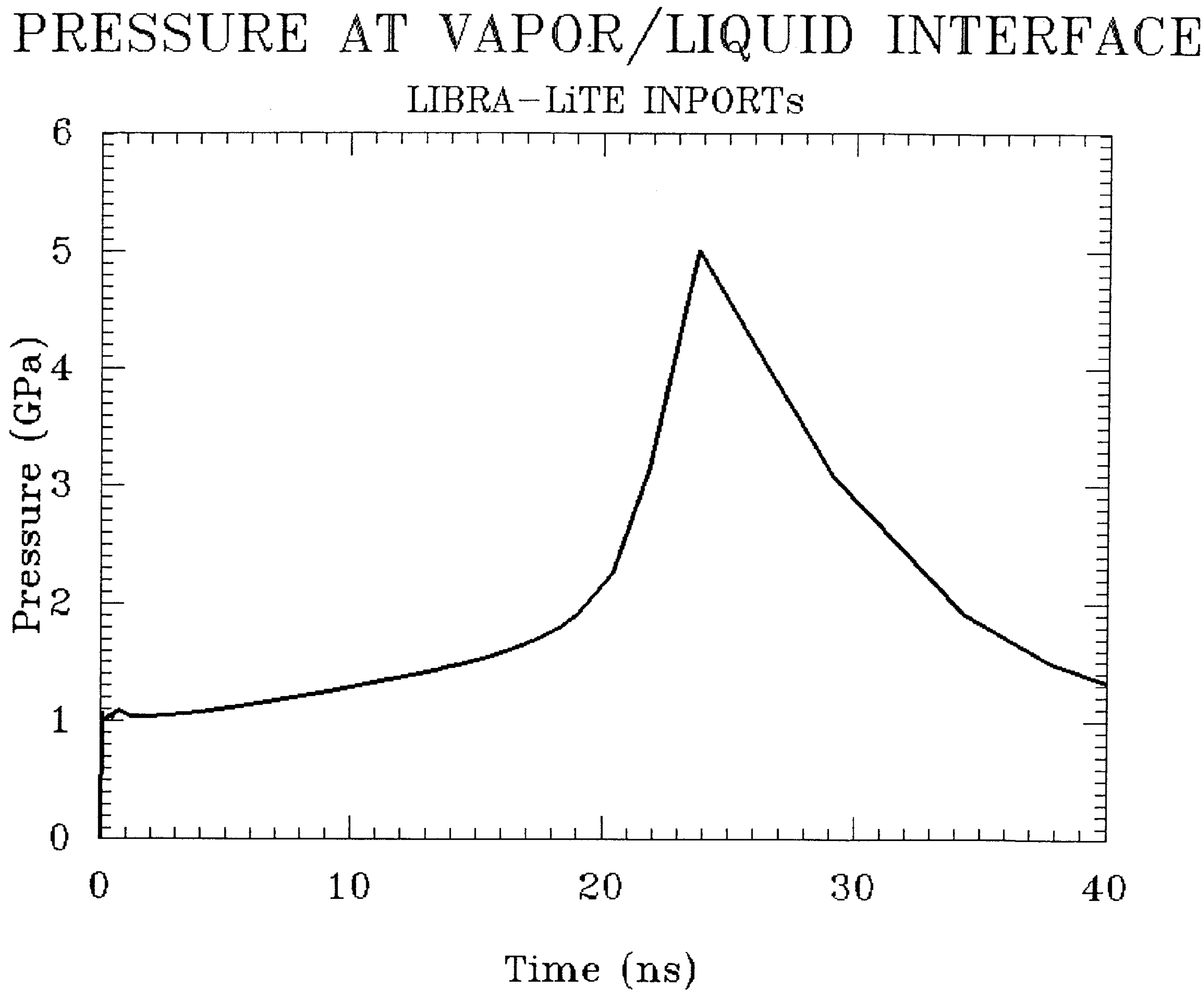

Pressure Pulse on Lens Magnets

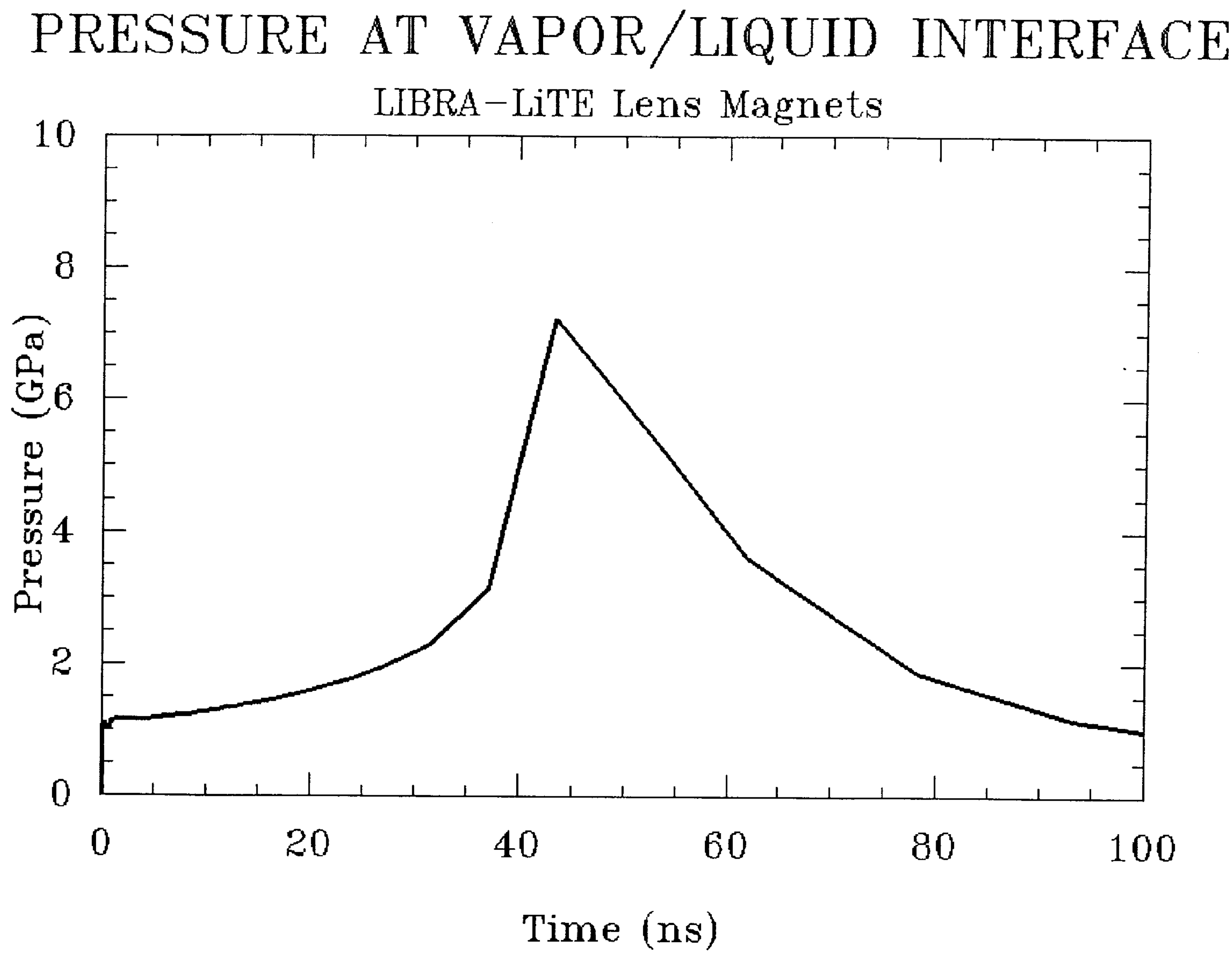

Schematic Picture of Gas Flow in Target Chamber

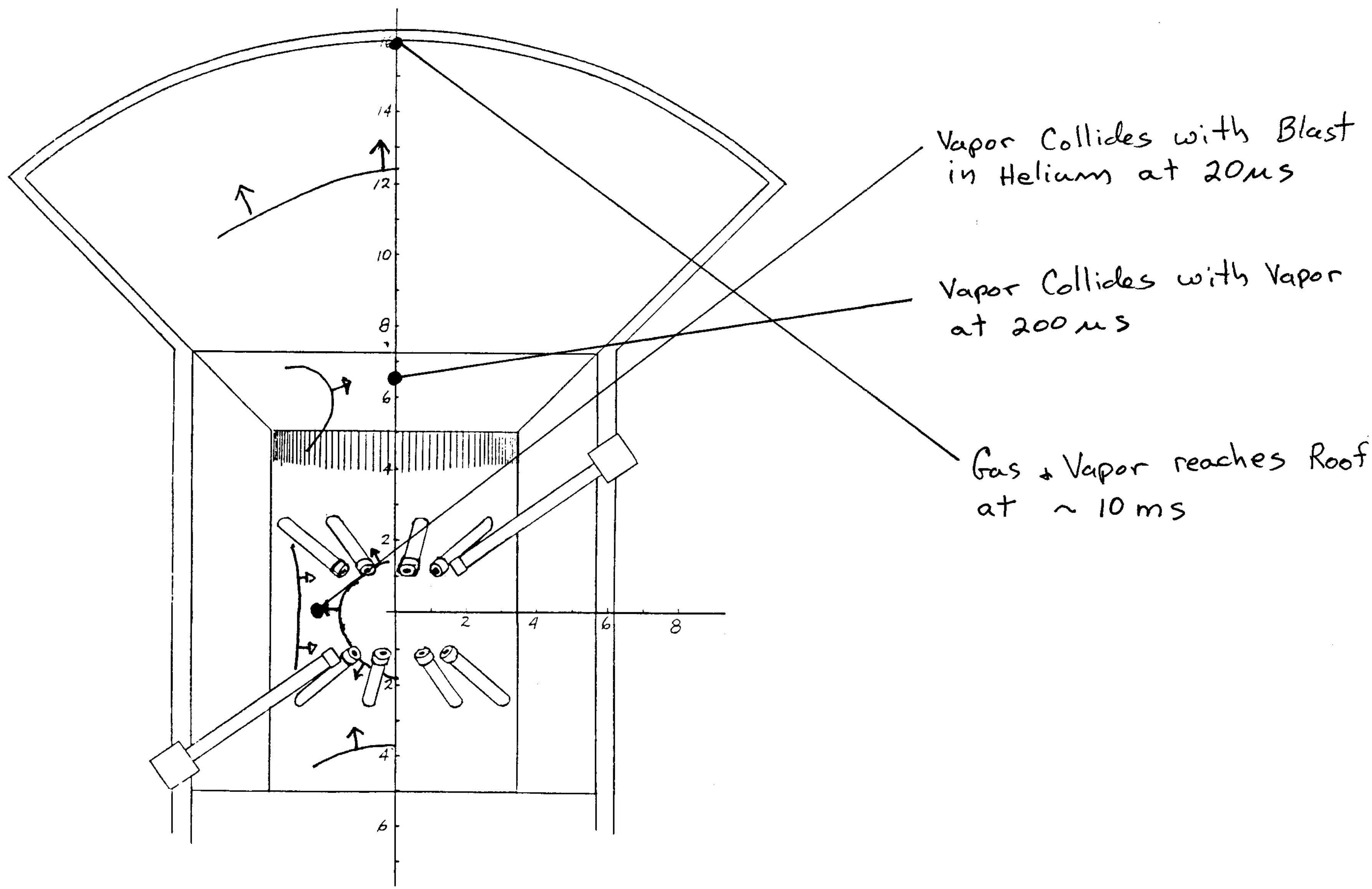

INPORT System Parameters

	LIBRA	LIBRA - LiTE
Tube Material	SiC	HT-9
Liquid Metal	LiPb	Li
Tube Diameter (cm)	3.0	5.0
Tube Thickness (mm)	2.0	3.0
Unsupported Length (m)	6.4	5.0
Flow Velocity (m/s)	2.60	2.44
Rep Rate (Hz)	3.0	3.0
Impulsive Pressure (Pa-s)	125	153

Preliminary INPORT Design Characteristics

Tube Structure:	67% solid density
Tension Bearing Fraction:	33% of HT-9
Yield Strength:	> 350 MPa at 550 °C
Creep-Rupture Strength:	> 200 MPa at 550 °C
Maximum Allowable Tension:	22.2 kN

(Design criterion based on creep rupture at 2.0×10^4 hr.)

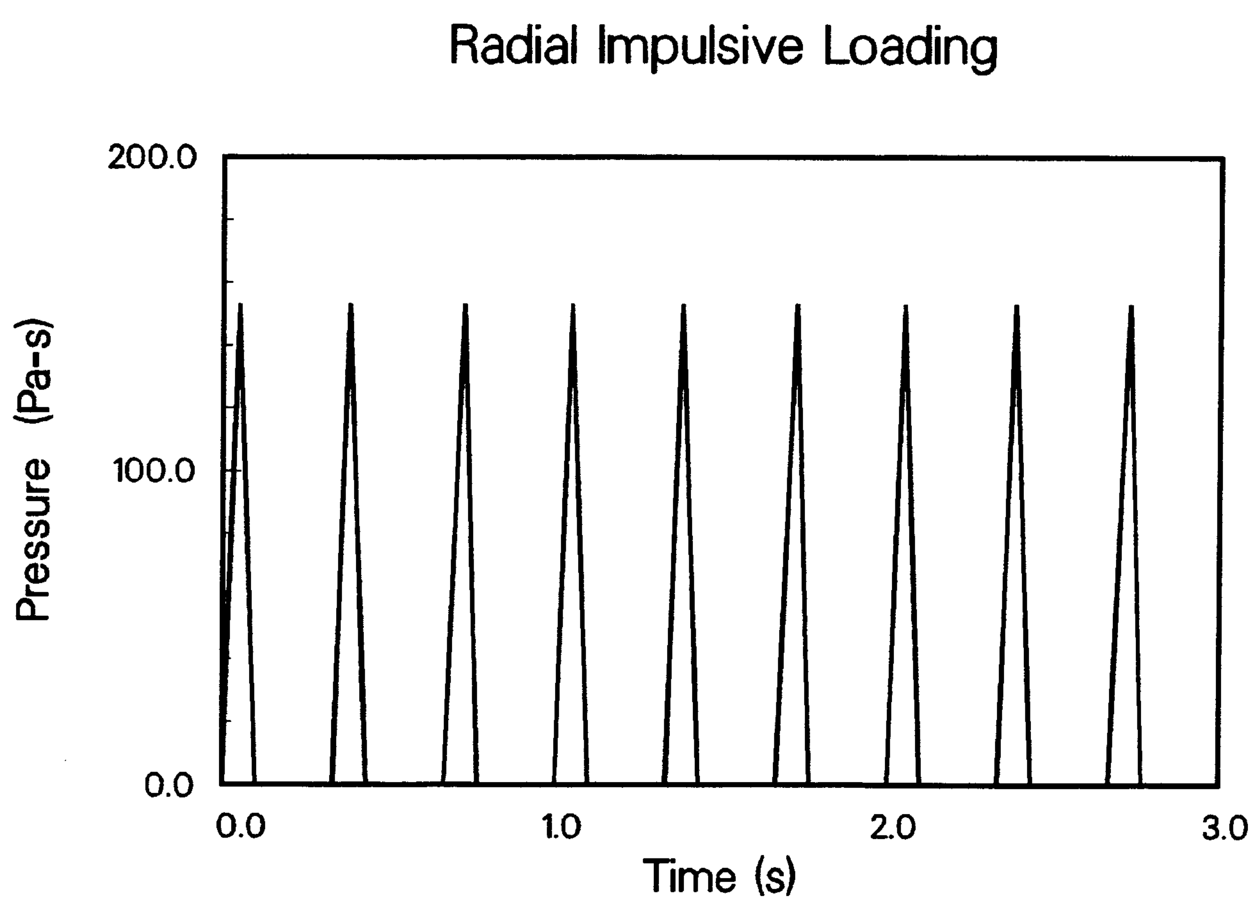
Radial Impulsive Loading
200.0
100.0
0.0
Pressure (Pa-s)
0.0
1.0
2.0
3.0
Time (s)

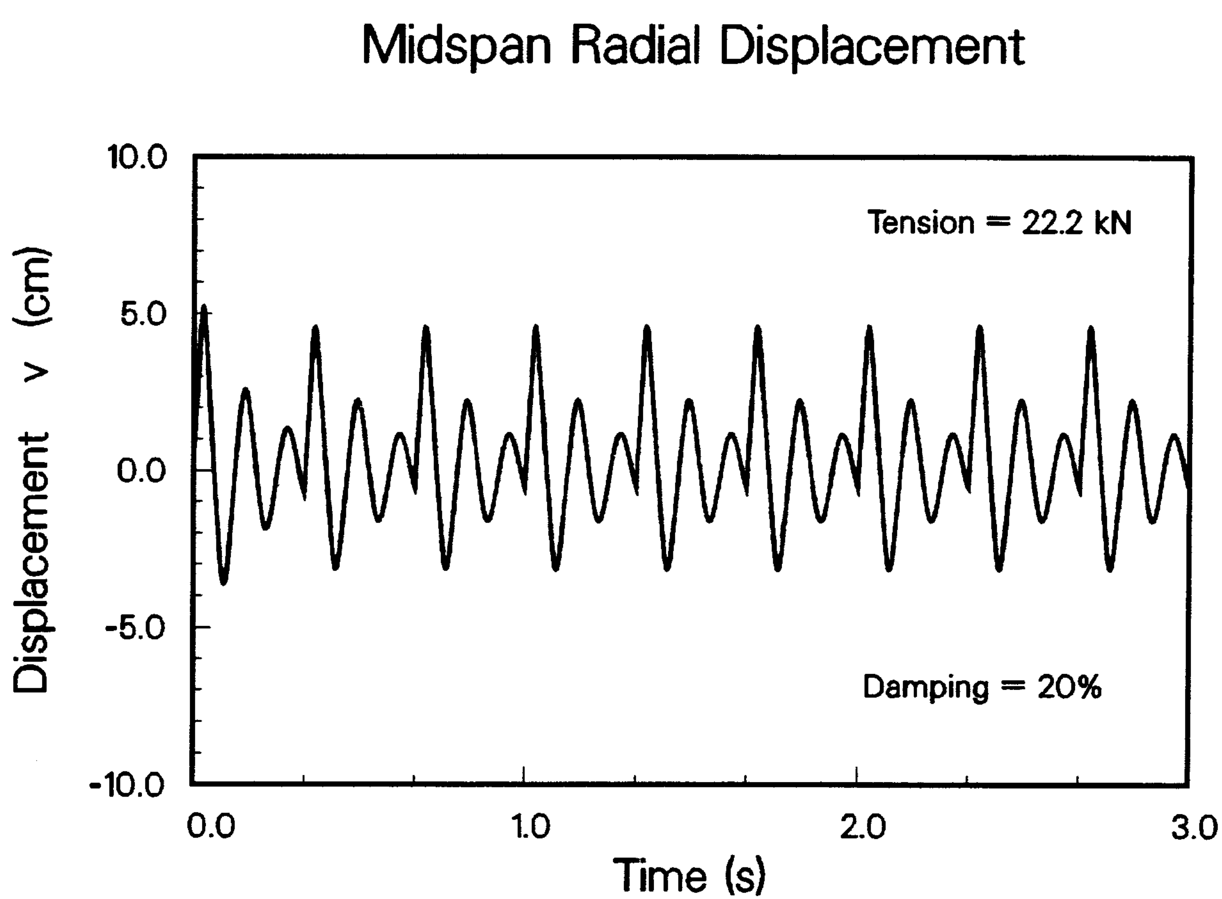

Midspan Radial Displacement
Tension = 22.2 kN
Damping = 20%
Displacement v (cm)
10.0
5.0
0.0
-5.0
-10.0
0.0
1.0
2.0
3.0
Time (s)

Circumferential Displacement

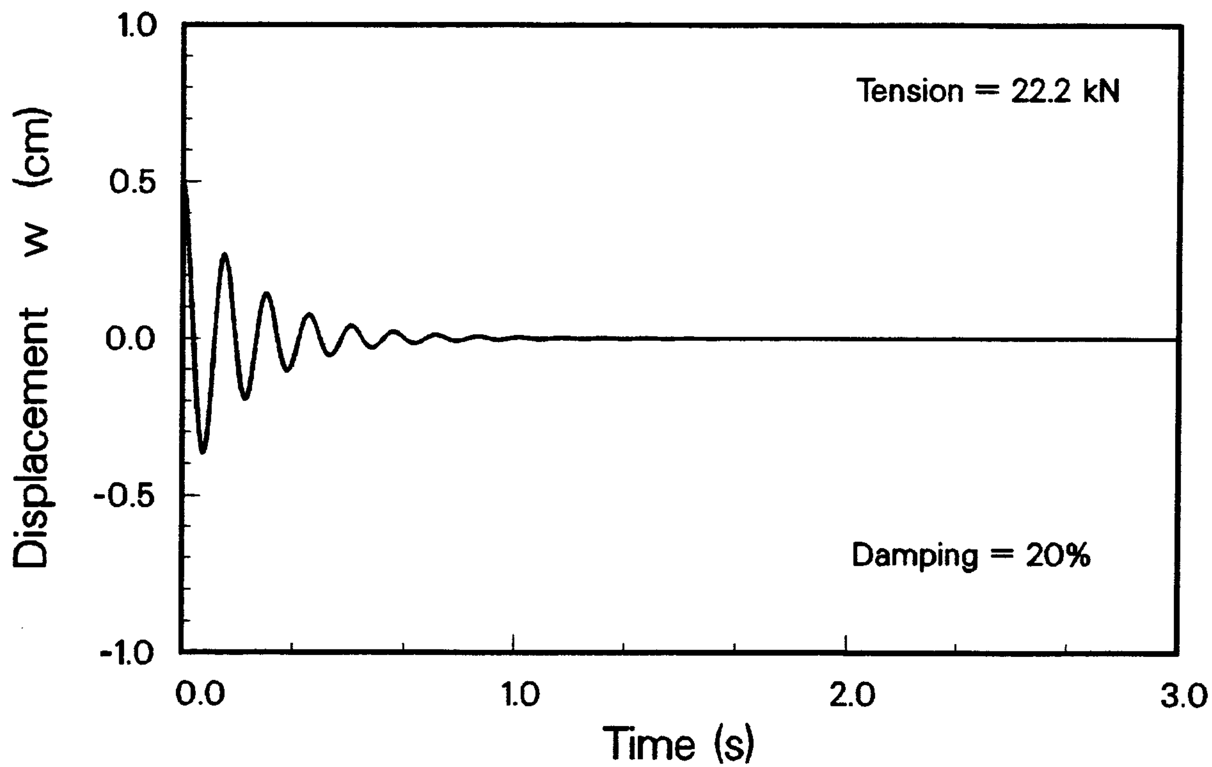

INPORT Response Summary

- For the design parameters the response is planar
- Maximum steady state displacement is 4.6 cm
- Maximum tension is used to control displacements
- For high tension, increases have a small effect on displacement
- Dynamic response depends on the natural frequencies vs. the rep rate
- Natural frequencies depend on the tension, flow velocity, mass, damping, etc.
- Parametric studies are in progress to optimize the design for acceptable displacements and life

Schematic Long-Term Pressure History on INPORT's

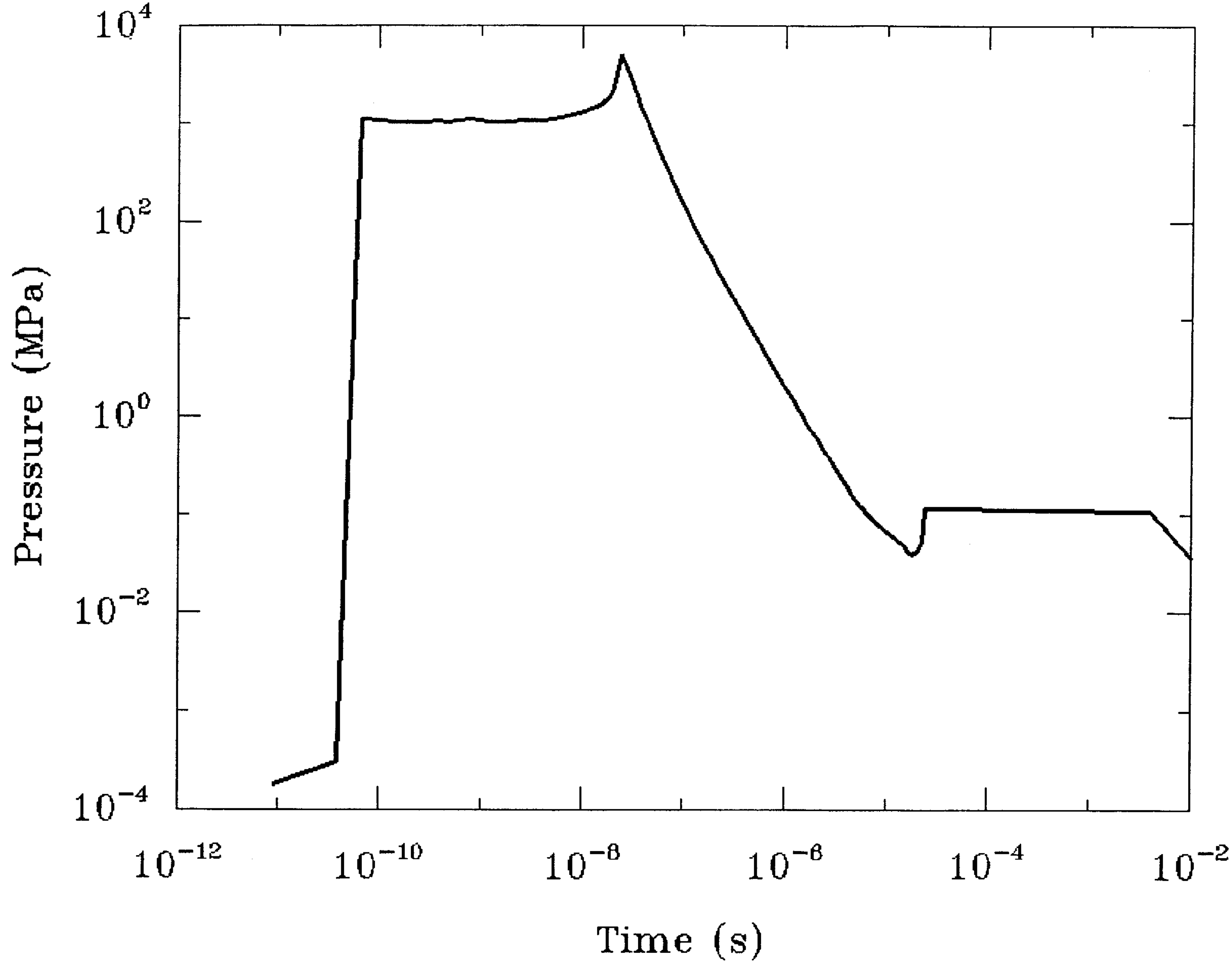

Conclusions

- Blasts have been simulated with the CONRAD computer code for a variety of target yields and chamber radii of relevance to LIBRA-LiTE.

- Pressure loadings on target chamber structures have been determined.

- Mechanical response of flexible INPORTs has been calculated.

- Long term behavior of target chamber fill gas has been estimated.

Other Reactor Features

Subject Covered

- Maintenance of Chamber Components
- Power Cycle
- Power Flow Diagram

Chamber Component Maintenance

Component	Estimated Lifetime
Lens Magnet	1 calendar year
Front INPORT Units	3 calendar years
Rear INPORT Units	4 calendar years

Maintenance of Lens Magnets and Front INPORTs

- Lens magnets and front INPORT units are mounted on a frame such that they constitute a single assembly

- The frame with the magnets and front INPORT units can be taken out of the chamber through the upper access port

- Coolant connections and electrical bus connections for the magnets can be integrated into the frame

- A seal must be provided at the interface of the beam tubes to prevent Li from leaking into them with the possibility of drips intercepting the beam

- With the assembly in the hot cell,magnet elements and INPORT units can be replaced

Maintenance of Rear INPORT Units

- With the lens magnet assembly out of the chamber, the rear INPORT units can be accessed for replacement.

- A transport column will be lowered into the chamber and fixed to the perforated plate. A carriage with manipulators can ride down the transport column into the chamber.

- The manipulator slides INPORT unit assemblies radially into the chamber, then an overhead crane pulls them out through the upper access port.

Power Cycle

- Li exchanges heat with an organic coolant which then goes to a steam generator and a steam cycle utilizing two reheat stages.

Power Cycle Parameters

Total thermal power (MWt)	3425
Li inlet temperature to heat exchanger (^oC)	500
Li outlet temperature from heat exchanger (^oC)	350
Li mass flow rate (kg/s)	$4.84x10^3$
Organic coolant inlet temperature (^oC)	310
Organic coolant outlet temperature (^oC)	425
Mass flow rate of organic coolant (kg/s)	$11.74x10^3$
Steam temperature (^oC)	399
Steam pressure (MPa)	17.3
Estimated gross power cycle efficiency (%)	44
Gross electric power (MWe)	1507

POWER FLOW DIAGRAM FOR LIBRA-LiTE